STUDIES ON THE ADSORPTION OF BOVINE SERUM ALBUMIN ONTO POLYMER LATICES

HIROYUKI SHIRAHAMA

1986

HIROSHIMA UNIVERSITY

PREFACE

The studies included in this thesis have been carried out under the instructive guidance of Professor Toshiro Suzawa, Faculty of Engineering, Hiroshima University, during 1980-1985. The contents are concerned with the adsorption of bovine serum albumin onto polymer latices.

I am greatly indebted to Professor Toshiro Suzawa for his continuous encouragement and advice in this work. And also, I am heartily grateful to all the members of the research group of Professor Suzawa.

Hiroyuki Shirahama

Suzawa Laboratory

Department of Applied Chemistry

Faculty of Engineering

Hiroshima University

CONTENTS

GENERAL INTRODUCTION

The adsorption phenomena of biological macromolecules such as proteins at interfaces have been of great importance in many industrial fields (e.g., cosmetics, pharmaceutics, foodstuffs, etc.).

Proteins are highly surface-active owing to their amphiphilic character. Hence, they can adsorb at almost any interface over a wide range of conditions. In particular, the adsorption behavior of serum proteins onto polymer surfaces has recently been of considerable interest for the development and the improvement of biomedical materials such as the artificial heart and kidney.

As is commonly accepted now, the primary incidents when a foreign material is in contact with blood are the initial rapid adsorption of plasma proteins[1)-3)] and the following adhesion of platelets.[2)] Aggregation and morphological changes of the platelets can lead to an activation of the coagulation system and the formation of thrombi finally. The initial rapid protein adsorption is strongly dependent on the chemical and physical surface properties of polymer materials. Therefore, it is one of important themes for developing antithrombogenic biomaterials to clarify the adsorption behavior of serum proteins such as bovine serum albumin (BSA) onto polymer surfaces.

Incidentally, there are now two material surfaces which can be expected for antithrombogenic biomaterials. One is the surface that is

preferentially adsorbed by serum albumin when exposed to blood. It has been reported[2),4),5)] that platelets did not adhere to albumin coated surfaces, whereas γ-globulin or fibrinogen coated surface caused not only platelet adhesion, but also aggregation and the release of platelet constituents. However, the desorption or denaturation of albumin molecules probably leads to the decrease in antithrombogenecity. The other is the material that has little interaction between its surface and serum proteins, that is, in this case, serum proteins are hard to adsorb onto this material. Hydrogels such as poly(2-hydroxyethyl methacrylate(HEMA))and polyacrylamide (PAAm) are designed by this concept. All these hydrogels contain a large amount of water (which is in a quasi-organized state in the gels[6)]).

Up to the present, from the above viewpoint, many investigations on the adsorbability of plasma proteins onto polymer surfaces have been reported. Brash et al.[1)] studied extensively the adsorption of albumin, γ-globulin, and fibrinogen onto various polymer surfaces. They supposed that these proteins adsorbed physically and irreversibly onto hydrophobic surfaces in a monolayer and a native state. However, many investigations after their study revealed that protein adsorption was not necessarily irreversible but was in the dynamic equilibrium state, repeating adsorption and desorption,[7)] and there were differences in the amount protein adsorbed, the rate of adsorption, etc. among those polymers.[5)]

As described above, recent studies on the adsorption of protein onto polymer surfaces have mainly been carried out under physiological conditions for the purpose of developing or improving the biomedical materials (especially antithrombogenic one). However, few papers (studied basically under various conditions) on the adsorption phenomena of protein onto polymer surfaces have been reported. The purpose of the current work, therefore, is to clarify the adsorption behavior of BSA onto polymer latices basically from the viewpoint of surface chemistry; the resulting information will make a contribution to the development of biomedical polymers.

The advantages in the application of polymer latices as adsorbents for proteins are as follows: (i) the surface area for adsorption is large, (ii) the kinds and quantities of dissociation groups existing on the surface of latex particles are clear, (iii) the surface characteristics of latex particles (e.g., hydrophilicity (or hydrophobicity) of the surface) can be varied relatively easily, etc.

Hitherto, polymer latices have mainly been used in the industrial fields of paint, adhesive, paper and textile, etc. In recent years, their uses are extending to the biomedical materials such as adsorbents for proteins,[8)-11)] enzyme immobilized latex,[12)] and medical diagnostics.[13)-15)] Norde[16)] studied systematically the adsorption of human plasma albumin (HPA) onto polystyrene (PS) latices, and indicated that HPA adsorption was entropically driven at least near the isoelectric point of this protein. However, using only PS latex,

it is not sufficient to study the relation between the adsorbability of the protein and surface properties of latices (such as hydrophilicity, hydrophobicity, surface charge groups, etc.). Therefore, in this work, various polymer latices (whose surface characteristics were different ~~from~~ from one another) were used as adsorbents for the protein.

The first part of this study was concerned with the preparation and the surface characterization of polymer latices. All the latices were prepared in the absence of emulsifier, and were highly monodisperse. In chapter I, polystyrene (PS)[17] and polymethyl methacrylate (PMMA)[18] latices were used as a hydrophobic homopolymer latex. These latices were prepared by the usual heterogeneous polymerization using potassium persulfate as initiator. In chapter II, carboxylated polymer (styrene / acrylic acid or styrene / methacrylic acid copolymer), styrene / 2-hydroxyethyl methacrylate copolymer (P(St/HEMA)), and styrene / acrylamide copolymer (P(St/AAm))[19),20)] latices were used as a hydrophilic latex. Carboxylated and P(St/HEMA) latices were prepared by a special polymerization technique, viz., the seed polymerization method with the successive addition of monomer, although P(St/AAm) latex was prepared by the same method as homopolymer latices. The surface characteristics of polymer latices were examined by conductometric and potentiometric titrations, ζ-potential and viscosity measurements, etc.

The second part of this study was concerned with the adsorbability of

BSA onto various polymer latices as a function of pH, ionic strength, etc. BSA is one of the proteins whose properties in solution are well-characterized. For example, the conformational alteration of BSA molecule is very sensitive to its environment (viz., pH, ionic strength, etc.). Therefore, it is of great interest to investigate BSA adsorption onto different polymer surfaces. In chapter I, BSA adsorption onto hydrophobic polymer (PS and PMMA) latices was examined. In chapter Ⅱ, BSA adsorption onto hydrophilic polymer (i.e., carboxylated, P(St/HEMA), and P(St/AAm)) latices was investigated. The adsorbability of BSA onto each latex was discussed by reference to the results of surface characteristics of latices. In chapter Ⅲ, the effects of coexistent electrolyte anions on BSA adsorption were studied. It is generally known that the binding of small electrolyte anions to BSA molecule completely dominates cation binding,[21] further, there is a difference in binding affinity between those anions.[22] Consequently, this will lead to the difference in the adsorbability of BSA onto the latex. In chapter Ⅳ, the adsorption of urea-denatured BSA onto latices was examined. Up to the present, many investigations on the denaturation of BSA in urea solution were carried out. However, little work on the adsorption of urea-denatured BSA onto polymer surfaces has been reported. Therefore, it is of great interest to study whether the adsorbability of urea-denatured BSA is different from that of native BSA.

PART I

Preparation and Surface Characterization of Polymer Latices

CHAPTER I

Hydrophobic Polymer Latices

Hydrophobic homopolymer latices, i.e., polystyrene (PS) and polymethyl methacrylate (PMMA) latices were prepared without emulsifier using potassium persulfate (KPS) as the initiator. Electron micrographs of these latices revealed the particles to be highly monodisperse. The conductometric titration curve of PS latex showed both strong and weak acid groups to exist on the latex surface, though that of PMMA latex showed only strong acid groups to exist on the surface. This was also supported by the results of the pH dependence of ζ-potentials for these latex particles. The surface charge density (or the ζ-potential) of PS latex was greater than that of PMMA latex in proportion to the amount of KPS used in the polymerization.

1. Introduction

A dispersion of polymer particles (whose diameters are about 0.1 −3 μm) in a liquid is referred to as a latex. Hydrophobic homopolymer latices, in particular, polystyrene (PS) and polymethyl methacrylate (PMMA) latices have been widely used as a model system in colloidal and adsorption studies, because their particles are rigid, spherical, and uniform in size, and they can be easily prepared. However, if the polymerization is carried out in the presence of emulsifier, emulsifier molecules adsorbed on the particle surface are hardly to remove even by prolonged dialysis.[23] For colloidal and adsorption studies, obviously, soap (emulsifier)-free polymer latices are desired. In the soap-free system, the latex surfaces are only stabilized by the ionic end-groups originating from decomposed initiator fragments.

In this chapter, hydrophobic PS and PMMA latices were prepared without soap, and the surface characteristics of these two latices were discussed by conductometric titration etc.

2. Experimental

2.1. Materials

Styrene and methyl methacrylate (MMA) were vacuum-distilled three times under a nitrogen atmosphere. Potassium persulfate (KPS) as the initiator was recrystallized twice from water. Cation- and

anion-exchange resins (porous ion-exchange resins PK-212 and PA-312, obtained from Mitsubishi Chemical Industries Ltd.) used for purifying latices were cleaned by reference to the method of van den Hul and Vanderhoff.[24] A carbonate-free sodium hydroxide (NaOH) solution used for titration was prepared from a "Sørensen liquid." All other chemicals such as sodium chloride (NaCl), hydrochloric acid (HCl)were of analytical grade. Distilled-deionized water was used in all experiments.

2.2.Methods

2.2.1.Preparation and purification of latices

PS and PMMA latices were prepared without soap under a nitrogen atmosphere.[17),18)] The polymerization recipe is given in Table 1. The latices obtained were first dialyzed against water for about one week using a well-boiled Visking tube. Subsequently, PS latex was purified by a batch procedure with a mixed bed of cation- and anion-exchange resins (the volume ratio of the latex dispersion to ion-exchange resin was 4:1), although PMMA latex was purified by electrodialysis for about one week. The particle diameters of latices were determined by electron microscopy (using a JEM-100U transmission electron microscope, JEOL Ltd.). All micrographs revealed the latices to be highly monodisperse. The specific surface areas of latices calculated from the particle diameter etc. was also given in Table 1.

Table 1. Preparation of PS and PMMA latices

	PS	PMMA
Styrene (mol/l)	0.871	———
MMA (mol/l)	———	2.0
KPS (mol/l)	1.83×10^{-3}	1.0×10^{-3}
Speed of agitation (rpm)	350	300
Polymerization temp. (℃)	70	70
Polymerization time (h)	11	8
Solid content [a] (g/l)	91	200
Particle diameter (nm)	526	413
Specific surface area (m^2/g)	10.86	12.16

[a] Theoretical value

2.2.2. Conductometric and potentiometric titrations

All titrations were carried out under a nitrogen atmosphere at 25 ℃. Conductometric titrations were carried out with a 1×10^{-3}N or 5×10^{-3}N NaOH aqueous solution as the titrant. The volume fractions (ϕ) of latices were about 1.3 and 1.7 % for PS and PMMA latices, respectively. During each titration, the latex dispersion was stirred with a magnetic stirrer. Conductivities were measured using a Toa digital conductivity meter CM-30ET.

Potentiometric titrations were carried out with a 1×10^{-2}N or 2×10^{-2}N NaOH solution as the titrant using a Hitachi-Horiba pH-meter F-7ss. Before titrating with an NaOH solution, the latex dispersion

was adjusted to a pH of about 3 and an ionic strength 0.01 by adding 1×10^{-2}N HCl and 0.1M NaCl. The ϕ for PS and PMMA latices were about 2.3 and 3.1 %, respectively. In the same way as in the conductometric titration, the latex dispersions were stirred during titrations except the time for reading pH values. The surface charge density (σ) of the latex was determined as a function of pH by titrating an equal volume of blank solution (containing only 1×10^{-2}N HCl and 0.1M NaCl) under the same conditions as for the latex dispersions.

2.2.3. Zeta (ζ)-potentials of latices

ζ-potentials of latex particles were measured by a microelectrophoresis apparatus (Mitamura Riken Co., Ltd) at 25 ℃. The electrophoretic mobilities were converted into ζ-potentials according to the treatment of Wiersema et al.[25] (in this treatment, both the retardation effect and the relaxation effect are taken into account). In measuring the ζ-potentials as a function of pH at a constant ionic strength 0.01, the pH and ionic strength were adjusted with aqueous HCl, NaOH, and NaCl.

3. Results and Discussion

3.1. Conductometric titrations of latices

Figures 1 and 2 show the conductometric titration curves of PS and PMMA latices, respectively. In the case of PS latex, two distinct inflection points (i,e., two endpoints of titration)are observed.

The first endpoint (a) corresponds to the equivalence point of strong acid ($-OSO_3^-$) derived from decomposed initiator fragments. The second endpoint (b) may correspond to that of weak acid ($-COO^-$). It appears that carboxyl groups ($-COO^-$) originate from the oxidation of hydroxyl groups ($-OH$),[26),27)] probably formed by the Kolthoff reaction[28)] of sulfate groups ($-OSO_3^-$). The oxidation of $-OH$ can be performed even under a nitrogen atmosphere.[28),29)] On the other hand, as can be seen from Figure 2, in PMMA latex, it is doubtful whether the second endpoint would be present. This may be because the amount of KPS used in the polymerization of PMMA latex (to be exact, a molar ratio of KPS to the monomer) is much smaller than that of PS latex. That is, the amount of weak acid groups existing on the latex surface may be too small to be titrated.

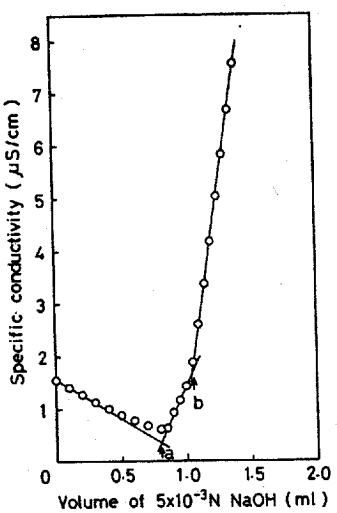

Fig.1. Conductometric titration curve of PS latex (25°C)

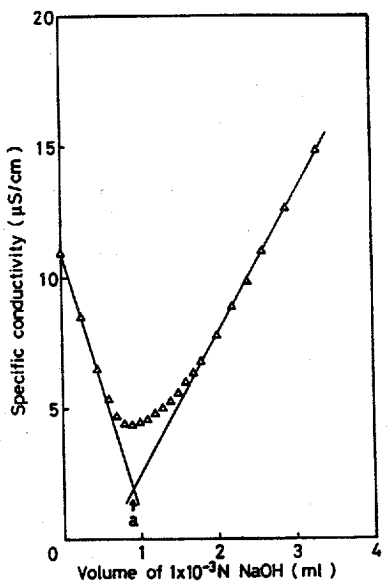

Fig.2. Conductometric titration curve of PMMA latex (25°C).

Surface charge densities (σ) of the latices were determined by the following equation:

$$\sigma = \frac{c \cdot f \cdot F}{S} \qquad (1)$$

where c is the titrant (viz., NaOH) quantity consumed up to the endpoint of titration (mol), f the factor of titrant, F the Faraday constant (C/mol), and S the total surface area of latex particles(cm^2). The σ-values obtained are given in Table 2. It can be seen from this table that the σ-value for PS latex is about 4.9 times greater than that for PMMA latex. The difference in σ-value between PS and PMMA latices is nearly proportional to that in a molar ratio of KPS to the monomer used in those polymerizations.

Table 2. Surface charge densities of PS and PMMA latices

	Surface charge density ($\mu C/cm^2$)		
Latex	σ_s	σ_w	$\sigma = \sigma_s + \sigma_w$
	Strong acid($-OSO_3^-$)	Weak acid($-COO^-$)	Total
PS	-4.52	-1.41	-5.93
PMMA	-1.20	——	-1.20

3.2. Potentiometric titrations of latices

The potentiometric titration curves of PS and PMMA latices are shown in Figures 3 and 4, respectively. The shapes of these two titration curves are similar to each other.

Assuming the difference in titration volume of NaOH solution between the latex dispersion and blank solution to be proportional to the number of charged groups on the surface of latex particles, one can determine the surface charge density (σ) of the latex as a function of pH using eq.(1). The results are shown in Figure 5.

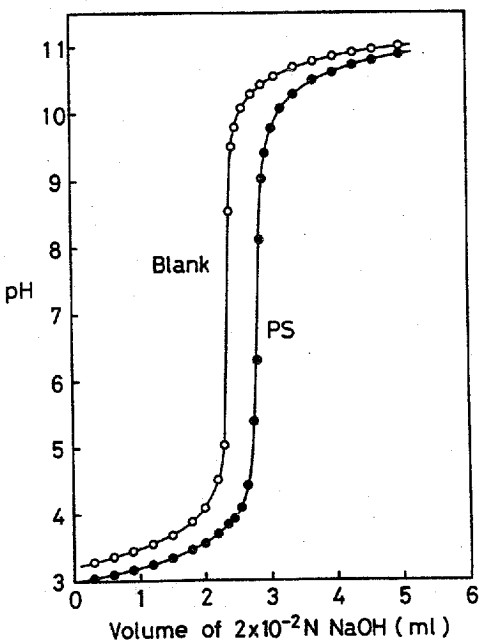

Fig. 3. Potentiometric titration curve of PS latex (25°C, ionic strength=0.01).

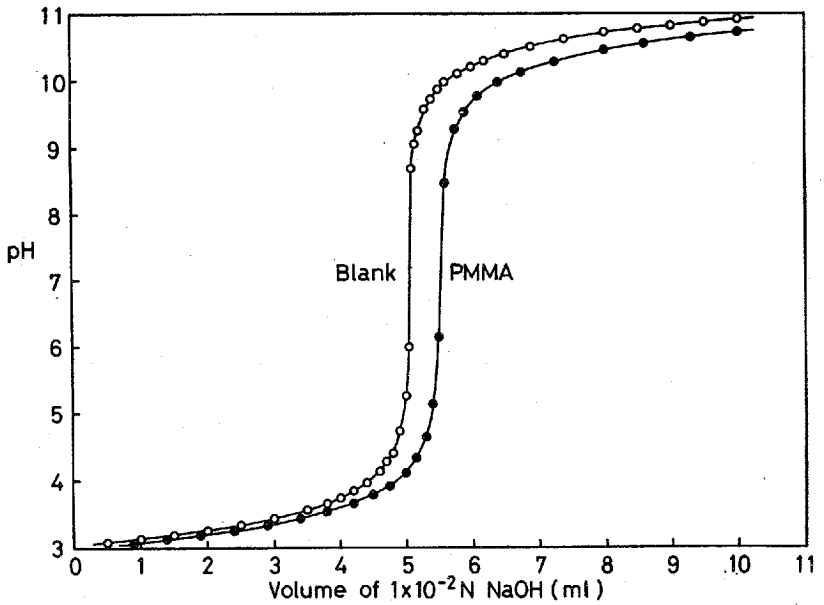

Fig.4. Potentiometric titration curve of PMMA latex (25°C, ionic strength ≈0·01).

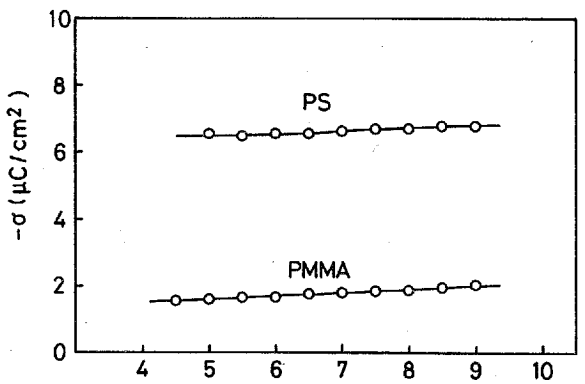

Fig.5. Surface charge densities for PS and PMMA latices as a function of pH (25°C, ionic strength ≈ 0·01).

As can be seen from this figure, σ for PS latex is about four times greater than that for PMMA latex over the whole range of measured pH. This may be attributed to the difference in a molar ratio of KPS to the monomer used in the polymerization, similarly to the results of the conductometric titrations of these latices. However, the pH dependence of σ for PS and PMMA latices is not very different from each other, because the surface charge of these latices is derived from decomposed initiator fragments (mainly strong acid groups) only.

3.3. ζ-potentials of latices

Figure 6 shows ζ-potentials of PS and PMMA latices as a function of pH at ionic strength 0.01. As can be seen from Figure 6, two latices have negative charges associated with initiator fragments. The ζ for PS latex is much greater than that for PMMA latex throughout the entire range of measured pH. This result is probably due to a greater σ of PS latex compared with that of PMMA latex. Moreover, the ζ for PS latex increases from acidic to neutral pH region, though that for PMMA latex remains almost constant throughout the whole pH range. This increase in ζ for PS latex is probably attributed to the dissociation of carboxyl groups (suggested their existence by conductometric titration of PS latex, see Figure 1) on the latex surface. In PMMA latex, since carboxyl groups were hardly discernible on the latex surface (see Figure 2), the ζ for this latex probably remains constant regardless of pH change. Thus, the ζ-potentials

(or the surface charges) of polymer latices (whose surface characteristics are similar to each other) appear to increase in proportion to the amount of initiator (KPS) used in the polymerization.

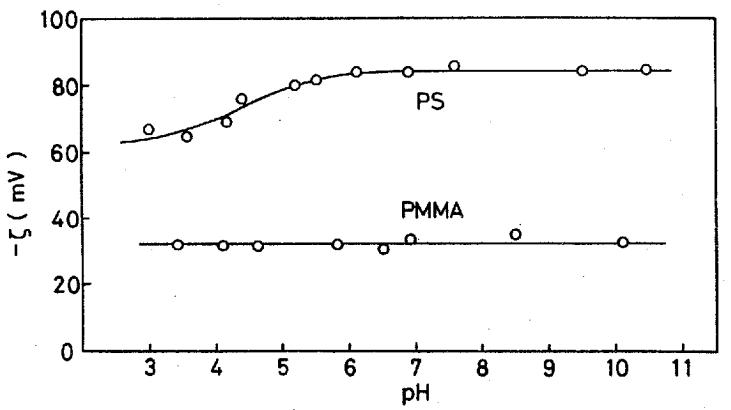

Fig. 6. ζ-potentials of PS and PMMA latices as a function of pH (25°C, ionic strength 0·01).

CHAPTER II

Hydrophilic Polymer Latices

Hydrophilic copolymer latices, viz., carboxylated latices —— styrene/acrylic acid (AA) copolymer (P(St/AA)) and styrene/methacrylic acid (MAA) copolymer (P(St/MAA)) —— , styrene/2-hydroxyethyl methacrylate (HEMA) copolymer (P(St/HEMA)) latices, and styrene/acrylamide (AAm) copolymer (P(St/AAm) latices were prepared in the absence of emulsifier using potassium persulfate (KPS) as the initiator. Polystyrene (PS) latex was used as a reference sample. To obtain stable and monodisperse copolymer latices, a special polymerization technique, i. e., the seed polymerization method with the successive addition of monomer was used for preparing P(St/HEMA) and carboxylated latices, though P(St/AAm) latices were prepared by the same method as PS latex. All these latices were found to be highly monodisperse from those electron micrographs. Conductometric titration curves of these latices except P(St/AAm) latices showed that both strong and weak acid groups existed on the surface of latex particles. The surface charge density (σ) for P(St/AA) latex was proportional to the amount of AA used in the copolymerization. However, the σ for P(St/MAA) latex was smaller than that for P(St/AA) latex, although the mol % of acid monomers used in the copolymerization was the same for both latices. The σ for carboxylated latices increased with an

increase of pH, but the pH dependence of σ for PS latex was not very pronounced. The pH dependence of σ for P(St/HEMA) latex was similar to that for PS latex. From this result, it was suggested that the surface of P(St/HEMA) latex was more hydrophilic than that of PS latex in spite of its having much the same surface charge as PS latex. The ζ- potentials of these copolymer latices were smaller than that of PS latex over the whole range of measured pH. This result was interpreted on the basis of the difference in the structure of the electrical double layer between PS and copolymer latices. Moreover, in the case of P(St/AAm) latex, the thickness of a hydrophilic polymer (viz., polyacrylamide (PAAm)) layer existing on the latex surface was estimated from the viscosity measurement. As a result, it was found that the thickness of PAAm layer increased with increasing the amount of AAm used in the copolymerization. Methylene Blue (basic dye) adsorption onto PS, P(St/AA), and P(St/HEMA) latices was measured as a function of pH. The overall tendency of the dye adsorption was more similar to the σ-pH curves than the ζ-pH curves. This may indicate that Methylene Blue adsorption onto latices mainly occurs electrostatically.

1. Introduction

As mentioned in GENERAL INTRODUCTION, polymer latices have many industrial applications in such fields as paint, paper and textile, etc. In particular, latices prepared by copolymerization of hydrophobic monomers with unsaturated hydrophilic monomers play important roles in those fields. Considering that their uses are now extending to the fields of biomedical materials such as medical diagnostics,[13)-15)] adsorbents for serum proteins,[8)-11)] etc., it is very important to clarify their surface characteristics. Moreover, in many cases, use of soap-free polymer latices is favorable because of the various effects of emulsifiers (e.g., the remaining emulsifier molecules may affect the protein adsorption). However, a special technique is necessary to prepare stable and monodisperse soap-free latices by copolymerization with a hydrophilic monomer.

In this chapter, the surface characteristics of copolymer latices (prepared by copolymerization of styrene with hydrophilic monomers) were compared with that of hydrophobic polystyrene latex. As hydrophilic monomers, acrylic acid (AA), methacrylic acid (MAA), 2-hydroxyethyl methacrylate (HEMA), and acrylamide (AAm) were used. Similarly to hydrophobic homopolymer latices, the polymerizations were carried out in the absence of emulsifier using potassium persulfate (KPS) as the initiator.

2. Experimental

2.1. Materials

Monomers used in the copolymerization were purified as follows: Styrene and hydrophilic monomers (AA, MAA, HEMA) were distilled three times and twice, respectively, under a nitrogen atmosphere in vacuo. AAm was recrystallized twice from benzene. Methylene Blue (obtained from Wako Pure Chemical Industries Ltd.) was purified by recrystallization from water twice. All other chemicals and water were similar to those described in chapter I.

2.2. Methods

2.2.1. Preparation and purification of latices

Styrene / AAm copolymer (P(St/AAm) latices[19),20)] were prepared by the usual heterogeneous polymerization similarly to homopolymer latices. Carboxylated latices —— styrene / AA copolymer (P(St/AA))and styrene / MAA copolymer (P(St/MAA)) —— , and styrene / HEMA copolymer (P(St/HEMA)) latices were prepared by the seed polymerization method with the successive addition of monomers. This method was newly developed for the current study, and was different from the usual seed polymerization. A practical polymerization method was as follows.

First, the prescribed amount of water was placed in a glass vessel equipped with a stirrer. The water was heated until it reached the

polymerization temperature. Then, the seed monomer (a few percent of total monomer mixture) was added to the reactor. When adding the prescribed amount of KPS dissolved in water, the seed polymerization step was initiated and performed for about 30 minutes. Subsequently, the residual monomer was successively added to the reactor with a feeding pump over a period of a few hours. The polymerization was carried out in a nitrogen atmosphere without soap, and was continued until it was substantially completed (this process after the successive addition of monomer was referred to as "After Polymerization").

The polymerization conditions for carboxylated, P(St/HEMA), and P(St/AAm) latices are given in Tables 3 — 5, respectively. The ratio of KPS to total monomer was adjusted to almost the same value in the preparation of each latex.

The latices obtained were first dialyzed against water for about 1 — 2 weeks. Further, P(St/AAm) latices were centrifuged in urea solution (ca. 6.7 mol/ l) to remove free polyacrylamide (PAAm) dissolved in the bulk solution, and redispersed in water by supersonic wave.[20] This procedure was repeated three times. Then, the latex dispersion was dialyzed for about two weeks to remove urea in the bulk solution. No PAAm was detected by Kjeldahl analysis in the final bulk solution of P(St/AAm) latices. Finally, all the copolymer latices were purified with ion-exchange resins in a similar procedure to PS latex. The volume ratios of latex dispersions to ion-exchange reins for

carboxylated, P(St/HEMA), and P(St/AAm) latices were 2:1, 3:1, and 3:1, respectively. The wt% of AAm in P(St/AAm) latex was determined by elemental analysis (using a Yanagimoto CHN Corder MT-2) and listed in Table 5. As can be seen from Table 5, the AAm fraction (wt%) in polymer latex is proportional to the amount of AAm used in the copolymerization.

Table 3. Preparation of carboxylated polymer latices (N_2 atmosphere)

Conditions	P(St/AA_2[a])	P(St/AA_5[a])	P(St/MAA_5[a])	PS[b]
Styrene (g)	73.96	72.36	71.87	45.34
AA (g)	1.045	2.640	—	—
MAA (g)	—	—	3.130	—
KPS (g)	0.3750	0.3750	0.3750	0.2473
Water (ml)	425	425	425	450
Seed monomer (g)	15	15	7.5	—
Speed of agitation (rpm)	350	350	350	350
Seed polymerization (℃,h)	70,0.5	70,0.5	70,0.5	—
Successive addition of monomer (℃,h)	70,1.0	70,1.0	70,1.0	—
After Polymerization (℃,h)	70,9.0	70,8.0	70,7.0	70,11.0[c]
Solid content [d] (g/l)	148	148	148	91

[a] Subscripts 2 and 5 represent the mol% of AA or MAA used in the copolymerization.

[b] This is the same PS latex as listed in Table 1 of chapter I.

[c] Polymerization time.

[d] Theoretical value.

Table 4. Preparation of P(St/HEMA) latices (Atmosphere N_2)

Conditions	P(St/HEMA$_5$[a)])	P(St/HEMA$_{10}$[a)])	PS[b)]
Styrene (g)	70.37	65.85	45.34
HEMA (g)	4.63	9.15	—
KPS (g)	0.3750	0.3750	0.2473
Water (ml)	425	425	450
Seed monomer (g)	15	7.5	—
Speed of agitation (rpm)	350	350	350
Seed polymerization (℃,h)	70,0.5	70,0.5	—
Successive addition of monomer (℃,h)	70,1.0	70,2.0	—
After Polymerization (℃,h)	70,5.5	70,4.5	70,11.0[c)]
Solid content [d)] (g/l)	149	149	91

[a)] Subscripts of 5 and 10 represent the mol% of HEMA.

[b)] This is the same PS latex as listed in Table 1 of chapter I.

[c)] This time corresponds to the polymerization time.

[d)] Theoretical values.

Table 5. Preparation of PS and P(St/AAm) latices (N_2 atmosphere)

Latex	PS	P(St/AAm$_5$[a)])	P(St/AAm$_{10}$[a)])	P(St/AAm$_{20}$[a)])
Styrene (mol/l)	0.871	0.910	0.856	0.768
Acrylamide (mol/l)	—	0.070	0.141	0.281
KPS (mol/l)	1.5×10^{-3}	1.72×10^{-3}	1.72×10^{-3}	1.72×10^{-3}
pH	3	3	3	3
Speed of agitation (rpm)	350	350	350	350
Polymerization temperature (℃)	70	70	70	60
Polymerization time (h)	14	10	8	10
Acrylamide fraction in polymer latex (wt%)[b)]	—	1.6	1.8	2.4

[a)] Subscripts 5, 10, and 20 represent acrylamide fraction in total monomer (wt%)

[b)] Obtained from elemental analysis.

The particle diameters of these latices were determined by electron microscopy, using a JEOL JEM-100U transmission electron microscope. As can be seen from Figure 7, all micrographs revealed the latices to be highly monodisperse. The average diameter, specific surface area, and uniformity ratio (U) for each latex are given in Table 6. U is defined by the following equation[30],

$$U = D_W / D_N \qquad (2)$$

where D_W and D_N are the weight-average and number-average diameters of latex particles, respectively. In the case of $U \leqq 1.01$, latices may be considered monodisperse.

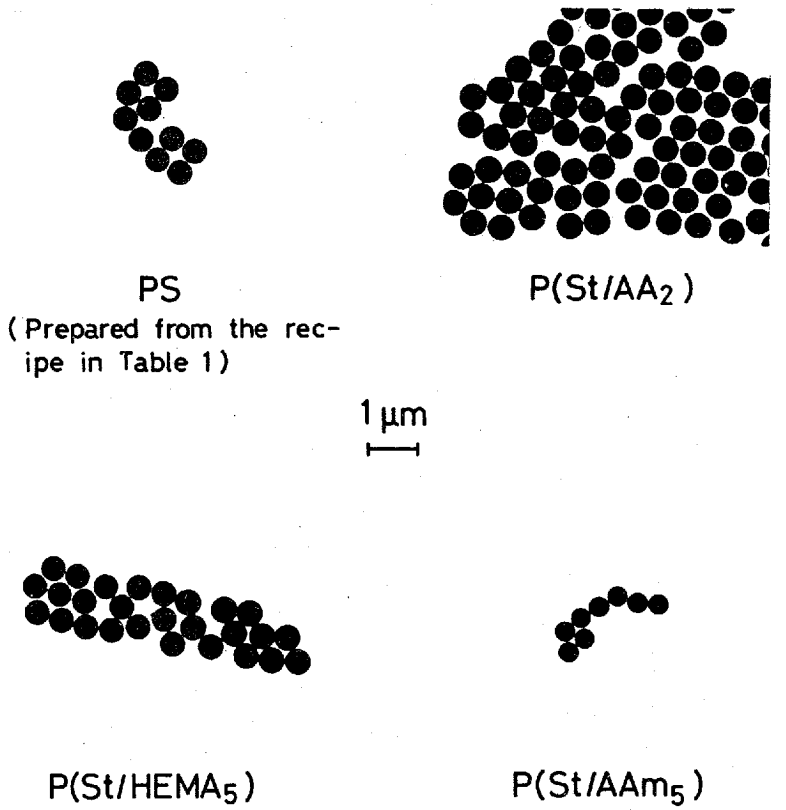

Fig. 7. Electron micrographs of various polymer latices (x 10,000).

Table 6.

Particle diameters, specific surface areas, and uniformity ratios of polymer latices.

Latex	Particle diameter (nm)	Specific surface area(m^2/g)	Uniformity ratio
PS *)	526	10.86	1.0003
P(St/AA_2)	541	10.54	1.0002
P(St/AA_5)	515	11.04	1.0011
P(St/MAA_5)	543	10.34	1.0007
P(St/$HEMA_5$)	510	11.13	1.0003
P(St/$HEMA_{10}$)	491	11.48	1.0006
PS **)	630	8.98	1.0004
P(St/AAm_5)	424	13.35	1.0017
P(St/AAm_{10})	420	13.48	1.0006
P(St/AAm_{20})	458	12.36	1.0109

*) and **) :These PS latices were prepared by the polymerization recipes listed in Table 3 and Table 5, respectively.

2.2.2. Conductometric and potentiometric titrations

These titrations were carried out by the same methods as described in chapter I. In the conductometric titrations of carboxylated latices, an NaCl aqueous solution (5×10^{-4} M/ ℓ) was added to facilitate the determination of the inflection point of the titration curve.[31] The volume fractions (ϕ) of latices were about 1.0, 1.3, and 2.4% for carboxylated, P(St/HEMA), and P(St/AAm) latices, respectively. In the potentiometric titrations, the ϕ for carboxylated and P(St/HEMA) latices were about 1.1 and 2.3%, respectively.

2.2.3. ζ-potentials of latices

ζ-potentials of latex particles were measured by a microelectrophoresis method described in chapter I.

2.2.4. Infrared (IR) spectra for P(St/HEMA) latices

For P(St/HEMA) latices, elemental analysis and conductometric (or potentiometric) titration can not give any data whether HEMA was surely incorporated into the latex particles. Thus, the IR absorption spectra for this latex were measured using an IR spectrometer (Hitachi, Type 215). The latex dispersion was first centrifuged, then the precipitate was dried in vacuo. This dried sample was made into a tablet with KBr powder. For example, the IR spectrum for P(St/HEMA$_{10}$) latex is shown in Figure 8. As observed in this figure, in addition to the characteristic absorption of polystyrene, it can be seen that

poly-HEMA absorbs at about 1730 and 3500 cm^{-1} (these peaks correspond to the stretching vibrations of — C=O and — OH, respectively).

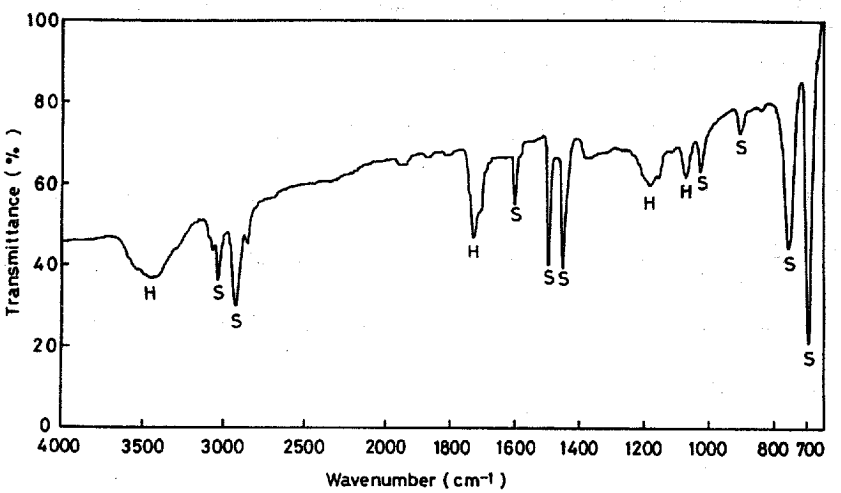

Fig. 8. The IR spectrum of P(St/$HEMA_{10}$) latex
(S, Polystyrene ; H, Poly-HEMA)

2.2.5. Viscosity measurement

In order to determine the thickness of polyacrylamide layer existing on the surface of P(St/AAm) latex, the viscosities of latex dispersions were measured with a Ostwald viscometer as a function of volume fraction of latex particles. The measurements were carried out at 25℃ in 1×10^{-3} M/ℓ NaCl solution.

2.2.6. Methylene Blue adsorption onto latices

Methylene Blue (basic dye) adsorption onto PS, P(St/AA), and P(St/HEMA) latices was measured at 25℃ by spectrophotometry, in order to compare the dye adsorption with the results of titrations and

ζ-potentials measurements. After a Methylene Blue solution was mixed with a latex dispersion, the sample solution was centrifuged in a high-speed centrifuge (Kubota KH-180). The amount adsorbed was determined from the difference between the initial and equilibrium concentrations. The wavelength of light used was 670nm. Preliminary experiments showed that adsorption equilibrium should be reached in 2h. Hence, all data were taken 2h after the test solutions were made. The pH and ionic strength of test solutions were adjusted with aqueous HCl, NaOH, and NaCl.

3. Results and Discussion

3.1 Conductometric and potentiometric titrations of latices

3.1.1. Carboxylated latices

The conductometric titration curves for carboxylated polymer latices are shown in Figure 9. These curves are similar to each other. Two distinct inflection points (viz., two endpoints of titration) are observed for each latex. The first endpoint (a) corresponds to the equivalence point of strong acid($-OSO_3^-$) derived from decomposed initiator fragments, and the second endpoint (b) to that of weak acid ($-COO^-$) derived from acid monomers. There is little difference in the titration volume of the strong acid among these latices, because the ratio of KPS to total monomer was adjusted to almost the same value for each latex.

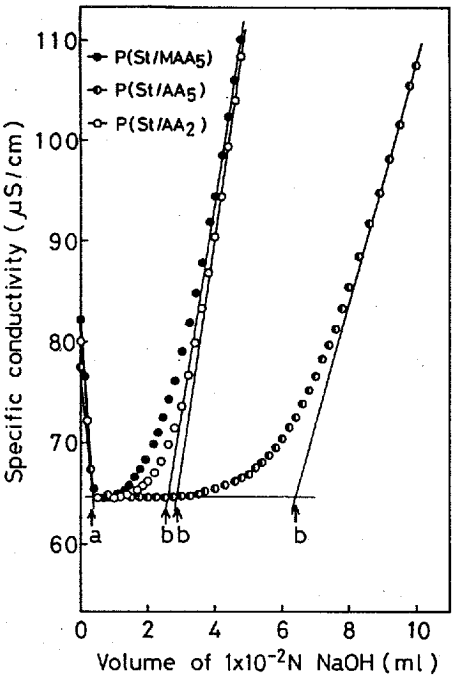

Fig.9. Conductometric titration curves of Carboxylated latices (25°C).

Surface charges (σ) of latices were determined using eq. (1) in chapter I. The σ-values obtained are given in Table 7. It can be seen from this table that the σ-value of weak acid (σ_w) for P(St/AA_5) latex is 2.61 and 2.47 times greater than those for P(St/AA_2) and P(St/MAA_5) latices, respectively. The difference in σ_w between P(St/AA_2) and P(St/AA_5) latices is proportional to the difference in mol% of acrylic acid (AA) used in the copolymerizations of these two latices. However, despite the same mol% of acid monomer being used in their copolymerizations, the σ_w of P(St/MAA_5) latex is much smaller than that of P(St/AA_5) latex. This may indicate that the total amount of acid monomer incorporated into the latex particles does not differ,

but there is a difference in the amount of acid monomers existing on the latex surfaces. That is, more AA can exist on the surface of latex particles than methacrylic acid (MAA), depending on the distribution coefficient between water and styrene monomer[32].

Figure 10 shows the potentiometric titration curves for PS and carboxylated latices. The curve of PS latex is similar to that of the blank solution, whereas the curves of carboxylated latices are fairly different from that of PS latex : the titration volume for carboxylated latices is considerably greater than that for PS latex, particularly in the alkaline pH region.

Table 7. Surface charge densities of various polymer latices

Latex	Surface charge density ($\mu C/cm^2$)		
	σ_s Strong acid($-OSO_3^-$)	σ_w Weak acid ($-COO^-$)	$\sigma = \sigma_s + \sigma_w$
PS *)	-4.52	-1.41	-5.93
P(St/AA_2)	-5.11	-33.3	-38.4
P(St/AA_5)	-5.49	-87.0	-92.5
P(St/MAA_5)	-6.08	-35.2	-41.3
P(St/$HEMA_5$)	-5.49	-1.65	-7.14
P(St/$HEMA_{10}$)	-5.04	-1.61	-6.65
PS **)	-3.45	-1.37	-4.82
P(St/AAm_5)	-1.79	——	-1.79
P(St/AAm_{10})	-0.52	——	-0.52
P(St/AAm_{20})	-1.47	——	-1.47

*) , **) Obtained from the polymerization recipes in Table 3 and Table 5, respectively.

In the same way as homopolymer latices, the surface charge densities (σ) of latices were determined as a function of pH using eq. (1) in chapter I. The results obtained are shown in Figure 11.

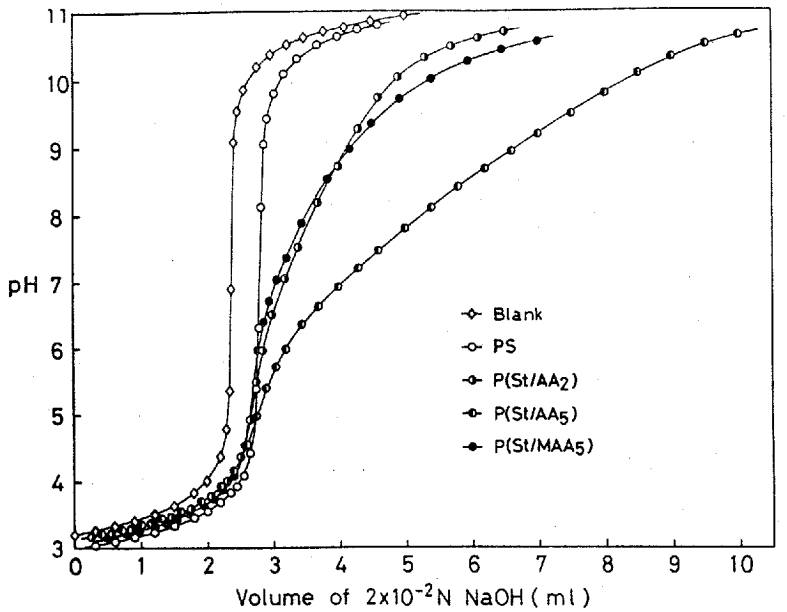

Fig10. Potentiometric titration curves of PS and Carboxylated latices (25°C, ionic strength≈0.01)

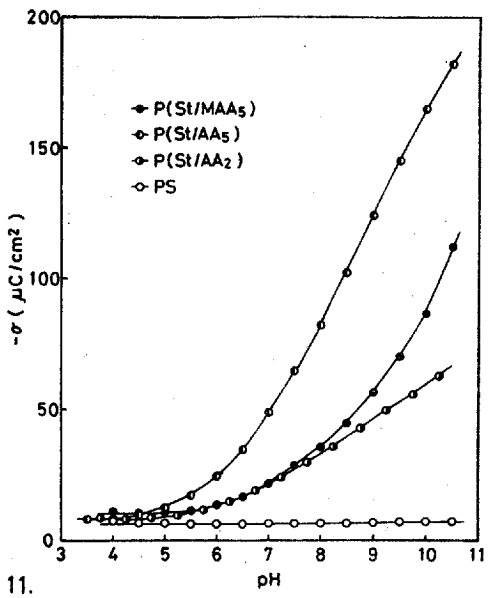

Fig. 11.
Surface charges as a function of pH for PS and Carboxylated latices (25°C, ionic strength≈0.01).

Up to a pH about 5, the σ for carboxylated latices is almost equal to that for PS latex, since carboxyl groups hardly dissociate in this pH region. However, at pH higher than about 5, the σ for carboxylated latices increases with increasing dissociation of carboxyl groups (i, e., with increasing pH). Further, at the same pH in the alkaline region, σ increases in the order, $P(St/AA_2) \leqq P(St/MAA_5) < P(St/AA_5)$. But little pH dependence of σ is observed for PS latex. This may be because carboxyl groups on PS latex surface are far fewer than those on carboxylated latices (see Table 7). The results of conductometric titrations (i,e., σ-values for carboxylated latices in Table 7) suggest the equivalence point of these latex dispersions to be found at a pH of about 8.4 at which σ for each carboxylated latex in Figure 11 is close to the value ($\sigma = \sigma_s + \sigma_w$) in Table 7. Therefore, the σ for carboxylated latices appear to approach their plateau values above pH 8.4, since all carboxyl groups on the particle surface are titrated at this pH. However, as can be seen from Figure 11, the σ for these latices still increase with increasing pH. Thus, not only the carboxyl groups on the latex surface but also those in the interior near the particle surface are titrated in this pH region since the surface polyacrylic (or polymethacrylic) acid layer of these latices swells with increasing pH. This is supported by the results on $P(St/AA_2)$ and $P(St/MAA_5)$ latices in Figure 11. That is, σ-values for $P(St/MAA_5)$ latex are greater than those for $P(St/AA_2)$ latex above pH ca. 8.4, because methacrylic acid is more

likely to exist in the interior of latex particles than acrylic acid.

3.1.2. P(St/HEMA) latices

The conductometric titration curves for PS and P(St/HEMA) latices are shown in Figure 12. The shapes of titration curves for P(St/HEMA) latices are similar to that for PS latex. Two distinct endpoints of titration are shown for each latex. These two endpoints correspond to the equivalence points of strong acid ($-OSO_3^-$) and weak acid ($-COO^-$), respectively, as described in chapter I. The surface charge densities (σ) of these latices obtained are given in Table 7. It can be seen from this table that the σ for these latices are not very different from one another.

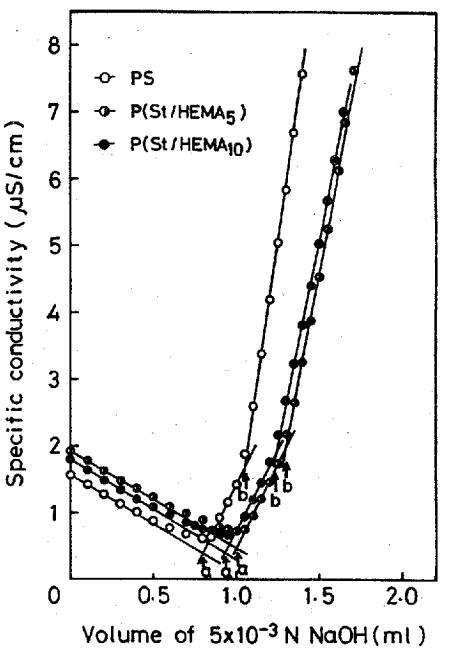

Fig.12. Conductometric titration curves of PS and P(St/HEMA) latices (25°C).

Figure 13 shows the potentiometric titration curves of PS and P(St/HEMA) latices. In the alkaline pH region, the titrant volume for P(St/HEMA) latex at the same pH-value is somewhat greater than that for PS latex. The σ for these latices as a function of pH were determined by the same manner as in homopolymer latices. The pH dependence of σ for these latices are shown in Figure 14. For each latex, $-\sigma$ somewhat increases from a neutral pH value (pH ca. 6). This may arise from the dissociation of weak acid groups on the latex surface. This tendency is greater for P(St/HEMA) latex than for PS latex. For this result, the following explanations are possible : (i) As HEMA is more hydrophilic than styrene, water-soluble initiator (viz., KPS) fragments may be incorporated more into P(St/HEMA) latex than into PS latex. Therefore, weak acid groups probably exist more on P(St/HEMA) latex than on PS latex. (ii) Weak acid groups may be formed by hydrolysis of HEMA during the polymerization. However, since HEMA is stable to hydrolysis except at high alkalinity,[33] this effect seems to be not very large. In general, the pH dependence of surface charges for these latices is relatively small. Thus, it appears that P(St/HEMA) latices are more hydrophilic than PS latex in spite of their having much the same surface charges as PS latex.

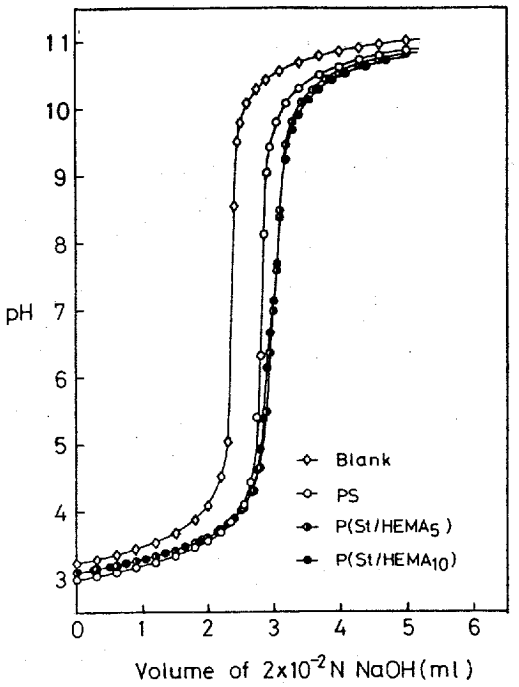

Fig.13.
Potentiometric titration curves of PS and P(St/HEMA) latices (25°C, ionic strength=0.01).

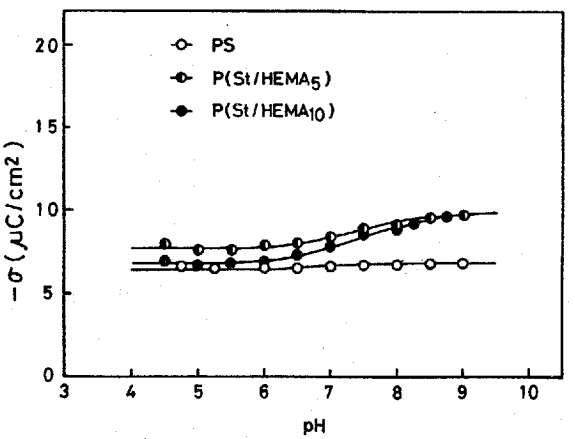

Fig.14. Surface charges for PS and P(St/HEMA) latices as a function of pH (25°C, ionic strength 0.01).

3.1.3. P(St/AAm) latices

Figure 15 shows the conductometric titration curves of PS and P(St/AAm_{20}) latices. In this case, PS latex listed in Table 5 was used. For

PS latex, there exist two endpoints in the titration curve as described previously. On the other hand, the second endpoint for P(St/AAm$_{20}$) latex is not so clear as to be identified as weak acid. For other P(St/AAm) latices, the titration curves obtained are similar to that of P(St/AAm$_{20}$) latex. The surface charge densities (σ) of these latices were determined by the same method described in chapter I. The σ obtained are given in Table 7. As can be seen from this table, the σ for each P(St/AAm) latex is rather smaller as compared with that for PS latex. Probably, this is because a part of the initiator (KPS) was consumed for homopolymerization of acrylamide (AAm) in the bulk solution, and the surface dissociation groups, i.e., strong acid groups masked with polyacrylamide (PAAm) layer on the latex surface, were not detectable by titration.

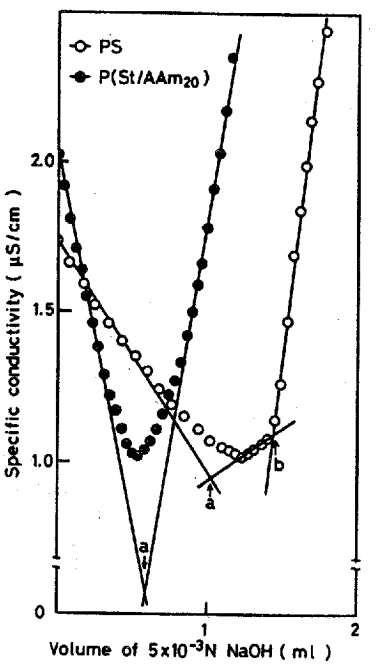

Fig. 15. Conductometric titration curves of PS and P(St/AAm$_{20}$) latices (25°C).

3.2. ζ-potentials of latices

3.2.1. Carboxylated latices

Figure 16 shows ζ-potentials of PS and carboxylated latices as a function of pH. It can be seen that these latices have negative charges associated with the acid monomer and/or initiator fragment. The ζ for each latex increases from acidic to neutral pH probably as a result of the dissociation of carboxyl groups on the latex surface. However, in contrast to the σ-pH curves (Figure 11), ζ for PS latex is larger than that for carboxylated latices throughout the entire range of measured pH. The following reason may explain the difference in tendency between σ-pH and ζ-pH curves: σ represents the charge of all ionized groups on the latex surface while ζ is the potential on the shear plane of the electrical double layer. To clarify this, I attempted to estimate the position of the plane of shear on the basis of the Gouy-Chapman-Stern model for double layers.

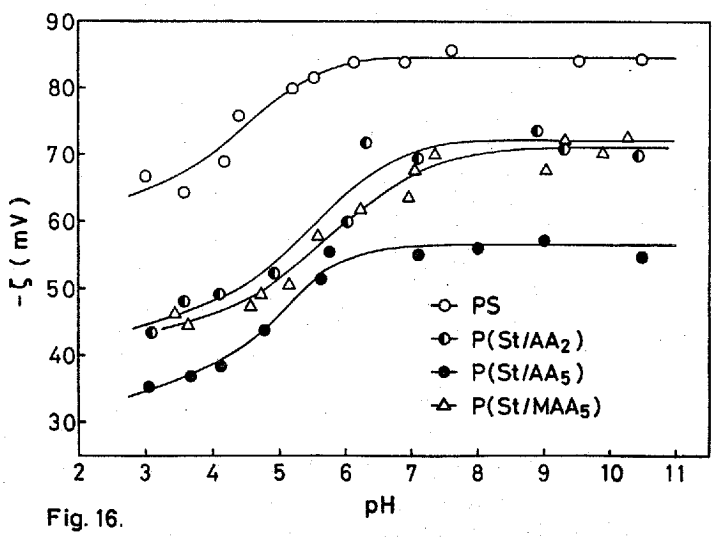

Fig. 16.
Zeta-potentials of PS and Carboxylated latices as a function of pH (25°C , ionic strength 0·01).

Figure 17 shows the potential (ψ) distribution in this double layer model as a function of the distance from the solid-liquid interface, where ψ_0 is the surface potential. The position (t) of the shear plane was estimated by the treatment of Eversole-Boardman,[34] who expressed the dependence of ζ-potential on the electrolyte concentration as

$$\ln \tanh (ze\zeta/4kT) = \ln \tanh (ze\psi_\delta/4kT) - \kappa t \qquad (3)$$

where z is the valence of ions, e, the charge of an electron, k, the Boltzmann constant, T, the absolute temperature, ψ_δ, the Stern potential, and κ, the Debye-Hückel parameter. For the 1-1 electrolyte, eq. (3) can be written for water solutions at 25℃ as follows:

$$\ln \tanh (9.727\times10^{-3}\zeta) = \ln \tanh (9.727\times10^{-3}\psi_\delta) - 0.3285\sqrt{c}\, t \qquad (4)$$

where ζ, c (electrolyte concentration), and t are in mV, mol/ℓ, and Å, respectively. Thus, t can be estimated from the slope of the straight line suggested by eq (4).

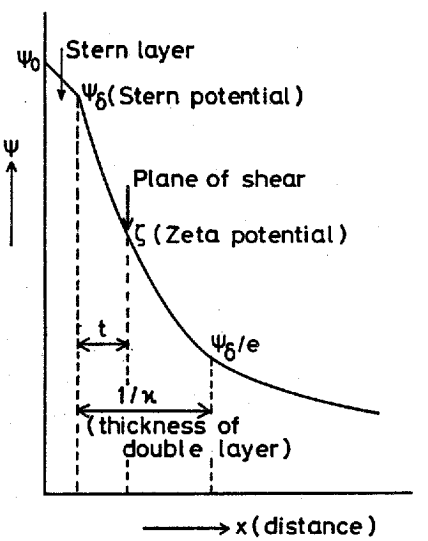

Fig. 17.
Potential distribution for the Gouy-Chapman-Stern model of the electrical double layer

First, the ζ-potentials of PS and carboxylated P(St/AA) latices were measured as a function of the electrolyte (NaCl) concentration. For $P(St/AA_5)$ latex, the ζ-potentials were also measured at an alkaline pH (pH of about 10.3 obtained by adding aqueous NaOH). In other cases, the pH was fixed to about 6 regardless of the electrolyte concentration, since the measurement solution of the latex dispersion contained only NaCl as the electrolyte. In Figure 18, the ζ-potentials of these latices exhibit maxima at ca. a 3×10^{-3} mol /ℓ NaCl concentration. The increase in the ζ-potential up to this NaCl concentration may be due to the adsorption of Cl^- from a bulk solution onto the particle surface.[35] The rapid decrease in the ζ-potential above this NaCl concentration most likely results from compression of the electrical double layer with increasing electrolyte concentration.

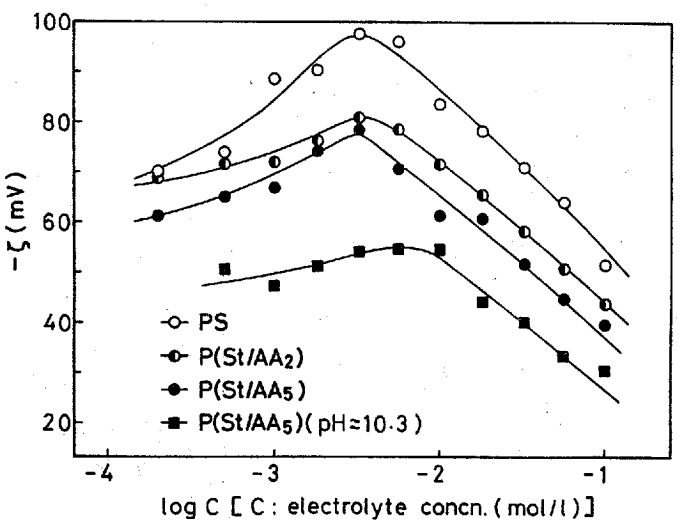

Fig.18. Zeta-potentials of PS and Carboxylated latices as a function of electrolyte concentration (25°C).

The data of Figure 18 were used to make the Eversole-Boardman's plot in Figure 19. The values of t and ψ_δ calculated by the least squares method from the slopes and intercepts of the indicated straight lines are given in Table 8. The values of t for P(St/AA) latices are larger than that for PS latex. Furthermore, t increases with increasing mol% of acrylic acid used in the copolymerization or pH.

These results indicate that, in the case of carboxylated latices, hydrous polyacrylic (or polymethacrylic) acid layers exist on the surfaces and shift the plane of shear away from the particle surfaces. Therefore, the greater the t value is, the smaller the potential at the plane of shear (i.e., ζ-potential) becomes (see Figure 17). This may be one reason why the ζ-potentials of carboxylated latices are smaller than that of the PS latex. The Stern potentials(ψ_δ) for P(St/AA) latices are smaller than that for PS latex (see Table 8). This probably leads to low ζ-potentials of carboxylated latices, even though the surface potentials (ψ_0) of the latices are high. Thus, it may be concluded that the lower ζ-potentials of carboxylated latices are due to larger t and smaller ψ_δ.

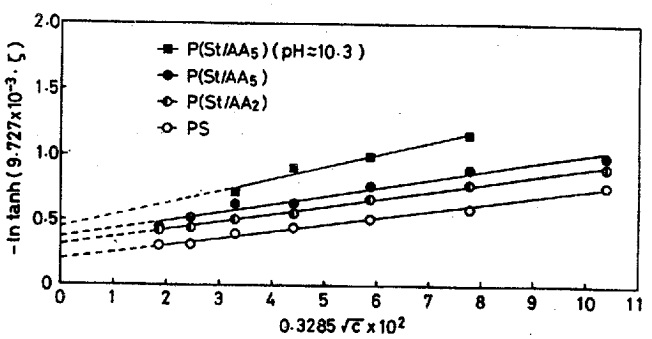

Fig.19. Eversole-Boardman's plot(25°C).

Table 8. Values of t and ψ_δ for various polymer latices

Latex	t(Å)	ψ_δ (mV)
PS *)	5.4	-119
P(St/AA_2)	5.9	-96.2
P(St/AA_5)	6.4	-87.8
P(St/AA_5) (pH≈10.3)	9.3	-78.0
P(St/$HEMA_5$)	10	-88.6
P(St/$HEMA_{10}$)	14	-82.7
PS **)	5.3	-136
P(St/AAm_5)	19	-114
P(St/AAm_{10})	27	-106
P(St/AAm_{20})	38	-50.7

*) and **) These PS latices were prepared according to the recipes in Table 3 and Table 5, respectively.

3.2.2. P(St/HEMA) latices

Figure 20 shows ζ-potentials of PS and P(St/HEMA) latices as a function of pH. From this figure, it can be seen that all these latices have negative charges derived from the initiator fragments. The ζ for P(St/HEMA) latices are smaller than that for PS latex over the whole range of measured pH; this tendency is proportional to the quantity of HEMA used in the copolymerization. Considering the difference in σ between PS and P(St/HEMA) latices not to be very large (strictly speaking, the σ for P(St/HEMA) latex is somewhat greater than that for PS latex), it is difficult to understand this trend in ζ-potentials (cf. Figures 14 and 20). Similarly to carboxylated latices, the difference in tendency between σ-pH and ζ-pH curves may be attributed to the structure of the electrical double layer for these latices.

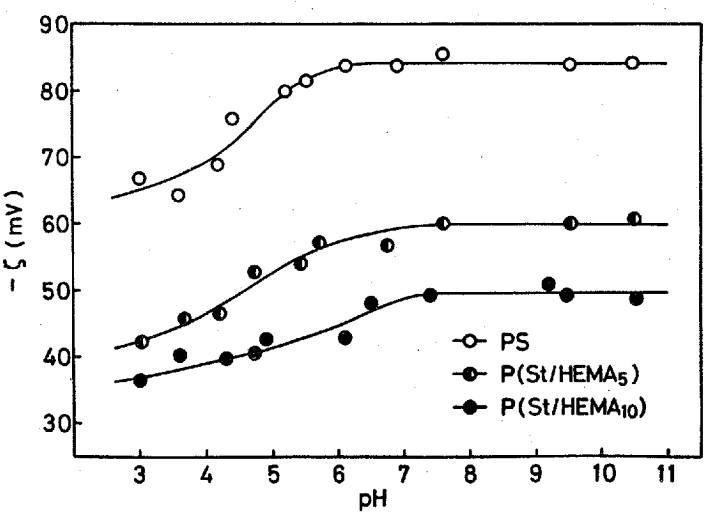

Fig. 20. ζ-potentials of PS and P(St/HEMA) latices as a function of pH (25°C, ionic strength 0.01).

First, the ζ-potentials of PS and P(St/HEMA) latices were measured as a function of the electrolyte (viz., NaCl) concentration (see Figure 21). As observed in this figure, the electrolyte concentration dependence of ζ for P(St/HEMA) latices is much the same tendency as carboxylated latices. In a similar manner, the Eversole-Boardman's plot for each latex was made (see Figure 22) ; the position (t) of the shear plane and the Stern potential (ψ_δ) were calculated from the slope and intercept of the straight line indicated in Figure 22, respectively. The values of t and ψ_δ obtained are given in Table 8. As can be seen from Table 8, the t for P(St/HEMA) latices are about two times greater than that for PS latex. Moreover, t increases with increasing the quantity of HEMA used in the copolymerization. Similarly to carboxylated latices, these indicate that hydrated poly-HEMA layers exist on the surface of P(St/HEMA) latex and shift the shear plane away from the particle surfaces in proportion to the values of t. This consideration is illustrated schematically in Figure 23. The smaller valve of ψ_δ for P(St/HEMA) latex may also contribute to its lower ζ-potential.

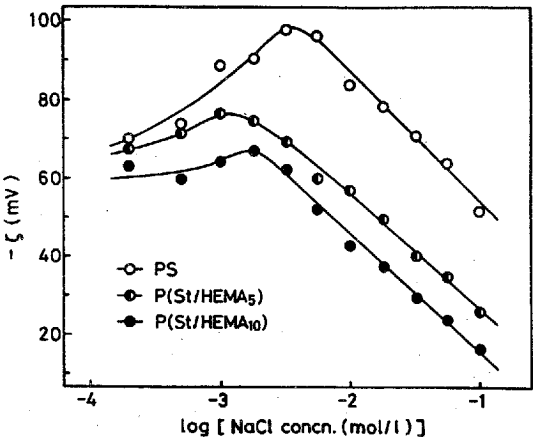

Fig. 21. ζ-potentials of PS and P(St/HEMA) latices as a function of NaCl concentration (25°C).

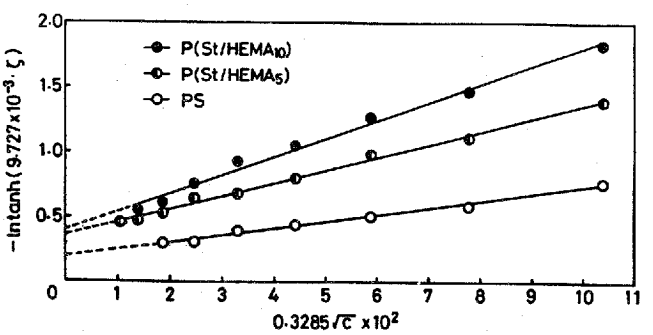

Fig. 22. Eversole-Boardman's plot (25°C).

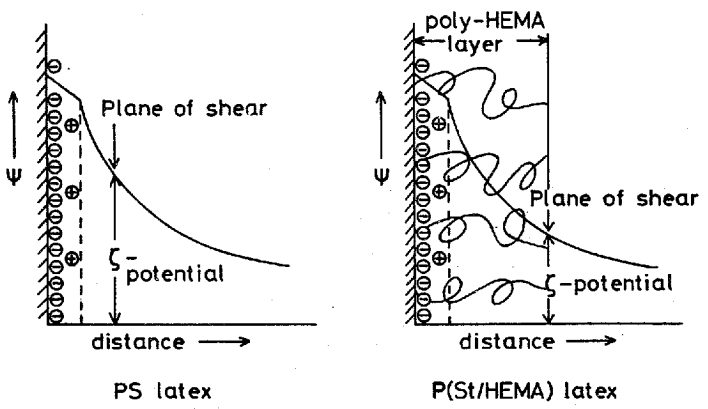

Fig. 23.
Schematic representation of the electrical double layer for polymer latex surfaces

3.2.3. P(St/AAm) latices

Figure 24 shows the ζ-potentials of PS and P(St/AAm) latices as a function of pH. All latices show negative ζ derived from the initiator fragments. The ζ for PS latex increases from acidic to neutral pH probably as a result of the dissociation of weak acid groups on the latex surface. For P(St/AAm) latex, a similar tendency is observed in a more alkaline pH region. Judging from the result of the conductometric titration for P(St/AAm) latex (which suggested only strong acid groups to exist on the latex surface), this increase in ζ may be attributed to the exposure of strong acid groups (masked with polyacrylamide (PAAm) layer existing on the particle surface) to the bulk solution.[36] The ζ for P(St/AAm) latices are smaller than that for PS latex over the whole range of measured pH; this tendency is proportional to the quantity of acrylamide (AAm) used in the copolymerization. This result is probably due to a smaller σ of P(St/AAm) latex, and to the difference in the structure of the electrical double layer between PS and P(St/AAm) latices. In the same manner as other latices, the values of t and ψ_δ for P(St/AAm) latices were estimated.

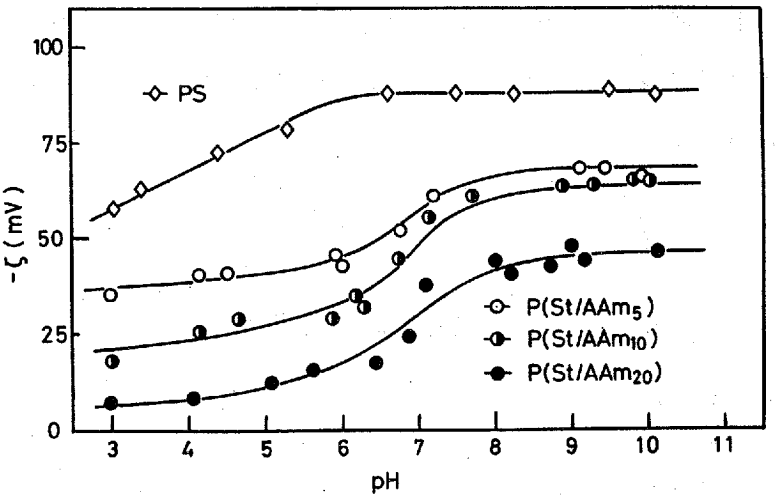

Fig. 24. ζ-potentials of PS and P(St/AAm) latices as a function of pH at 25°C and ionic strength 0·01.

First, the ζ-potentials of PS and P(St/AAm) latices were measured as a function of NaCl concentration; the Eversole-Boardman's plot for these latices is shown in Figure 25. As can be seen from this figure, this plot for each latex shows a good linearity. The values of t and ψ_δ obtained are listed in Table 8. The values of t for P(St/AAm) latices are about four times greater than that for PS latex; t increases with increasing the quantity of AAm used in the copolymerization similarly to P(St/HEMA) latices. However, when the comparable amount of the comonomer (AAm or HEMA) was used in each polymerization, t for P(St/AAm) latices are greater than those for P(St/HEMA) latices (see Table 8). Probably, this is because the chain length (in other words, the molecular weight) of PAAm layer on the latex surface was larger than that of poly-HEMA, and/or AAm was incorporated more effectively on the latex surface than HEMA. On the

other hand, the values of ϕ_δ for P(St/AAm) latices are smaller than that for PS latex. This may also lead to the lower ζ-potentials of P(St/AAm) latices.

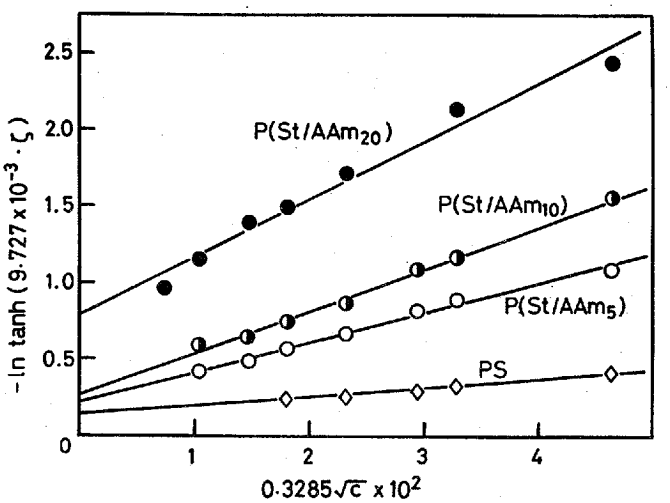

Fig. 25. Eversole-Boardman's plot for PS and P(St/AAm) latices (25°C).

3.3. Thickness of polyacrylamide (PAAm) layer

The conductometric titration and the measurement of ζ-potential for P(St/AAm) latex suggested the hydrated PAAm layer to exist on the surface of the latex particle. The thickness of this PAAm layer can be estimated from the extended-equation[37] of the Einstein's viscosity theory by measuring the specific viscosity (η_{sp}) of the latex dispersion.[20)36)] According to this viscosity theory, the dependence of η_{sp} on the volume fraction (ϕ) of the dispersed phase can be written as

$$\eta_{sp} / \phi = K_E + k' \cdot K_E^2 \cdot \phi \qquad (5)$$

where K_E is the Einstein coefficient (K_E is 2.5 for spherical particles), k' the Huggins constant. If now an (adsorbed) polymer (such as PAAm) layer is present on the latex surface, the volume fraction increases by a factor f to become $f\phi$, and eq. (5) can be written as follows.

$$\eta^*_{sp}/\phi = K_E \cdot f + k'(K_E \cdot f)^2\phi \quad (6)$$

where η^*_{sp} is the specific viscosity of the colloidal dispersion system having an (adsorbed) polymer layer. Equations (5) and (6) applied to PS and P(St/AAm) latices, respectively. A factor f was obtained from the ratio of the intercept of the straight line indicated by eq. (6) to that of the straight line indicated by eq. (5). Finally, the thickness (Δ) of PAAm layer was estimated from the following equation,

$$\Delta = a\,(f^{1/3} - 1) \quad (7)$$

where a is the particle radius of P(St/AAm) latex.

Figure 26 shows the dependence of η_{sp} on ϕ for PS and P(St/AAm) latices. As can be seen from this figure, the intercept of the straight line for P(St/AAm) latex increases (from the standard value of 2.5 for PS latex) with increasing the quantity of AAm used in the copolymerization. The thickness of PAAm layer was calculated from eq.

(7) described above, and listed in Table 9. Similarly to the previous studies,[20) 36)] the thickness of PAAm layer increases with an increase in the quantity of AAm used, i.e., in the order, $P(St/AAm_5) < P(St/AAm_{10}) < P(St/AAm_{20})$. This may indicate the surface of P(St/AAm) latex to be more hydrophilic in this order.

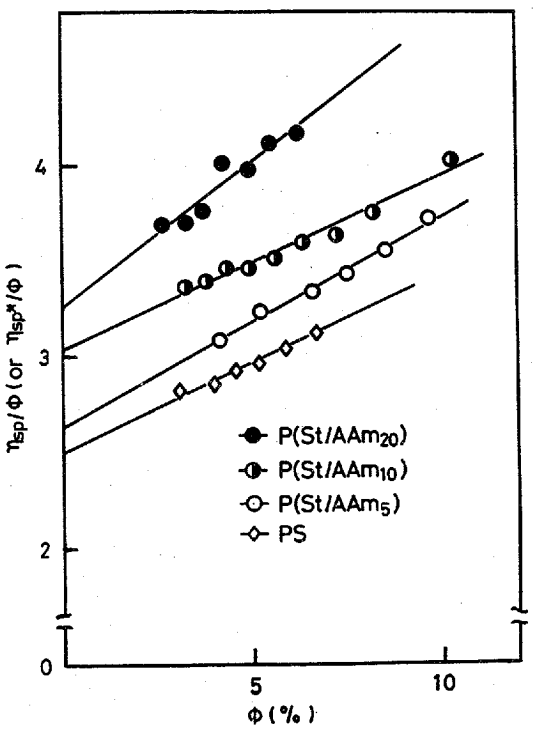

Fig. 26. Plots of η_{sp}/Φ vs. Φ for PS and P(St/AAm) latices (25°C, ionic strength 0·001).

Table 9. Thickness (Δ) of PAAm layer for P(St/AAm) latex

Latex	Δ (nm)
$P(St/AAm_5)$	3.6
$P(St/AAm_{10})$	14
$P(St/AAm_{20})$	21

3.4. Methylene Blue adsorption onto latices

Prompted by the results of titrations and ζ-potential measurements, Methylene Blue (basic dye) adsorption onto PS, P(St/AA), and P(St/HEMA) latices was investigated as a function of pH.

3.4.1. P(St/AA) latices

Figure 27 shows the pH dependence of Methylene Blue adsorption onto PS and P(St/AA) latices. The overall tendency of the adsorption is similar to the σ-pH curves (Figure 11) but not to the ζ-pH curves (Figure 16). This may be explained by the fact that ~~thses~~ these latices and Methylene Blue molecules have opposite charges and consequently, the dye molecules are adsorbed electrostatically on the surface charge groups regardless of the value of the ζ-potential. Therefore, the pH dependence of Methylene Blue adsorption onto PS latex can hardly be observed, as is the case for the σ-pH curves, and the amount of Methylene Blue adsorbed onto P(St/AA) latices increases with

increasing pH (i.e., with increasing dissociation of carboxyl groups). Furthermore, it can be seen that the amount adsorbed onto P(St/AA_5) latex is larger than that onto P(St/AA_2) latex at the same pH value.

The ratio (r) of the number of Methylene Blue molecules adsorbed (n_1) to the number of surface charged groups (n_2) was calculated as a function of pH, where n_1 and n_2 were obtained from the amount of dye adsorbed and the surface charge density of the latices, respectively. r for PS latex was found to be about 1.09, independent of pH. However, r for P(St/AA) latices decreased gradually with an increase in pH (i.e., r for P(St/AA_2) decreased from 1.74 to 0.61, and r for P(St/AA_5) decreased from 2.05 to 0.31). The ratio r is a measure of electrostatic interaction between dye and latex. For $r = 1$, each dye molecule is adsorbed on a single site of surface charge groups of latex particles. Thus, Methylene Blue adsorption onto PS latex is considered to occur mainly electrostatically. In the acidic region (where the dissociation of carboxyl groups is not very large), r for P(St/AA) latices was larger than 1. This may be attributed to hydrogen bonding of the nitrogen atoms of the dye molecules with the carboxyl groups of the latex as well as to the effect of electrostatic attraction. In the alkaline pH region, r was smaller than 1, indicating the number of dye molecules adsorbed to be smaller than that of the surface charge groups. Since the Methylene Blue molecule has a definite area for adsorption, dye molecules cannot adsorb any more even if the adsorption sites increase.

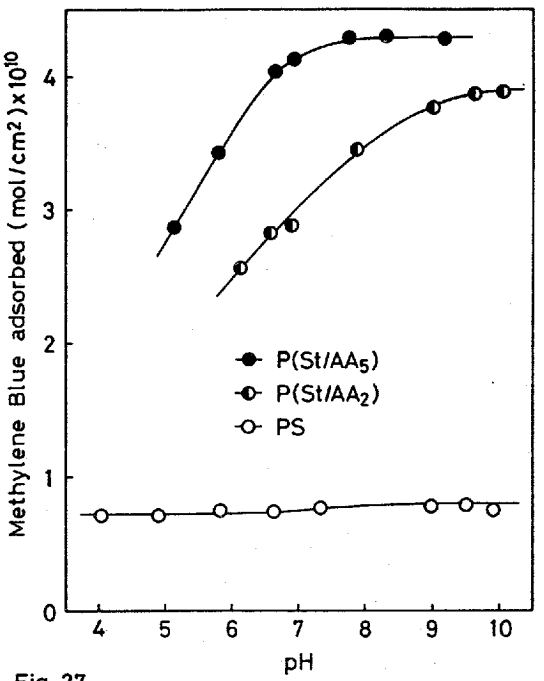

Fig. 27.
pH dependence of Methylene Blue adsorption onto PS and P(St/AA) latices (25°C, ionic strength 0.01).

3.4.2. P(St/HEMA) latices

Figure 28 shows the pH dependence of Methylene Blue adsorption onto PS and P(St/HEMA) latices. As described in the results for P(St/AA) latices, the overall tendencies in the dye adsorption onto these latices are similar to the σ-pH curves (cf. Figures 14 and 28). However, contrary to the σ-pH curves, Methylene Blue adsorption onto PS latex is somewhat greater than that onto P(St/HEMA) latex. To better understand this result, in the same manner as described previously, the ratio (r) of the number of the dye molecules adsorbed to the number of surface charged groups was calculated as a function

of pH. As a result, r for PS, P(St/HEMA$_5$), and P(St/HEMA$_{10}$) latices were about 1.09, 0.71, and 0.74, respectively regardless of pH. Judging from these values, it appears that Methylene Blue adsorption onto these latices mainly occurs electrostatically. Nevertheless, r for PS latex is larger than that for P(St/HEMA) latex. This fact may be because the hydrophobic interaction between PS latex and Methylene Blue molecule is greater than that between P(St/HEMA) latex and the dye molecule. In other words, when Methylene Blue molecules adsorb onto polymer latices, this dye must displace the hydrated layer of the latex surface. Thus, the more hydrophilic the latex surface is, the more difficult Methylene Blue adsorbs. This tendency is also observed in the adsorption of sodium dodecyl sulfate onto these latices.[38]

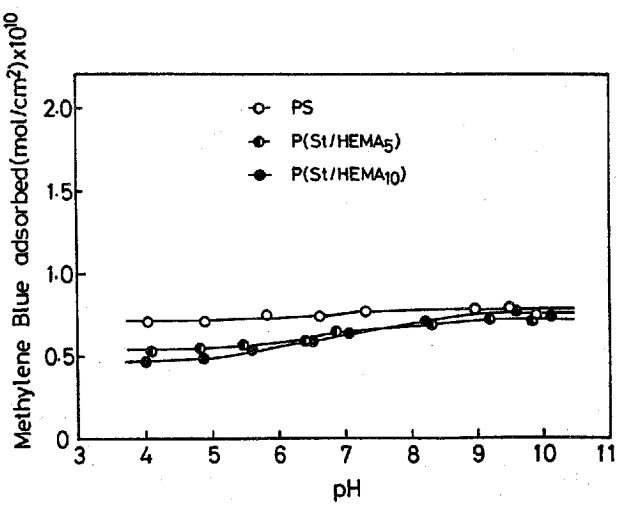

Fig. 28. pH dependence of Methylene Blue adsorption onto PS and P(St/HEMA) latices (25°C, ionic strength 0.01).

PART II

Adsorption of Bovine Serum Albumin onto Latices

CHAPRER I.

Hydrophobic Polymer Latices

In this chapter, the adsorbability of bovine serum albumin (BSA) onto hydrophobic polystyrene (PS) and polymethyl methacrylate (PMMA) latices was studied. Affected by the electrostatic interactions between BSA molecules and the latices, the initial slopes of the adsorption isotherms of BSA for these latices decreased with increasing pH. The isotherms for these latices showed steps at some concentrations of BSA. The cross-sectional area of an adsorbed BSA molecule and the thickness of the adsorbed BSA monolayer suggested that BSA molecules adsorbed onto PS latex in a " side-on " mode near the isoelectric point (iep) of this protein. With an increase of ionic strength, the amount of BSA adsorbed onto each latex increased except in the iep regin. The amount adsorbed showed a maximum near the iep of BSA (pH about 5), and the pH at maximum adsorption shifted to a more acidic pH region with increasing ionic strength. The amount of BSA adsorbed onto PS (more hydrophobic) latex was greater than that onto PMMA latex over the whole range of measured pH.

1. Introduction

As described previously, to investigate the adsorbability of plasma proteins onto solid polymer surfaces is of great importance for biological and medical applications, particularly, for the development of artificial internal organs. In recent years, a large number of investigations on the above theme have been reported.[1)-5),7)-11),16),39)-49)]

In part II, the adsorption of bovine serum albumin (BSA) onto various polymer latices was investigated basically (the advantages in the use of latices as adsorbents for proteins were described in GENERAL INTRODUCTION). First, this chapter is concerned with BSA adsorption from solution onto hydrophobic surfaces (i.e., polystyrene (PS) and polymethyl methacrylate (PMMA) latices). The variables in the experiment are pH, ionic strength, protein concentration. As a rule, the conformational alteration of proteins, especially that of BSA molecule, is very sensitive to environmental factors such as pH. Therefore, the variations in these factors may cause the great change in the adsorbability of BSA onto latices. In order to keep the system as simple as possible, buffer solutions were used in the experiments only for obtaining the adsorption isotherms.

2. Experimental

2.1. Materials

PS and PMMA latices used were the same samples as described in chapter I of part I. BSA (Sigma Chemical Co., Crystallized and Lyophilized, Cat. No. A-4378) as the protein was used without further purification. BSA (crystalline) and its stock solution were stored at 0−5 ℃. In order to facilitate the following discussion about BSA adsorption onto polymer latices, the physicochemical properties of BSA will now be reviewed briefly.

The biological function of serum albumin is concerned with the binding and transport of small molecules and ions. Serum albumin is able to bind these substances to a considerable extent nonspecifically.[22),50)] This nonspecific binding affinity of serum albumin is considered to be due to its configurational adaptability[51)] and the hydrophobic patch[52)] existing on its surface. Albumin plays an important role in maintaining an osmotic pressure and a constant pH in the blood.

BSA consists of a single polypeptide chain of 582 amino acid residues[53)] and has a molecular weight of about 67,000. The amino acid composition was already known[54)], and the sequence has recently been established by Reed et al[55)]. The molecule contains 17 disulfide (S-S) bonds, 19 tyrosine (Tyr) and 2 tryptophan (Try) residues, ca. 100 basic amino acid residues (lysine, histidine, and arginine) and ca.100

acidic amino acid residues (aspartic and glutamic acids) which cause positively- and negatively-charged groups, respectively. Normally, BSA contains 0.6−0.7 molecule of sulfhydryl group (−SH) per molecule, thus, it is assumed that two classes of albumin, i,e., mercaptalbumin (having −SH) and non-mercaptalbumin, exist in the cluster of BSA molecules. In non-mercaptalbumin, the sulfhydryl group is blocked by cysteine and/or glutathione[56].

BSA molecule is considered to be a prolate spheroid of revolution with a major axis of 140Å and a minor axis of 40Å by the results of low angle X-ray scattering[57] etc. Some physicochemical properties of BSA are summarized in Table 1[58]. These are the values measured in a neutral pH region. Since BSA molecule is subject to change in its conformation with the environment such as pH, these values in Table 1 probably change.

The isoelectric point of BSA usually lies in the pH region of 4.2−5.0 depending on the ionic strength and the kind of the medium.[59)-61)] The isoionic point, viz., the pH at which the charge would be zero if no ions other than protons were bound, is about 5.3.[62]

Analytical grade chemicals and distilled-deionized water were used in all experiments.

Table 1. Some physicochemical properties of BSA[58)]

Molecular weight (Obtained from amino acid composition)	66,267
Size (Å)	140× 40
Sedimentation constant, $s_{20,w} \times 10^{13}$(S)	4.5
Diffusion constant, $D_{20,w} \times 10^{7}$(cm^2/s)	5.9
Partial specific volume, v_{20}(ml/g)	0.733
Intrinsic viscosity, $[\eta]$ (dl/g)	0.0413
Isoelectric point, (pH units)	4.2−5.0
Isoionic point, (pH unit)	ca.5.3

2.2. Methods

2.2.1. Determination of BSA concentration

The BSA concentration was determined by the Microbiuret method.[63)] The principle of this method is that the protein forms a complex (which absorbs light in the ultraviolet region) with Cu^{2+} in a strongly alkaline solution. This method is convenient for the measurement; the complex is stable for a long time even at a high temperature. The wavelength of light used was 310nm. The calibration curve showed a good linearity within the experimental error of a few %.

2.2.2. Adsorption experiment

All adsorption experiments were carried out at 25℃. The amount of

BSA adsorbed was determined as follows: After a BSA solution was mixed with a latex dispersion, the test solution was centrifuged using a high-speed refrigerated centrifuge (Kubota KR-20000T ; 15 min at 24,000g, twice). The residual concentration of BSA in the supernatant was determined by the above method. The amount adsorbed per unit area of the latex was calculated from the difference between the initial and equilibrium concentrations. From the results of preliminary experiments, an equilibration time of 2h was chosen for the adsorption experiments. The pH and ionic strength of the sample solutions were adjusted with aqueous HCl, NaOH, and NaCl. Buffer solutions (viz., acetate and phosphate buffers) were used for obtaining the adsorption isotherms.

3. Results and Discussion

3.1. Adsorption isotherms

Figures 1 and 2 show the adsorption isotherms of BSA onto PS and PMMA latices, respectively. The measurements were carried out at pH 4.2, 5.0 (or 4.8), and 7.4 (or 6.5). These pH values correspond to the acidic pH lower than the isoelectric point(iep) of BSA, the neighborhood of the iep, and the alkaline pH higher than the iep, respectively. As can be seen from these figures, the initial parts of the isotherms, where the interaction between the protein molecule and the latex is important because the interaction between adsorbed

protein molecules are negligible, appear to be affected by electrostatic interactions between BSA molecules and the latices. That is, their slopes decrease with increasing pH.[16),45)] Apparently, the isotherms except that at pH 7.4 (or 6.5) show steps at some concentrations of BSA. These steps probably reflect a conformational rearrangement of adsorbed BSA molecules (becoming more native and ordered structures) rather than a multilayer adsorption.[8),9),16),45)] The maximum plateau values of the isotherms were obtained near the iep of BSA, i.e., at pH 5.0 (or 4.8).

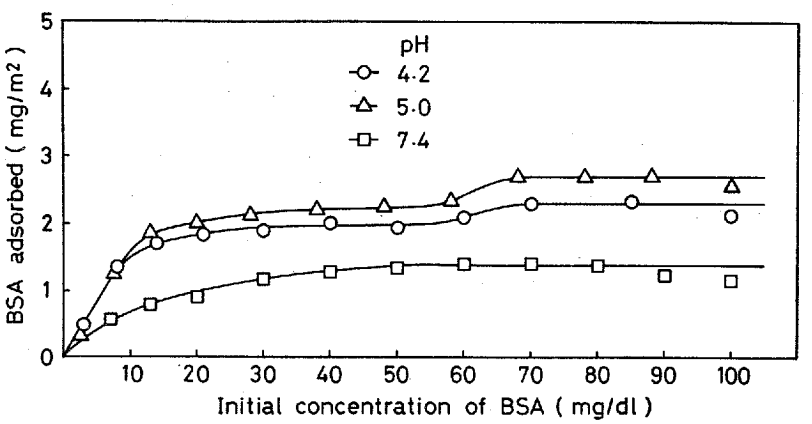

Fig. 1. Adsorption isotherms of BSA onto PS latex at 25°C and ionic strength 0.01.

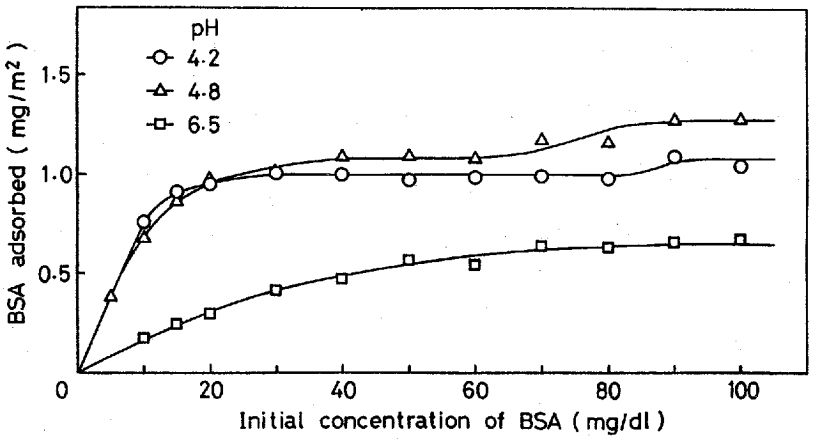

Fig. 2. Adsorption isotherms of BSA onto PMMA latex at 25°C and ionic strength 0.01.

In the iep region of BSA, because the intramolecular electrostatic repulsions are minimized, BSA molecules probably form most compact structures. Further, since the electrostatic repulsions hardly act in this pH region between the protein molecule and the latex and between the adsorbed protein molecules, BSA molecules can adsorb onto the latex in their native states. In the iep region of BSA (pH ca. 5.0), to estimate the adsorption mode of BSA onto the latex, the cross-sectional area (S) of an adsorbed BSA molecule and the thickness (δ) of the adsorbed BSA monolayer were calculated from the following equations.[64]

$$S = \frac{\pi}{2\sqrt{3}} \cdot \frac{M}{A \cdot N_A} = 0.907 \frac{M}{A \cdot N_A} \quad (1)$$

$$\delta = \frac{3\sqrt{3}}{\pi} \cdot \frac{A}{d} = 1.654 \frac{A}{d} \quad (2)$$

where $\pi/2\sqrt{3}$ and $3\sqrt{3}/\pi$ are the "packing factor", M the molecular weight of BSA (taken as 6.7×10^4), A the plateau value of the amount adsorbed at pH 5.0 (or 4.8) (converted into $g/\mathring{A}^2$), N_A the Avogadro number, d the density of BSA (which corresponds to the reciprocal of its known partial specific volume). The values (obtained by using equations (1) and (2)) of S and δ for PS and PMMA latices are given in Table 2. Incidentally, taking the BSA molecule to be a prolate spheroid of revolution with major and minor axes 2a and 2b respectively, the "side-on" cross-sectional area (S*) of the molecule is given by πab. Here, using the values listed in Table 1 (2a=140$\mathring{A}$, 2b=40$\mathring{A}$), πab yields 4400$\mathring{A}^2$. Judging from the values of S and S* (or the values of δ and the minor axis (40$\mathring{A}$) of BSA molecule), BSA molecules appear to adsorb onto PS latex in a "side-on" mode near the iep region. Fair et al.[9] studied protein adsorption onto PS latex and indicated the hydrodynamic thickness of adsorbed BSA monolayer to be about 42$\mathring{A}$. This result also shows that BSA molecule adsorbs onto PS latex in a "side-on" mode. However, the value of S (or δ) for PMMA latex is much larger (or smaller) than that expected for a "side-on" adsorption mode. This may indicate BSA molecules to adsorb onto this

latex rather sparsely than expansively.

Table 2. Values of S and δ for PS and PMMA latices

Latex	S(Å²)	δ (Å)
PS	3700	33
PMMA	7900	16
Theoretical value	4400 ($S^* = \pi ab$)	40×140 (Ellipsoidal size of BSA)

In the following experiments, the initial BSA concentration of 50mg/dl, which corresponds to the first plateau level of the isotherms, was used.

3.2. Effects of pH and ionic strength

Figures 3 and 4 show the effects of pH and ionic strength on the adsorption of BSA onto PS and PMMA latices, respectively. The amount adsorbed for each latex shows a maximum near the iep of BSA as many authors have demonstrated.[8),16),42),65)-68)] This fact is probably because BSA molecules form most compact structures near the iep region, hence, more molecules can adsorb on the given surface area.

These figures also show that the pH at maximum adsorption shifts to a more acidic pH region with increasing ionic strength. This result may correlate to the shift[61),69)] of the iep of BSA toward an acidic pH region with increasing ionic strength. Further discussion about this phenomenon is given in chapter Ⅲ.

In the region of acidic pH lower than the iep of BSA, the amount adsorbed increases with increasing ionic strength. For this result, the following explanations are possible: (i) With an increase of ionic strength, electrostatic repulsions in the interior of protein molecules decrease. This leads protein molecules to more compact structures. (ii) Moreover, lateral repulsions between adsorbed protein molecules decrease with increasing ionic strength.[45)] Thus, more molecules can adsorb on the given surface area. (iii) Electrostatic attractions between protein molecules and the substrate also decrease with increasing ionic strength. Nevertheless, the amount adsorbed increases with increasing ionic strength in this pH region. This is probably because factor(iii) affects BSA adsorption less than the above two factors ((i) and (ii)).

In the neighborhood of the iep of BSA , if the conformational alteration of BSA is not affected very much by the ionic strength, the amount adsorbed appears to remain constant regardless of the ionic strength (this almost holds true in the case of PMMA latex). However, the amount adsorbed onto PS latex in this pH region decreases with increasing ionic strength. This suggests that BSA adsorption onto PS

latex is affected by the electrostatic interaction to some extent even in this pH region. That is, the decrease in the amount adsorbed (near the iep region with an increase of ionic stength) is probably due to the decrease in the electrostatic attraction between BSA molecule and PS latex with increasing ionic strength.

In the alkaline pH region (pH > 7), the amount of BSA adsorbed onto each latex increases with increasing ionic strength similarly to the acidic pH region. At a low ionic stength (0.001), the amount adsorbed onto these latices in this pH region is scarcely discernible because of the electrostatic repulsion between BSA molecule and the latex. However, at a high ionic strength (0.1), the amount adsorbed onto PS latex in the alkaline region is almost comparable to that in the iep region. Since the electrostatic interaction between BSA molecule and the latex particle decreases relatively at a high ionic strength, the hydrophobic interaction between the adsorbate and the adsorbent appears to be a dominant factor in the adsorption. Consequently, BSA adsorption onto PS latex is little affected by pH change. Also the increase in the conformational stability of a protein molecule with increasing ionic strength[70] probably affects this result. At a high ionic strength, therefore, it seems that BSA molecules adsorb onto PS latex in a "side-on" mode even in the alkaline pH region. On the other hand, at ionic strength 0.1, the amount adsorbed onto PMMA latex increases again from pH ca. 7 and reaches a plateau level. This result may be attributed to the

hydrophobic interaction between the methyl side chain of PMMA latex and BSA molecule (more detail discussion about this is given in the next chapter).

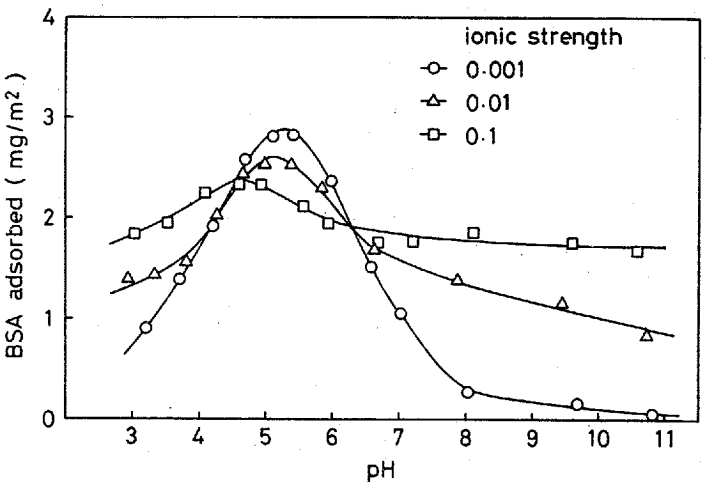

Fig. 3. pH dependence of BSA adsorption onto PS latex
(25°C , BSA initial concn. 50mg/dl)

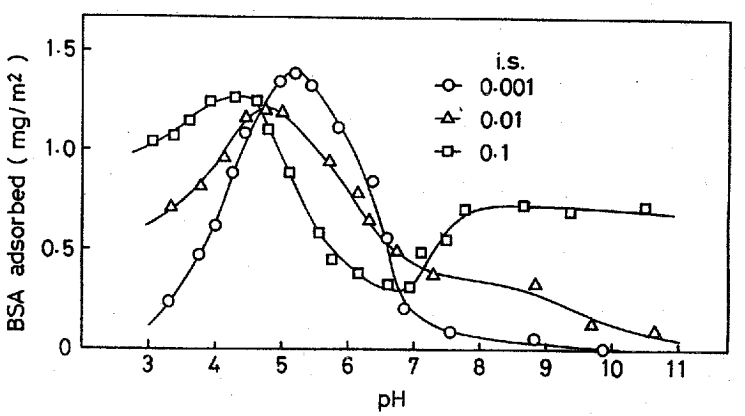

Fig. 4. BSA adsorption onto PMMA latex as a function of pH and ionic strength(i.s.), 25°C, initial BSA concn. 50mg/dl.

To compare the adsorbability of BSA onto PS latex with that onto PMMA latex, the pH dependence of the amount adsorbed onto these latices at ionic strength 0.1 is shown in Figure 5. As can be seen from this figure, the amount adsorbed onto PS latex is greater than that onto PMMA latex over the whole range of measured pH. Norde[8),16)] showed that the amount of albumin adsorbed onto PS latex increased with increasing the surface charge of the latex. Since, in this case, the surface charge density of PS latex is higher than that of PMMA latex (see chapter I in part I), the result obtained seems to be the same as that by Norde. However, using the PMMA latex having much the same surface charge as PS latex, the amount of BSA adsorbed onto PS latex was greater than that onto PMMA latex.[71)] Generally, it is often said that protein adsorption on a hydrophobic surface is greater than that on a hydrophilic one.[40),72)] Incidentally, the values of critical surface tensions for PS and PMMA are 33 and 37−39 dyn/cm, respectively.[73)] This indicates that PS is more hydrophobic than PMMA. Hence, the result obtained in this study appears to be consistent with the general tendency described above.

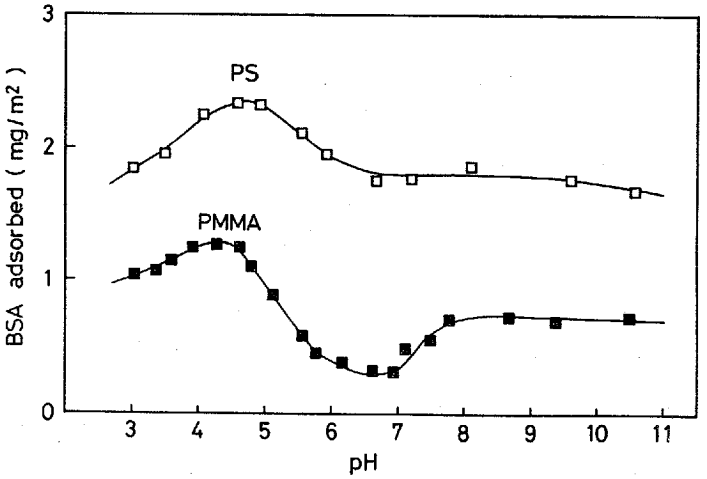

Fig. 5. pH dependence of BSA adsorption onto PS and PMMA latices at 25°C and ionic strength 0·1 (initial BSA concentration 50 mg/dl).

CHAPTER Ⅱ.

Hydrophilic Polymer Latices

Introduction

The initial rapid adsorption of plasma proteins onto polymer materials plays an important role in the thrombus formation. Therefore, it is very reasonable to investigate the adsorbability of such protein as bovine serum albumin (BSA) onto various polymer surfaces. From the above viewpoint, the adsorption behavior of BSA onto hydrophobic polymer latices was studied in chapter Ⅰ. However, using only hydrophobic latices, we may be unable to obtain much useful information about biocompatible (particularly, antithrombogenic) materials.

In recent years, hydrophilic crosslinked gels (viz., crosslinked hydrogels) have become of great interest with respect to their biocompatibility, because they have a very low interfacial free energy between their polymers and the aqueous environment.[74)-76)] This low free energy probably leads to the low interaction between the gels and the protein molecules. Therefore, the more hydrophilic the polymer surface is, the less the protein adsorption occurs. On the other hand, superhydrophobic polymer surfaces can be also expected for blood-compatible materials.[77)] However, hydrophilic polymers appear to

be more practicable surfaces for biocompatible materials, because it is almost impossible to synthesize a more hydrophobic polymer than perfluoropolymers such as polytetrafluoroethylene. Thus, it seems to be of great interest to compare the adsorbability of BSA onto hydrophilic polymer latices having different surface properties.

II－1. Carboxylated Polymer Latex

The adsorbability of bovine serum albumin (BSA) onto carboxylated polymer latices was investigated in this section. The carboxylated latices used in this work were styrene/acrylic acid (AA) copolymer (P(St/AA)), styrene/methacrylic acid (MAA) copolymer (P(St/MAA)), and styrene/methyl methacrylate (MMA)/methacrylic acid (MAA) copolymer (P(St/MMA/MAA)). The adsorption isotherms of BSA onto P(St/AA) latices showed a stepwise nature. The thickness of the adsorbed BSA monolayer suggested that BSA molecules adsorbed onto P(St/AA_2) latex (here, the subscript 2 represents the mol% of AA used in the copolymerization) in a "side-on" mode near the isoelectric point (iep) of this protein. However, in the case of P(St/AA_5) latex, a part of BSA molecules seemed to adsorb in a "loop" or an "end-on" mode. Similarly to hydrophobic latices, the amount of BSA adsorbed onto carboxylated latices increased with increasing ionic stength except in the iep region, and showed a maximum near the iep of BSA (pH ca. 5); the pH at maximum adsorption shifted to a more acidic pH region with increasing ionic strength. The amount adsorbed onto carboxylated latices except in the alkaline pH region was greater than that onto polystyrene (PS) latex. Moreover, the amount adsorbed onto P(St/AA_5) latex was greater than that onto P(St/AA_2) or P(St/MAA_5) latex throughout almost the range of measured pH (i.e., the amount adsorbed onto carboxylated latices was proportional to the quantity of surface carboxyl groups of

the latices). These results are probably due to the hydrogen bonding between BSA molecule and carboxylated latex. Further, for all carboxylated latices, the amount of BSA adsorbed increased again from pH ca. 7 at a high ionic strength; this tendency was proportional to the quantity of surface carboxyl groups of the latices. Nevertheless, probably owing to the additional hydrophobic interaction between the methyl group of MMA unit of P(St/MMA/MAA_5) latex and BSA molecule, this increase in the amount adsorbed in the alkaline pH region was most remarkable for the case of P(St/MMA/MAA_5) latex.

1. Introduction

In general, carboxylated polymer latices (having many industrial applications) are prepared by copolymerization with unsaturated acid monomers (viz., acrylic acid (AA), methacrylic acid (MAA), and itaconic acid (IA)), with the purposes of improving mechanical and freeze-thaw stabilities,[78)-80)] allowing adhesion and cross-linked reactions,[81),82)] and preparing hydrosols.[83)] On the other hand, little investigation on the biomedical use of carboxylated latices, particularly on the adsorbents for serum proteins, has been reported. As described in chapter Ⅱ of part Ⅰ, the amount of surface carboxyl groups were dependent on the kinds and quantities of acid monomers. Therefore, it is of great interest to investigate the effect of carboxyl groups (existing on the latex surface) on BSA adsorption onto various carboxylated latices.

2. Experimental

2.1. Materials

Styrene/acrylic acid (AA) copolymer (P(St/AA)), styrene/methacrylic acid (MAA) copolymer (P(St/MAA)), and styrene/methyl methacrylate (MMA)/methacrylic acid (MAA) copolymer (P(St/MMA/MAA)) latices were used. P(St/AA)) latices were the same samples as listed in Table 3 of part Ⅰ. P(St/MAA) and P(St/MMA/MAA) latices were prepared by the same method as that used in P(St/AA) latex according to the

polymerization recipe in Table 3, and purified by dialysis and electrodialysis. The particle diameters and the surface charge densities of latices were determined by electron microscopy and conductometric titration, respectively.

BSA was the same sample described in chapter I. Other reagents and water were similar to those used in chapter I.

Table 3. Preparation of P(St/MAA) and P(St/MMA/MAA) latices (N_2 atmosphere)

Conditions	$P(St/MAA_5$ [a])	$P(St/MMA/MAA_5$ [a]) [b]
Styrene(g)	71.87	48.49
MMA(g)	—	23.35
MAA(g)	3.130	3.167
KPS(g)	0.375	0.375
Water(ml)	425	425
Seed monomer(g)	3.75	15
Speed of agitation(rpm)	350	350
Seed polymerization(℃,h)	70, 1.0	65, 0.4
Successive addition of monomer (℃,h)	70, 3.0	65, 1.0
After Polymerization (℃,h)	70, 5.0	65, 8.0
Solid content [c] (g/ℓ)	148	148
Paticle diameter(nm)	578	488
Surface charge density($\mu C/cm^2$)	-54.3	-49.2

a) Subscript 5 represents the mol% of MAA used in the copolymerization.

b) The molar ratio of styrene to MMA is 2 : 1.

c) Theoretical value.

2.2. Methods

2.2.1. Determination of BSA concentration

2.2.2. Adsorption experiment

These determination and experiment were carried out at 25 ℃ by the same methods as described in chapter I.

3. Results and Discussion

3.1. Adsorption isotherms

Figure 6 shows the adsorption isotherms of BSA onto P(St/AA) latices. The measurements were carried out at pH 4.2, 5.0, and 7.4. Similarly to hydrophobic latices, the isotherms show steps; the maximum plateau values are obtained near the isoelectric point (iep) of BSA, i.e., at pH 5.0. As can be seen from the initial parts of the isotherms, BSA adsorption onto these latices occurs rapidly at pH 4.2 and 5.0, because the electrostatic repulsion hardly acts at these pH values between the latex and BSA molecule. Further, at pH 4.2 and 5.0, the plateau values of the amount adsorbed onto P(St/AA) laticas are greater than those onto hydrophobic polystyrene (PS) and polymethyl methacrylate (PMMA) latices (see Figures 1 and 2 in chapter I).

This suggests that the hydrogen bonding between BSA molecule and carboxyl group of P(St/AA) latex affects the protein adsorption more effectively than hydrophobic interaction between BSA molecule and PS (or PMMA) latex. The fact that the plateau value of the amount adsorbed onto $P(St/AA_5)$ latex is greater than that onto $P(St/AA_2)$ latex (i. e., the amount adsorbed is proportional to the quantity of acrylic acid (AA) used in the copolymerization) also supports the effect of hydrogen bonding on BSA adsorption. Moreover, Kim et al.[84] also demonstrated that the hydrogen bonding between segmented copolyether-urethane-urea (PEUU) and BSA molecule increased the amount of protein adsorbed.

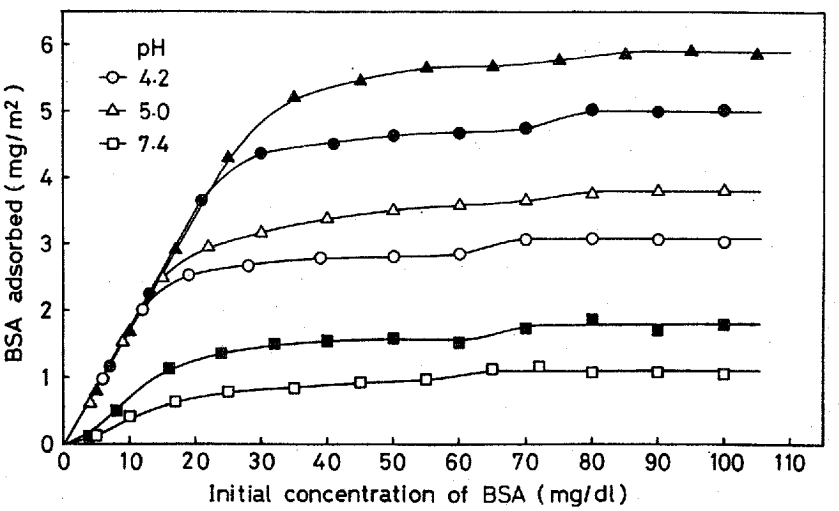

Fig.6. Adsorption isotherms of BSA onto P(St/AA) latices at 25°C and ionic strength 0.01. Open symbols, $P(St/AA_2)$; filled symbols, $P(St/AA_5)$.

In the same manner as described in chapter I, the cross-sectional area (S) of an adsorbed BSA molecule and the thickness (δ) of the adsorbed BSA monolayer were calculated using the plateau values of the amount adsorbed at pH 5.0. The obtained values of S and δ for P(St/AA) latices are given in Table 4. As can be seen from comparing the δ-value with the ellipsoidal size of BSA molecule, BSA molecules probably adsorb onto P(St/AA_2) latex in a "side-on" mode near its iep region. However, the S-value for this latex appears to be somewhat smaller than that expected for a "side-on" adsorption mode (i.e., 4400 $\mathring{A}^2$). The difference in the tedency between S- and δ-values may be attributed to the questionable values of the molecular weight (taken as 6.7×10^4) and the density (taken as 1.364) of BSA. Apart from the molecular weight, it seems to be very difficult to estimate the density of the adsorbed BSA layer (which is probably less than that of the crystalline BSA[1]). On the other hand, the δ-value for P(St/AA_5) latex is greater (or the S-value is smaller) than that expected for a "side-on" adsorption mode. This may indicate that a part of BSA molecules adsorb onto this latex in a "loop" or an "end-on" mode.

At pH 4.2, BSA molecules probably adsorb onto the latices in a flatter mode than that at pH 5.0 because of the electrostatic attraction between the latex and the protein molecule. At pH 7.4, it appears that BSA molecules adsorb onto these latices sparsely, since the electrostatic repulsions between the protein molecule and the latex and between the adsorbed protein molecules are acting at this

pH. Similarly to hydrophobic latices, the initial BSA cocentration of 50mg/dl was used in the following adsorption experiments.

Table 4. Values of S and δ for P(St/AA) latices

Latex	S(Å²)	δ (Å)
P(St/AA_2)	2700	46
P(St/AA_5)	1700	72
Theoretical value [a)]	4400 ($S^* = \pi ab$)	40× 140 (Ellipsoidal size of BSA)

a) See section 3.1. in chapter I.

3.2. Effects of pH and ionic strength

Figures 7 and 8 show the effects of pH and ionic strength on the adsorption of BSA onto P(St/AA_2) and P(St/AA_5) latices, respectively. As can be seen from these figures and Figure 3 in chapter I, the adsorbability of BSA onto P(St/AA) latices in the acidic pH region (pH < 6) shows a similar tendency to that onto PS latex. That is, the amount adsorbed shows a maximum near the iep of BSA; the pH at maximum adsorption shifts to a more acidic region with increasing ionic strength.

In the acidic region lower than a pH of about 4, the amount adsorbed onto these latices increases with increasing ionic strength similarly to the case of hydrophobic latices. The amount adsorbed in the pH region lower than the iep of BSA decreases with decreasing pH, in spite of the electostatic attraction between the protein and the latex. This decrease in the amount adsorbed is probably due to the increase in the expansion of BSA molecule with decreasing pH. That is, the greater the size of the protein molecular, the smaller the amount adsorbed on a definite area. Thus, BSA adsorption onto polymer latices depends on not only the electrostatic interaction but also the conformational alteration of the protein molecule.

In the neighborhood of the iep of BSA, the amount absorbed onto P(St/AA) latices is greater than that onto PS latex (cf. Figures 7 and 8 with Figure 3 in chapter I), and this tendency is proportional to the quantity of AA used in the copolymerization (i. e., the amount adsorbed onto $P(St/AA_5)$ latex is greater than that onto $P(St/AA_2)$ latex). As described above, this is probably attributed to the hydrogen bonding between BSA molecule and P(St/AA) latex. The amount adsorbed in this region decreases with increasing ionic strength similarly to PS latex.

In the alkaline pH region (pH > 7), the amount of BSA adsorbed onto P(St/AA) latices at low ionic strength (0.001) is hardly discernible because of the increase in the electrostatic repulsion between the protein molecule and the latex. As described in chapter II of part I,

since the surface charge density of P(St/AA) latex increases with increasing pH, the opportunity for acting the electrostatic repulsion between BSA molecule and this latex is much greater than that between BSA molecule and PS latex in the alkaline pH region of a low ionic strength. However, with an increase of ionic strength, the amount adsorbed onto P(St/AA) latices increases even in this pH region as in the case of PS latex. At a high ionic strength, the electrostatic interaction between BSA molecule and the latex decreases. As a result, the hydrogen bonding and the hydrophobic interaction probably affect BSA adsorption onto latices greatly. Similar results were obtained for other carboxylated latices (i.e., $P(St/MAA_5)$ and $P(St/MMA/MAA_5)$ latices).

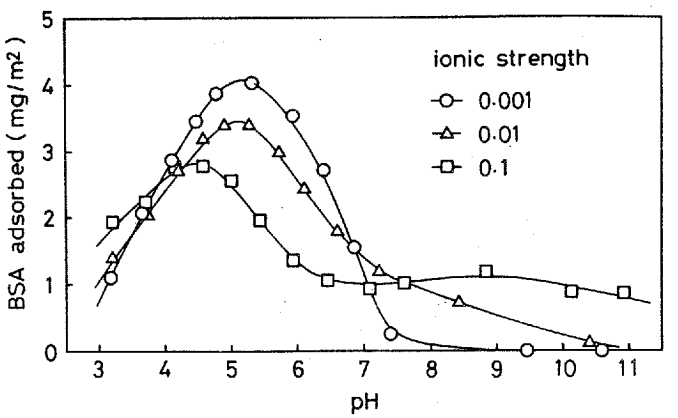

Fig. 7. pH dependence of BSA adsorption onto $P(St/AA_2)$ latex at 25°C (BSA initial concn. 50 mg/dl).

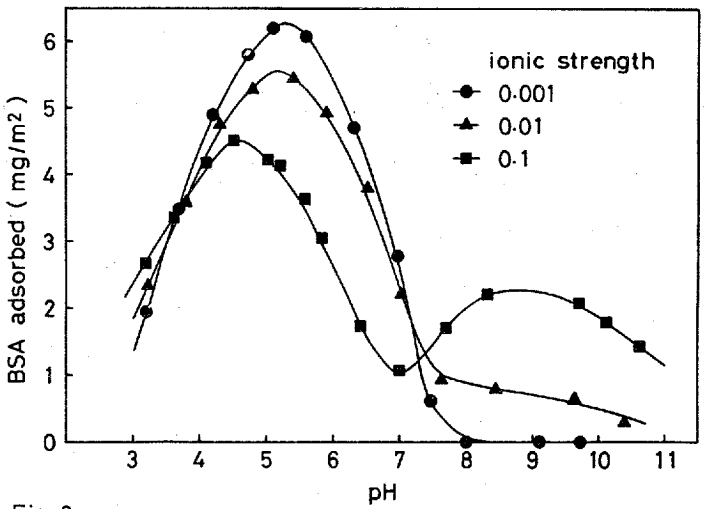

Fig. 8.
pH dependence of BSA adsorption onto P(St/AA_5) latex.
(25°C , BSA initial concn. 50mg/dl)

Figure 9 shows the pH dependence of BSA adsorption onto various carboxylated latices at ionic strength 0.1. As can be seen from this figure, the amount adsorbed onto P(St/AA_5) latex is greater than that onto P(St/AA_2) or P(St/MAA_5) latex throughout almost the pH range measured, particularly in the iep region of BSA. This is probably because the hydrogen bonding between BSA moleccule and P(St/AA_5) latex is greater than that between BSA molecule and P(St/AA_2) or P(St/MAA_5) latex, in proportion to the quantity of surface carboxyl groups of the latices (see the results of surface characterization for these latices in chapter Ⅱ of part Ⅰ). Despite the increase in the electrostatic repulsions between BSA molecules and these latices with increasing pH, the amount of the protein adsorbed onto each latex increases again

from pH ca. 7 at this high ionic strength. As observed in this figure, this phenomenon appears to be a common feature to carboxylated latices. In the alkaline pH region, a part of masked amino acid residues (such as tyrosine and tryptophan) may be exposed to the aqueous phase,[85] because the degree of unfolding of BSA molecule increases with increasing pH.[45] Hence, the interaction, mainly the hydrogen bonding between BSA molecule and the latex probably increases at a high ionic strength. This leads to the increment of BSA adsorption. Thus, in this pH region, the amount adsorbed onto carboxylated latices seems to change from a decrease to an increase. This increase in the amount adsorbed is more remarkable for P(St/AA_5) latex than that for P(St/AA_2) or P(St/MAA_5) latex, in proportion to the quantity of surface carboxyl groups of these latices. The pH region of this change in the amount adsorbed is consistent with that of "N-B transition[85)-87)] " of BSA molecule (i. e., the region of pH 7−9). Accordingly, the increment of the amount adsorbed from pH 7 may be correlated with "N-B transition " to a certain extent. However, further work is necessary to clarify this relation. This increase in the amount adsorbed in the alkaline pH region was also observed in PMMA latex (see Figure 4 in chapter I). At that time, this result might be attributed to the hydrophobic interaction between the methyl groups of PMMA latex and BSA molecule. The fact that the amount adsorbed onto P(St/MMA/MAA_5) latex in this pH region is greater than that onto P(St/MAA_5) latex also appears to reflect this effect of the

methyl groups of MMA unit in P(St/MMA/MAA_5) latex. In the region up to a neutral pH, the amount adsorbed onto P(St/MMA_5) latex is greater than that onto P(St/MMA/MAA_5) latex as the relation between PS and PMMA latices (judging from the concept of core-shell emulsion,[88] MMA is more likely to exist on the surface of P(St/MMA/MAA_5) latex than styrene).

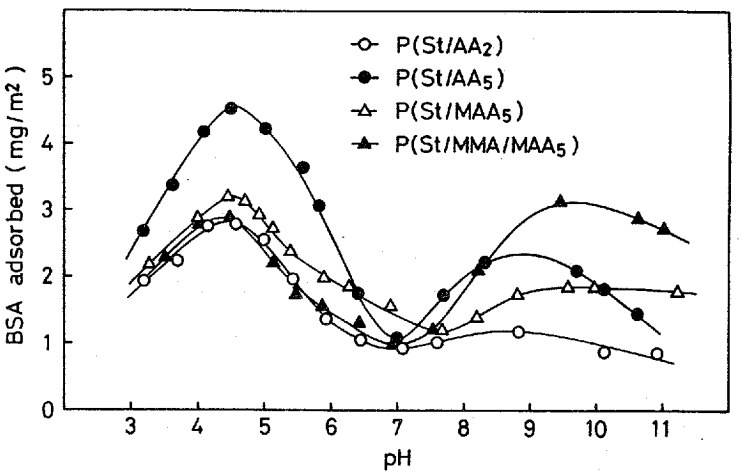

Fig. 9. pH dependence of BSA adsorption onto various carboxylated latices (25°C, ionic strength 0.1, initial BSA concentration 50 mg/dl).

II－II. Styrene/2-Hydroxyethyl Methacrylate Copolymer Latex

In this section, the adsorbability of bovine serum albumin (BSA) onto styrene/2-hydroxyethyl methacrylate (HEMA) copolymer (P(St/HEMA)) latex was investigated. Polystyrene (PS) latex was used as a reference sample. The cross-sectional area of an adsorbed protein molecule and/or the thickness of the adsorbed protein monolayer suggested that BSA molecules adsorbed onto P(St/HEMA) latex rather in a "side-on" mode than in an "end-on" mode near the isoelectric point (iep) of the protein. In the acidic pH region lower than the iep of BSA, the adsorbability of the protein onto P(St/HEMA) latex showed a similar tendency to that onto PS latex. However, in the alkaline pH region especially at a high ionic strength, BSA adsorption onto this latex was quite different from that onto PS latex. That is, the amount adsorbed onto P(St/HEMA) latex was scarcely discernible in this pH region regardless of ionic strength; this tendency was proportional to the quantity of HEMA used in the copolymerization. These results are probably because the hydrophobic interaction between BSA molecule and this latex is much smaller as compared with that between BSA molecule and PS latex. Moreover, the diffuse layer effect of poly-HEMA layer existing on the P(St/HEMA) latex, which is characteristic of the materials having hydrogel layers on their surfaces, probably affects this decrease in the amount of BSA adsorbed greatly.

1. Introduction

As described in chapter II of part I, the surface of styrene/2-hydroxyethyl methacrylate (HEMA) copolymer (P(St/HEMA)) latex is much more hydrophilic than that of polystyrene (PS) latex in spite of its having about the same surface charge density (σ) as PS latex. The surface of carboxylated polymer latex is also hydrophilic, whereas the σ of this latex increased with increasing pH. Therefore, using P(St/HEMA) latex, it is possible to discuss the adsorbability of bovine serum albumin (BSA) without considering the effect of σ-values of polymer latices. Poly-HEMA is a typical hydrogel and widely used as a material for soft contact lenses. In recent years, HEMA-copolymerized materials can be expected for medical diagnostics[14] and antithrombogenic biomaterials.[89),90)] In this section, from the above viewpoint, BSA adsorption onto P(St/HEMA) latex was investigated as a function of pH, ionic strength, etc. PS latex was used as a reference sample.

2. Experimental

2.1. Materials

P(St/HEMA) and PS latices used in this section were the same samples as listed in Table 4 of part I.

BSA, other reagents, and water were similar to those used in chapter I.

2.2. Methods

2.2.1 Determination of BSA concentration

2.2.2 Adsorption experiment

These determination and experiment were carried out at 25 ℃ by the same methods as described in chapter Ⅰ.

3. Results and Discussion

3.1 Adsorption isotherms

For example, Figure 10 shows the adsorption isotherms of BSA onto P(St/$HEMA_5$) latex (here, the subscript 5 represents the mol% of HEMA used in the copolymerization). Similarly to hydrophobic and carboxylated latices, at pH 4.2 and 5.1, the isotherms show steps at some concentrations of BSA; the maximum plateau value of the isotherms is obtained near the isoelectric point (iep) of BSA, i. e., at pH 5.1. However, at pH 7.5, the amount adsorbed onto P(St/$HEMA_5$) latex is scarcely observed regardless of BSA concentration. This tendency is more remarkable for P(St/$HEMA_{10}$) latex (the data are not shown), and will be discussed in the following section.

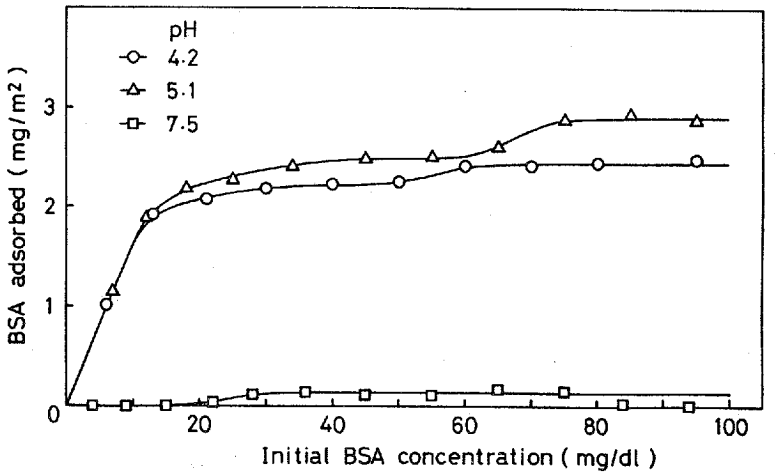

Fig.10. Adsorption isotherms of BSA onto P(St/HEMA$_5$) latex (25°C, ionic strength 0.01).

In the same manner as described in chapter I, the cross-sectional area (S) of an adsorbed BSA molecule and the thickness (δ) of the adsorbed BSA monolayer were calculated using the plateau values of the amount adsorbed onto each latex at pH 5.1. The obtained values of S and δ are given in Table 5. Judging from these values listed in Table 5, BSA molecules appear to adsorb onto P(St/HEMA) latices in a "side-on" mode rather than in an "end-on" mode near the iep region of the protein. The initial BSA concentration of 50mg/dl was used in the following adsorption experiments.

Table 5. Values of S snd δ for P(St/HEMA) latices

Latex	S(Å²)	δ (Å)
P(St/HEMA$_5$)	3500	35
P(St/HEMA$_{10}$)	4800	25
Theoretical value [a)]	4400 ($S^* = \pi ab$)	40×140 (Ellipsoidal size of BSA)

a) See section 3.1 in chapter I.

3.2. Effects of pH and ionic strength

Figure 11 shows the effects of pH and ionic strength on BSA adsorption onto P(St/HEMA$_5$) latex. In the acidic pH region lower than the iep of the protein, the adsorbability of BSA onto this latex shows a similar tendency to that onto polystyrene (PS) latex (see Figure 3 in chapter I). That is, the amount adsorbed shows a maximum near the iep (pH ca. 5) of BSA; with increasing ionic strength, the pH at maximum adsorption shifts to a more acidic region and the amount adsorbed increases except in the iep region. On the other hand, in the alkaline pH region, the adsorbability of BSA onto P(St/HEMA$_5$) latex is quite different from that onto PS latex, i. e., the amount adsorbed onto P(St/HEMA$_5$) latex in this pH region is scarcely discernible

regardless of ionic strength. Similar results are obtained for $P(St/HEMA_{10})$ latex. Thus, when the electrostatic repulsion between BSA molecule and the latex is acting, the protein molecules appear to be hard to adsorb onto P(St/HEMA) latex.

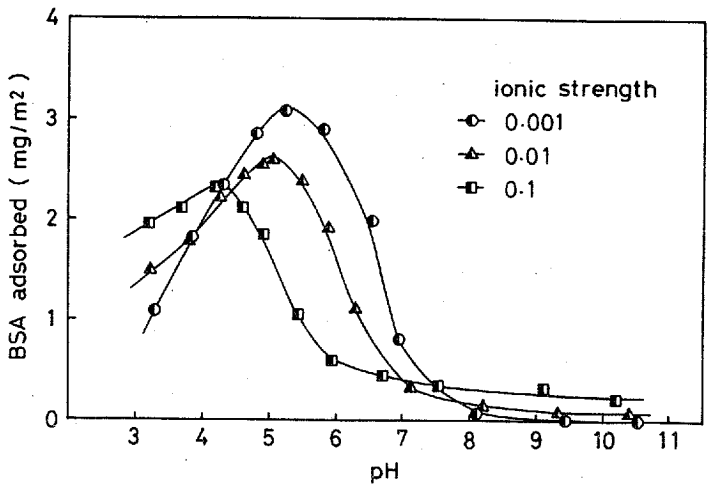

Fig.11. pH dependence of BSA adsorption onto $P(St/HEMA_5)$ latex (25°C , BSA initial concn. 50mg/dl).

As described previously, the surface of P(St/HEMA) latex is more hydrophilic than that of PS latex despite its having much the same surface charge as PS latex. Therefore, it is of great interest to compare the adsorbability of BSA onto P(St/HEMA) latices with that onto PS latex.

Figure 12 shows the pH dependence of BSA adsorption onto PS and P(St/HEMA) latices at a lower ionic strength (0.001). The adsorbability of BSA onto these latices shows almost the same tendency

over the whole range of measured pH. At a low ionic strength, except in the neighborhood of the iep of BSA, it seems that the main interaction between adsorbate and adsorbent concerned with BSA adsorption is electrostatic interaction. Namely, electrostatic attraction force (pH < 5) and repulsion one (pH > 5) may act on the adsorbability of BSA onto these latices almost equally regardless of the magnitude of ζ-potentials of latices. Hence, the influence of hydrophilic and hydrophobic properties of latex surfaces on BSA adsorption would be hardly discernible.

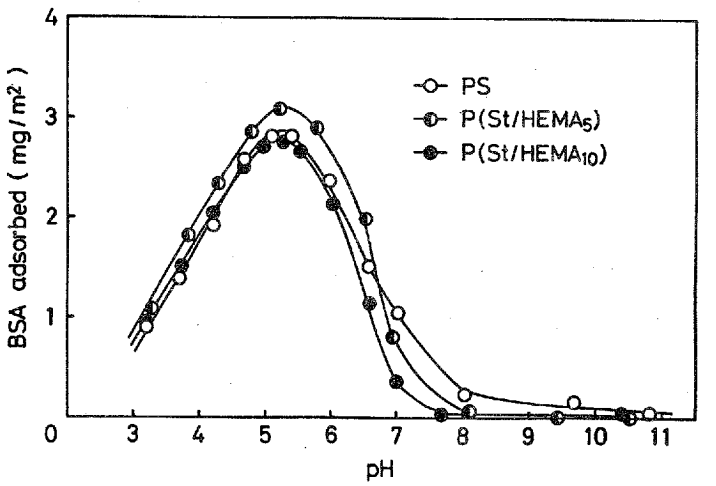

Fig.12. pH dependence of BSA adsorption onto PS and P(St/HEMA) latices (25°C, i.s. 0.001, BSA initial concn. 50mg/dl)

The results at a higher ionic strength (0.1) are shown in Fig. 13. It can be seen that the difference in BSA adsorption between PS and P(St/HEMA) latices is very great. Especially in the alkaline pH region,

the amount adsorbed onto P(St/HEMA) latex is much smaller than that onto PS latex. Moreover, this tendency is proportional to the quantity of copolymerized-HEMA. At a high ionic strength, it appears that factors such as hydrophobic interaction and hydrogen bonding in addition to electrostatic interaction significantly affect BSA adsorption. In the case of PS latex, it is probably hydrophobic interaction which is the predominant driving force to BSA adsorption. However, in the case of P(St/HEMA) latex, a hydrous poly-HEMA layer possibly exists on its surface as mentioned before, and that will lead to the decrease in the (hydrophobic) interaction between this latex and BSA molecules. Therefore, the amount adsorbed onto P(St/HEMA) latices in the alkaline pH region would greatly decrease compared with PS latex. In other words, when an electrostatic repulsion force is acting, there appears to be little interaction between P(St/HEMA) latex and BSA molecules. On the other hand, the amount adsorbed onto carboxylated latex in this pH region was comparable to that onto PS latex at a high ionic strength because of hydrogen bonding (see section Ⅱ－Ⅰ). In the acidic pH region, there is little difference in the adsorbability of BSA onto these latices, because an electrostatic attraction force between the latex and BSA molecules is acting. This similarity in the adsorbability may indicate that poly-HEMA covers the latex surface not wholly but partially.

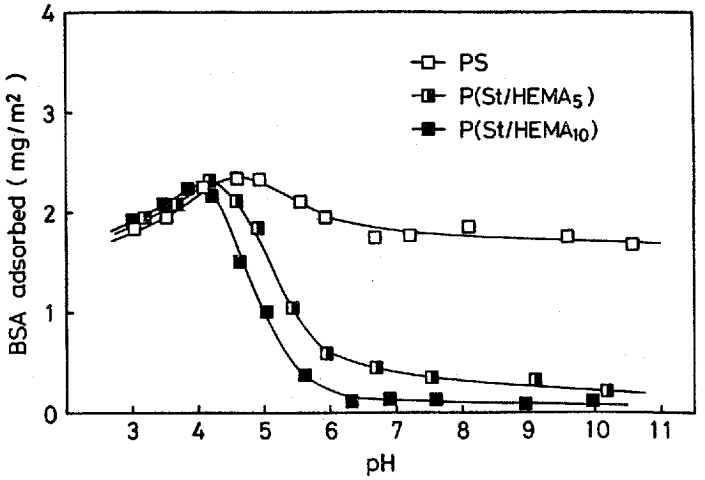

Fig.13. pH dependence of BSA adsorption onto PS and P(St/HEMA) latices (25°C, i.s.0.1, BSA initial concn. 50 mg/dl).

In conclusion, the amount adsorbed onto P(St/HEMA) latices in the alkaline pH region is hardly discernible regardless of ionic strength. This finding is also observed in the adsorption of plasma proteins onto hydrated polymer surfaces such as polyvinyl alcohol[91], hydrogels having polyoxyethylene as a side chain[92]. The decrease in the amount adsorbed onto these polymer surfaces could be explained by the volume restriction effect[92] or the diffuse layer effect.[91] Also in P(St/HEMA) latices, the amount of BSA adsorbed appears to be decreased by the above effect in addition to the decrease of hydrophobic interaction.

Hydrogels such as poly-HEMA are expected as biocompatible materials. That is because their surface structures resemble those of living

cells, i. e., there exists a large amount of water (which is in a quasi-organized state[6]) in the gels or cells. This similarity probably makes the interaction between hydrogels and living cells (or blood components) very small. The surface of P(St/HEMA) latex also appears to resemble those of hydrogels and living cells. Thus, BSA adsorption onto this latex would be hardly discernible at least in the alkaline pH region.

II－III. Styrene/ Acrylamide Copolymer Latex

This section was concerned with the adsorbability of bovine serum albumin (BSA) onto styrene/ acrylamide (AAm) copolymer (P(St/AAm)) latex. Polystyrene (PS) latex was used as a reference sample. The plateau values of the adsorption isotherms for the latices except that for $P(St/AAm_{20})$ latex (here, the subscript 20 represents the wt% of AAm used in the copolymerization) showed that BSA molecules adsorbed onto P(St/AAm) latex in a "side-on" mode near the isoelectric point (iep) of this protein. Similarly to other polymer latices, the amount adsorbed onto P(St/AAm) latex showed a maximum near the iep of BSA; the pH at maximum adsorption shifted to a more acidic region with increasing ionic strength. Moreover, BSA adsorption onto this latex, particularly at a high ionic strength, decreased with increasing the quantity of AAm used in the copolymerization, i. e., the amount adsorbed decreased in the order, PS > $P(St/AAm_5)$> $P(St/AAm_{10})$> $P(St/AAm_{20})$, throughout the entire range of measured pH. Similar results were obtained for P(St/HEMA) latex mainly in the alkaline pH region (see Figure 13). Therefore, the diffuse layer effect of P(St/AAm) latex appears to be greater than that of P(St/HEMA) latex. By comparison of BSA adsorption onto every latex, it was found that fewer BSA molecules adsorbed onto P(St/AAm) latex even in the acidic pH region lower than the iep of this protein.

1. Introduction

As described in the section of the surface characterization for polymer latices, the hydrated polymer layer existing on styrene/ acrylamide (AAm) copolymer (P(St/AAm)) latex is probably thicker than that existing on styrene/ 2-hydroxyethyl methacrylate (HEMA) copolymer (P(St/HEMA)) latex. Therefore, the tendency observed in the adsorbability of bovine serum albumin (BSA) onto P(St/HEMA) latex appears to become more remarkable for that onto P(St/AAm) latex. In this section, to investigate the effect of the hydrated polymer layer (existing on the latex surface) on BSA adsorption in more detail, three P(St/AAm) latices having different quantities of copolymerized-AAm were used. Hydrophobic polystyrene (PS) latex was used as a reference sample. And finally, the adsorbability of BSA onto P(St/AAm) latex was compared with that onto other hydrophilic latices (viz., styrene/acrylic acid copolymer (P(St/AA)) and P(St/HEMA)).

2. Experimental

2.1. Materials

P(St/AAm) and PS latices used in this study were the same samples as listed in Table 5 of part Ⅰ.

BSA, other reagents, and water were similar to those used in chapter Ⅰ.

2.2. Methods

2.2.1. Determination of BSA concentration

2.2.2. Adsorption experiment

These determination and experiment were carried out at 25 ℃ by the same methods as described in chapter Ⅰ.

3. Results and Discussion

3.1. Adsorption isotherms

The adsorption isotherms of BSA onto PS and P(St/AAm) latices at pH 5.1 (viz., near the isoelectric point (iep) of the protein) are shown in Figure 14. The isotherms for P(St/AAm) latices were obtained also at other pH-values (i. e., at a lower and a higher pH-values than the

iep of BSA); those tendencies were similar to those for P(St/HEMA) latex rather than those for PS latex. As can be seen from Figure 14, the adsorption isotherms for all latices are pseudo-Langmuir types and show steps at ca. 60 mg/dl of BSA concentration, similarly to hydrophobic and other hydrophilic latices. The plateau value of the amount adsorbed shows a maximum for PS latex, and decreases in the order, PS > P(St/AAm$_5$) > P(St/AAm$_{10}$) > P(St/AAm$_{20}$) (here, the subscripts 5, 10, and 20 represent the wt % of AAm used in the copolymerization). This result will be discussed in the following section.

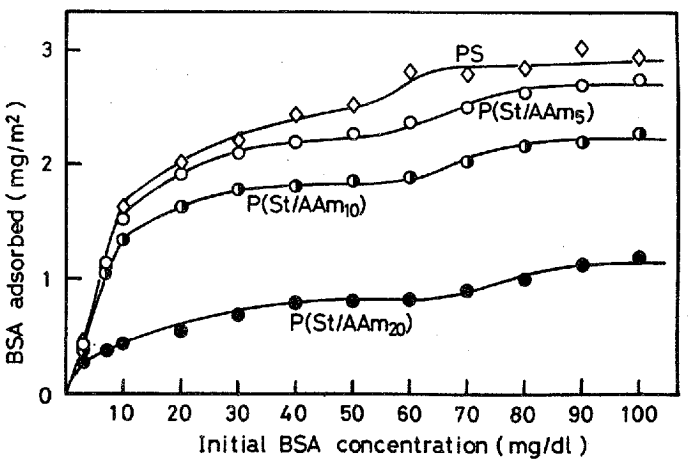

Fig. 14. Adsorption isotherms of BSA onto PS and P(St/AAm) latices (25°C, pH 5.1, ionic strength 0.01).

In the same manner as described in chapter I, the cross-sectional area (S) of an adsorbed protein molecule and the thickness (δ) of the

adsorbed protein monolayer were calculated using the plateau values of the amount adsorbed onto PS and P(St/AAm) latices at pH 5.1. The obtained values of S and δ are given in Table 6. Judging from these values in Table 6, BSA molecules seem to adsorb onto PS, P(St/AAm_5) and P(St/AAm_{10}) latices in a "side-on" mode rather than in an "end-on" mode near the iep region of this protein. However, the values of S and δ for P(St/AAm_{20}) latex are very far from those expected for a "side-on" adsorption mode. This probably indicates that BSA molecules adsorb onto P(St/AAm_{20}) latex sparsely not expansively. Similarly to other polymer latices, the initial BSA concentration of 50 mg/dl was used in the following adsorption experiments.

Table 6. Values of S and δ for PS and P(St/AAm) latices

Latex	S($\AA^2$)	δ ($\AA$)
PS	3500	35
P(St/AAm_5)	3700	33
P(St/AAm_{10})	4600	27
P(St/AAm_{20})	9200	13
Theoretical value [a)]	4400 ($S^* = \pi ab$)	40×140 (Ellipsoidal size of BSA)

a) See section 3.1. in chapter I.

3.2. Effects of pH and ionic strength

Figure 15 shows the pH dependence of BSA adsorption onto PS and P(St/AAm) latices at a lower ionic strength(0.001). At a low ionic strength, a predominant driving force to BSA adsorption except in the iep region appears to be the electrostatic interaction between the protein molecule and the latex. Therefore, similar results of BSA adsorption are obtained for these latices except $P(St/AAm_{20})$ latex. In particular, the adsorbability of BSA onto $P(St/AAm_5)$ latex shows almost the same tendency as that onto PS latex. This may indicate that polyacrylamide (PAAm) layer does not cover the surface of $P(St/AAm_5)$ latex wholly. In contrast to other P(St/AAm) latices, the amount adsorbed onto $P(St/AAm_{20})$ latex is considerably smaller than that onto PS latex over the whole range of measured pH. However, the maximum adsorption onto each latex is obtained near the iep (pH ca.5) of BSA.

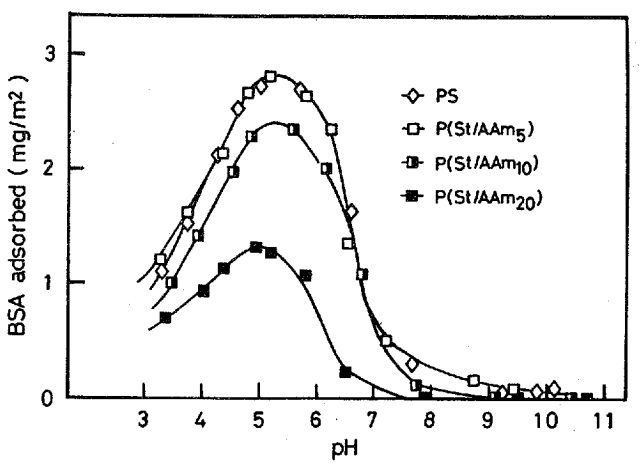

Fig.15. pH dependence of BSA adsorption onto PS and P(St/AAm) latices (25°C, ionic strength 0.001, initial BSA concentration 50 mg/dl).

Figure 16 shows the pH dependence of BSA adsorption onto PS and P(St/AAm) latices at a high ionic strength (0.1). At a high ionic strength, since the electrostatic interaction decreases relatively, such factors as the hydrophobic interaction and the van der Waals attraction between the protein molecule and the latex probably become a dominant driving force to BSA adsorption. It can be seen from Figure 16 that the pH at maximum adsorption onto P(St/AAm) latices shifts to a more acidic region as compared with that at a low ionic strength similarly to PS latex (cf. Figures 15 and 16). The amount adsorbed onto P(St/AAm) latices is considerably smaller than that onto PS latex particularly in the alkaline pH region; this tendency is proportional to the quantity of AAm used in the copolymerization. This is probably because the hydrated PAAm layer existing on the latex surface leads to the decrease in the hydrophobic interaction between BSA molecule and the latex with increasing the quantity of AAm copolymerized. This phenomenon was also observed in the case of P(St/HEMA) latex, however, in the acidic pH region lower than the iep of BSA, the amount adsorbed onto this latex was almost the same as that onto PS latex (see Figure 13 in section II- II). On the other hand, even in the acidic pH region, BSA adsorption onto P(St/AAm) latex (especially onto $P(St/AAm_{10})$ and $P(St/AAm_{20})$ latices) is smaller than that onto PS latex. This is probably because the volume restriction effect[92] (or the diffuse layer effect[91]) of PAAm layer on BSA adsorption is greater than that of poly-HEMA layer.

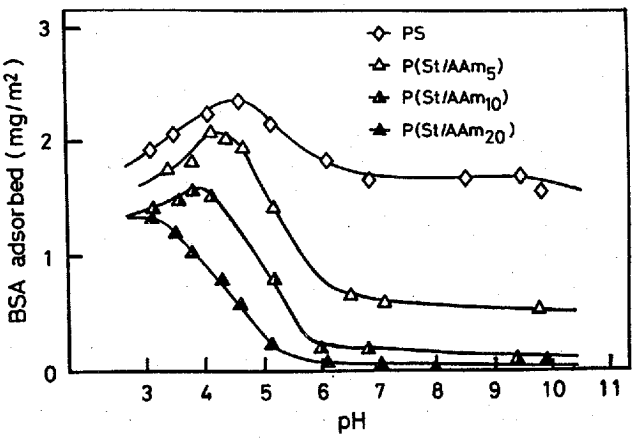

Fig.16. pH dependence of BSA adsorption onto PS and P(St/AAm) latices (25°C, ionic strength 0.1, initial BSA concentration 50 mg/dl).

3.3. Effects of surface characteristics of latices

As described so far, it has become clear that the adsorbability of BSA onto polymer latices depends on not only the surroundings of the system such as pH but also the surface characteristics of latices. Hence, the effects of surface characteristics of latices on BSA adsorption are discussed here at a high ionic strength. At a low ionic strength, as mentioned before, a predominant driving force to BSA adsorption is the electrostatic interaction between the protein molecule and the latex. Therefore, it seems that the surface characteristics of polymer latices have little effect on BSA adsorption at a low ionic strength.

Figure 17 shows the pH dependence of BSA adsorption onto various polymer latices at ionic strength 0.1. As can be seen from this figure, the amount of BSA adsorbed onto PS latex is little affected by pH change. This is probably because the hydrophobic interaction between the protein molecule and PS latex acts over a wide pH range. On the other hand, BSA adsorption onto hydrophilic polymer (P(St/HEMA) and P(St/AAm)) latices is considerably smaller than that onto PS latex particularly in the alkaline pH region, probably because the hydrophobic interaction between these latices and the protein molecule decreases greatly as compared with that between PS latex and the protein molecule. The amount adsorbed onto $P(St/AAm_{10})$ latex is rather smaller than that onto PS latex even in the acidic pH region lower than the iep of BSA. As mentioned before, probably the hydrogel (poly-HEMA or PAAm) layer existing on the latex surface also affects greatly this decrease in the amount adsorbed. However, the amount of BSA adsorbed onto $P(St/AA_5)$ latex especially in the iep region of the protein is much greater than those onto other hydrophilic latices. As described previously, this is probably due to the hydrogen bonding between BSA molecule and carboxyl groups of $P(St/AA_5)$ latex.

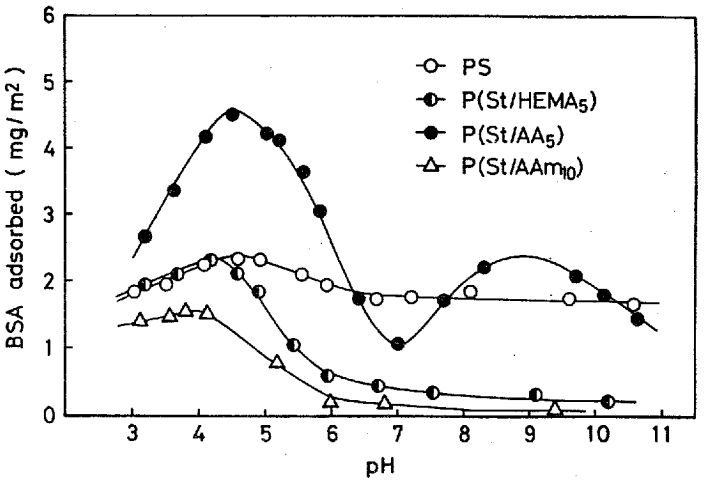

Fig. 17. pH dependence of BSA adsorption onto various latices (25°C, ionic strength 0.1, BSA initial concn. 50 mg/dl).

CHAPTER Ⅲ

Effects of Coexistent Electrolyte Anions

The effects of coexistent electrolyte anions on the adsorption of bovine serum albumin (BSA) onto polystyrene (PS) latex were investigated. Three electrolyte anions (viz., Cl^- , CH_3COO^- ,and SCN^-) were used as the sodium salt. The adsorbability of BSA onto PS latex in both Cl^- and CH_3COO^- media showed a similar tendency. However, BSA adsorption onto PS latex in SCN^- medium especially at a high ionic strength was very different from that in other anions (Cl^- and CH_3COO^-) media. That is to say, in SCN^- medium, the pH at maximum adsorption shifted to a more acidic pH region and the maximum adsorption was greater as compared with those in other anions media. These results were interpreted on the basis of the difference in the binding affinity of those small anions to BSA molecule.

1. Introduction

It is generally known that numerous organic and inorganic ions are nonspecifically bound to serum albumin. Recently, by taking advantage of this binding affinity, serum albumin has been applied to drug delivery systems as a carrier.[93]

Bovine serum albumin (BSA) molecule is sensitive to the surrounding medium. For example, this molecule alters easily its conformation by changes in pH. Moreover, the isoelectric point of BSA shifts when the kinds and concentrations of coexistent electrolyte ions change.[59),61)] In particular for the 1-1 electrolyte, it has been shown that the binding of the anions to BSA molecule completely dominates cation binding,[21)] and also there is a difference in binding affinity between those anions.[22)]

From the above view point, in this chapter, the effects of coexistent electrolyte anions on BSA adsorption onto polystyrene (PS) latex were investigated. Three electrolyte anions (CH_3COO^-, Cl^-, SCN^-) were used. All these anions were used as the sodium salt in order to avoid the effects of cations on BSA adsorption.

2. Experimental

2.1. Materials

As described before, PS latex was prepared by the usual heterogeneous polymerization without emulsifier according to the recipe of Table 7, and purified by dialysis and ion-exchange treatment. The particle diameter of the latex was measured by electron microscopy; its micrograph revealed the latex to be highly monodisperse. The surface charge density of the latex was determined by conductometric titration.

Table 7. Preparation of PS latex

Styrene (mol/ℓ)	0.871
KPS (mol/ℓ)	1×10^{-3}
Speed of agitation (rpm)	350
Polymerization temp. (℃)	70
Polymerization time (h)	24
Solid content [a] (g/ℓ)	91
Particle diameter (nm)	532
Specific surface area (m^2/g)	10.64
Surface charge density ($\mu C/cm^2$)	-2.47

a) Theoretical value

BSA was the same sample as described in chapter Ⅰ. Three electrolytes (CH_3COONa, NaCl, NaSCN) and other reagents were of analytical grade. Distilled-deionized water was used in all experiments.

2.2. Methods

2.2.1. Determination of BSA concentration

This determination was carried out by the same method as described in chapter Ⅰ. The calibration curve of BSA was not affected by the electrolytes (up to at least 0.1 mol/ℓ).

2.2.2. Adsorptoin experiment

The adsorption experiments were carried out at 25℃ by the same method as described in chapter Ⅰ.

2.2.3. Measurement of electrophoretic mobility

The electrophoretic mobilities of bare and BSA-covered latex particles were measured at 25℃ as a function of pH and ionic strength by microelectrophoresis method. The pH and ionic strength of the sample solutions were adjusted with aqueous HCl, NaOH, and electrolytes.

3. Results and Discussion

3.1. Electrophoretic mobilities of bare PS particles

Figure 18 shows the electrophoretic mobilities of PS latex particles as a function of pH and ionic strength. It can be seen from this figure that PS latex has a negative charge derived from decomposed initiator fragments throughout the entire range of measured pH. Further, the mobility values at ionic strength 0.1 are smaller than those at ionic strength 0.01. This result is probably attributed to the compression of the electrical double layer with increasing ionic strength.

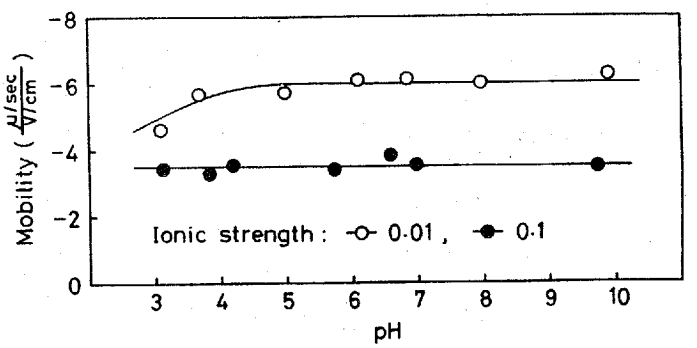

Fig. 18. Electrophoretic mobilities of PS latex particles as a function of pH at 25°C.

3.2. Effects of electrolyte anions on BSA adsorption

The effects of three electrolyte anions (Cl^-, CH_3COO^-, SCN^-)

on BSA adsorption are shown in Figures 19–21. An initial BSA concentration of 50 mg/dl, which corresponds to the plateau region of the adsorption isotherm, was the same one as in the previous studies.

Figures 19 and 20 show the effects of chloride (Cl^-) and acetate (CH_3COO^-) ions on BSA adsorption onto PS latex, respectively, as a function of pH and ionic strength. By comparison of these two figures, it can be seen that the adsorbability of BSA onto PS latex in these two anion media shows almost the same tendency. That is, as described before, the amount adsorbed increases with an increase of ionic strength except in the region of the isoelectric point (iep) of BSA (pH about 5). The amount adsorbed shows a maximum near the iep of BSA, and the pH at maximum adsorption shifts to a more acidic pH region with increasing ionic strength. Probably this pH shift correlates to the shift of the iep of BSA. The binding of these small anions (such as Cl^-, CH_3COO^-) to BSA molecule dominates cation binding.[21] This will lead to the shift of the iep of BSA to a more acidic region with increasing ionic strength. This phenomenon will be discussed in the following section. At a high ionic strength, as described in chapter I, since the hydrophobic interaction between BSA molecule and PS latex may be a predominant driving force to adsorption, BSA adsorption is not affected very much by pH change.

In the iep region of BSA, the amount adsorbed in acetate medium is little affected by the ionic strength, although that in chloride one decreases with increasing ionic strength (cf. Figures 19 and 20). The

binding of Cl^- to BSA molecule in this pH region is somewhat greater than that of CH_3COO^-. [94] Consequently, the number of positive sites in BSA molecules decreases more in chloride medium than in acetate one with an increase of ionic strength. This leads to the decrease in the electrostatic attraction between BSA molecule and PS latex. Thus, in chloride medium, the amount adsorbed in the iep region possibly decreases with increasing ionic strength. This result suggests that BSA adsorption even in the iep region is affected to some extent by the electrostatic attraction.

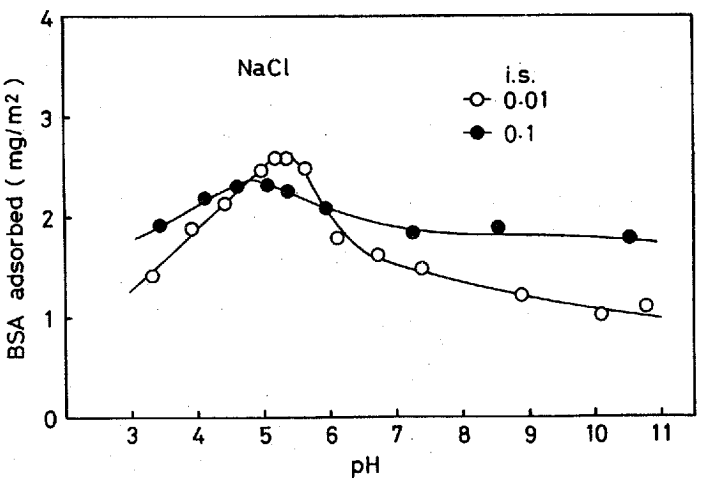

Fig.19. BSA adsorption onto PS latex as a function of pH and ionic strength (i.s.) in NaCl solution. 25°C, initial BSA concentration 50 mg/dl.

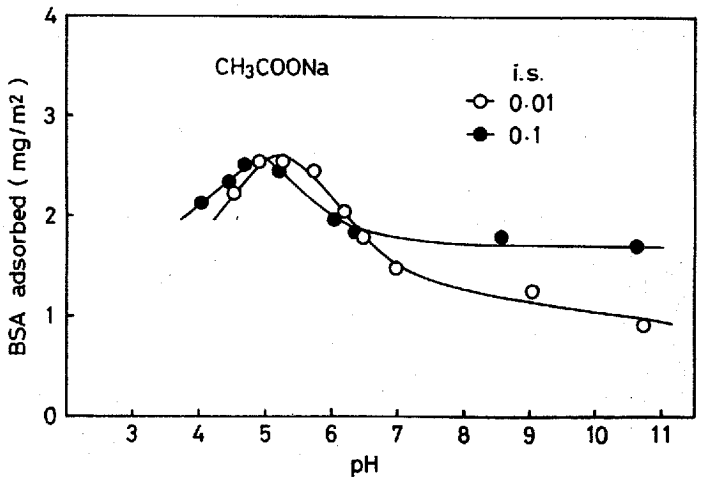

Fig.20. BSA adsorption onto PS latex as a function of pH and ionic strength (i.s.) in CH_3COONa solution. 25°C, initial BSA concentration 50 mg/dl.

Figure 21 shows the effect of thiocyanate ion (SCN^-) on BSA adsorption onto PS latex. The adsorbability of BSA at a higher ionic strength (0.1) is very different from that in other anions (viz., Cl^- and CH_3COO^-) media, although that at a lower ionic strength (0.01) shows almost the same tendency in every anion medium. As reported in many investigations[22),50),95),96)], the binding affinity of SCN^- to BSA molecule is much greater than that of Cl^-, especially in the iep and acidic pH regions. Consequently, the iep of BSA in SCN^- medium shifts to a more acidic pH region than that in Cl^- one[59),61)], and more compact structures of BSA molecules form in SCN^- medium[60)] because of the decrease in the electrostatic repulsions of intramolecules. Therefore, in SCN^- medium at ionic strength 0.1, the

maximum adsorption and its pH shift to an acidic region are much greater than those in other anion media (see Figure 22).

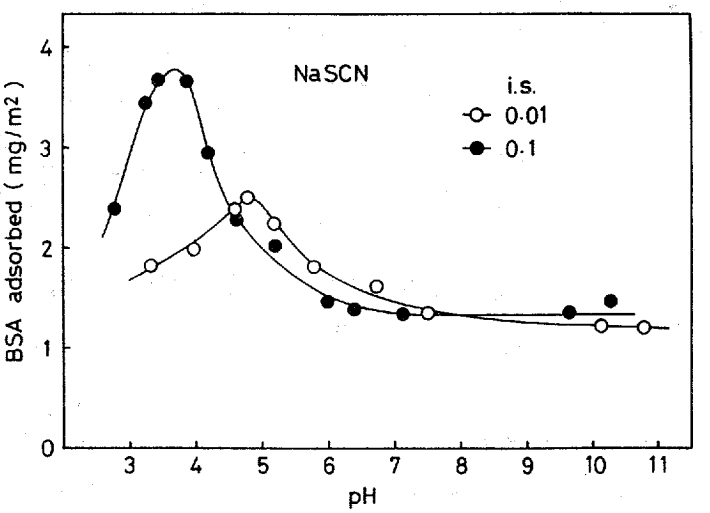

Fig.21. BSA adsorption onto PS latex as a function of pH and ionic strength (i.s.) in NaSCN solution. 25°C, initial BSA concentration 50 mg/dl.

Further, in SCN^- medium, the amount adsorbed in the alkaline pH region does not increase with increasing ionic strength (see Figure 21). Although the binding of small anions to protein molecules decreases with an increase of pH [22),50),96)], those anions are bound to some extent even in the alkaline region unless the pH is very high [50),96)]. Small anions used in this work are in the lyotropic series (or Hofmeister series) in the order, $SCN^- < Cl^- < CH_3COO^-$. [61),97)] This indicates that the dehydration power of these anions becomes stronger in this order. When protein molecules adsorb onto polymer latices, the hydrated water of the adsorbate and

adsorbent must be displaced. Hence, in SCN^- medium (whose dehydration power is weaker than that of other anions), BSA adsorption onto PS latex in the alkaline pH region may be little affected by the ionic strength.

Furthermore, it was reported that SCN^- reacted mainly with tryptophan (viz., hydrophobic residues) of BSA at neutral pH, in addition to the electrostatic interactions with positively charged groups surrounding the hydrophobic area.[98] Also, the binding entropy of SCN^- to BSA molecule, $\triangle S$ (positive value), is greater than that of Cl^-.[99] These facts suggest the decrease in the hydrophobic interaction between the BSA molecule and PS latex in SCN^- medium. At a high ionic strength and in the alkaline pH region, as mentioned before, the hydrophobic interaction is probably a dominant driving force to BSA adsorption onto PS latex. Therefore, in the alkaline pH region as shown in Figure 22, the amount of BSA adsorbed in SCN^- medium is smaller than those in other anions media. Judging from the above results and discussion, consequently, it appears that SCN^- in the alkaline pH region acts as a breaker ion in the hydrophobic interaction between the BSA molecule and PS latex.

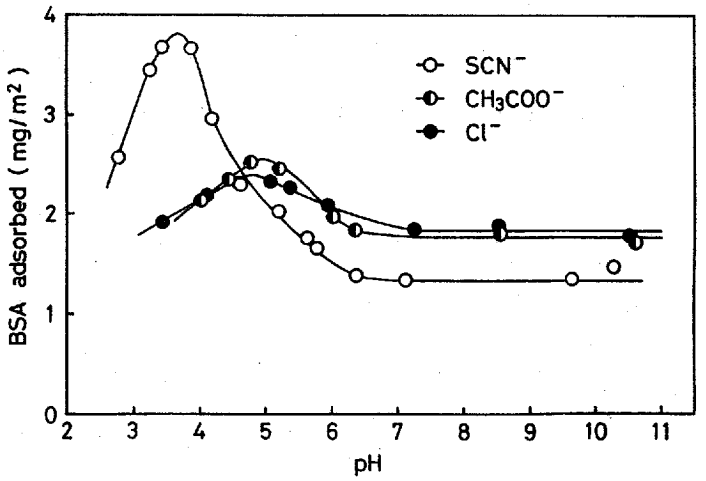

Fig.22. Effects of electrolyte anions on BSA adsorption onto PS latex as a function of pH. 25°C, initial BSA concentration 50 mg/dl, ionic strength 0·1.

3.3. Electrophoretic analysis of BSA-covered latex particles

Figure 23 shows the effects of three electrolyte anions on electrophoretic mobilities of BSA-covered PS particles as a function of pH. As described previously, in the isoelectric pH region of BSA, BSA molecules adsorb onto (a negatively charged) PS latex in a "side-on" mode, and probably complete the monolayer adsorption without a large interfacial denaturation.[8),100)] Therefore, the isoelectric point (iep) of BSA in the adsorbed state will not be very different from that in the dissolved one. As can be seen from Figure 23, in all anions media, the iep of BSA shifts to a more acidic pH with increasing ionic strength. This result corresponds to the pH shift of the maximum adsorption to an acidic side with an increase of ionic strength (see Figures 19-21).

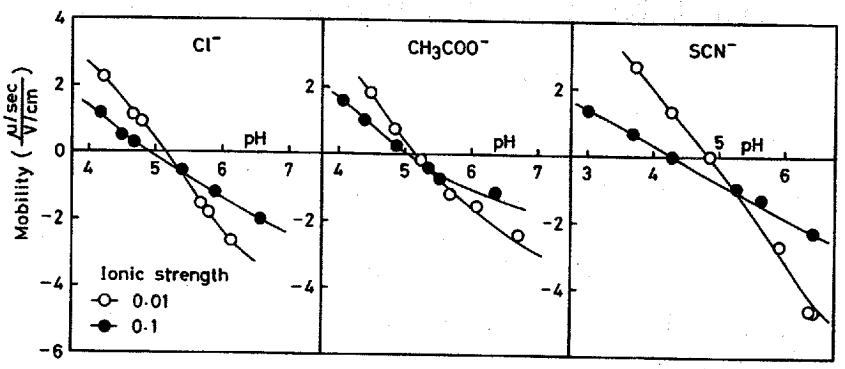

Fig.23. Effects of electrolyte anions on electrophoretic mobilities of BSA-covered PS particles as a function of pH at 25°C.

To understand better the effects of these anions on BSA adsorption onto PS latex, the pH at maximum adsorption ($pH(A_{max})$), the iep of adsorbed BSA determined by microelectrophoresis method (pH(iep)), and the iep of dissolved BSA determined by Longsworth et al.[61] (pH*(iep)) are summarized in Table 8. It can be seen from this table that in all anions media the values of $pH(A_{max})$ are in good agreement with those of pH(iep) except the results at ionic strength 0.1 in SCN^- medium. Further, the pH(iep) values are in fair agreement with pH*(iep) values. These demonstrate that the maximum adsorption is obtained near the iep of BSA, and the $pH(A_{max})$ shifts to a more acidic region with increasing ionic strength. Moreover, the pH(iep) (or pH *(iep)) in these anions media shifts to a more acidic region in the order of CH_3COO^-, Cl^-, and SCN^-. This indicates that the binding affinity of small anions to BSA molecule increases in the order, $CH_3COO^- < Cl^- \ll SCN^-$.[61] However, it is not clear that the $pH(A_{max})$ is rather lower than the pH(iep) at ionic strength 0.1 in SCN^- medium.

Table 8. Values of pH(A_{max}) and pH(iep) in various anion media

Anion	CH_3COO^-		Cl^-		SCN^-	
Ionic strength	0.01	0.1	0.01	0.1	0.01	0.1
pH(A_{max})	5.2	5.0	5.3	4.8	4.8	3.7
pH(iep)	5.2	5.0	5.2	4.9	4.9	4.3
pH*(iep)	—	4.7	—	4.6	—	4.2

As described above, it was found that BSA adsorption onto PS latex is strongly affected by coexistent electrolyte anions, especially by SCN^-.

CHAPTER Ⅳ

Adsorption of Urea-denatured BSA

The adsorbability of urea-denatured bovine serum albumin (BSA) onto polymer latices was investigated. The latices used were polymethyl methacrylate (PMMA) and styrene/methyl methacrylate/methacrylic acid copolymer (P(St/MMA/MAA)) latices. In the presence of urea, the initial slopes of the adsorption isotherms of BSA were very sharp regardless of pH. The pH at maximum adsorption of urea-denatured BSA shifted to a more alkaline region by ca. 1 pH unit as compared with that of native one. This pH shift agreed with the shift of the isoelectric point of BSA to a alkaline pH region in urea solution. In the alkaline pH region particularly at a high ionic strength, the amount adsorbed of urea-denatured BSA was considerably greater than that of native BSA. This may be because the hydrophobic interaction between urea-denatured BSA molecule and the latex is greater than that between native BSA molecule and the latex, and the aggregates of BSA molecules adsorb onto the latex in an "end-on" or a "loop" mode. It was found that the amount of BSA adsorbed onto P(St/MMA/MAA) latex was greater than that onto PMMA latex in the presence and absence of urea.

1. Introduction

The mechanism of the denaturation of BSA in aqueous urea solution has been studied by many different methods.[101)-114)] For instance, Kauzmann et al.[101)-103)] investigated extensively urea denaturation of BSA by means of optical rotation and viscosity methods. Katz et al.[109)-111)] and Aoki et al.[114)] analyzed it by polyacrylamide gel electrophoresis. Their papers can be summarized as follows: Urea breaks hydrogen bonding and hydrophobic interaction which contribute to the stability of the tertiary structure of BSA, and unfolds BSA molecules.[108)] In concentrated urea solution (above 5M), unfolded BSA molecules show a tendency to aggregate.[113)] This is much more pronounced in neutral and alkaline pH region.[107),114)] The aggregated forms of BSA appear to be due to an intermolecular SH/S-S exchange reaction.[107),112),114)] The isoelectric point of BSA in urea solution shifts to a more alkaline region than that in the absence of urea.[105),112)]

As described above, much information about the urea denaturation of BSA has been obtained. However, little work about the adsorbability of urea-denatured BSA onto solid surfaces has been reported. Therefore, this chapter is concerned with the adsorption of urea-denatured BSA onto polymer latices. The latices used were polymethyl methacrylate (PMMA) and styrene/methyl methacrylate/methacrylic acid copolymer (P(St/MMA/MAA)).

2. Experimental

2.1. Materials

PMMA and P(St/MMA/MAA) latices used were the same samples as described in chapter Ⅰ and section Ⅱ-Ⅰ of chapter Ⅱ, respectively. Urea (analytical grade) was purified by recrystallization from distilled ethanol.

BSA, other reagents, and water were similar to those used in chapter Ⅰ.

2.2. Methods

2.2.1. Determination of BSA concentration

The BSA concentration in urea solution was determined by the same method as described in chapter Ⅰ. The calibration curve of BSA showed a good linearity, although the absorbance of the protein in the presence of urea was somewhat higher than that in the absence of urea.

2.2.2. Adsorption experiment

In the presence of urea, the adsorption experiments were carried out as follows: A portion of BSA stock solution was exposed to the urea solution (including NaCl, HCl, or NaOH), and this mixture was kept at 25℃ for 1 hr. According to Ref.114), it was found that it took 1 hr to denature BSA sufficiently under similar conditions. The latex was added to this solution. The subsequent operation was the same as that

in the absence of urea; namely, after a centrifugation of the mixing solution, the amount adsorbed was determined by the microbiuret method (λ = 310 nm).

As described in chapter I, the pH and ionic strength of the sample solutions were adjusted with aqueous HCl, NaOH, and NaCl. Acetate (at pH 5.1 and 6.2) and phosphate (at pH 7.0) buffer solutions were used for obtaining the adsorption isotherms.

2.2.3. Measurement of electrophoretic mobility

To obtain the isoelectric point of BSA (adsorbed onto polymer latices), the electrophoretic mobilities of BSA-covered latex particles were measured as a function of pH by microelectrophoresis method.

3. Results and Discussion

3.1. Adsorption isotherms

Figure 24 shows the adsorption isotherms of BSA onto PMMA latex in the presence of urea. The isotherms are considerably different from that in the absence of urea (see Figure 2 in chapter I). That is, the initial slopes are very sharp regardless of pH. From the concept of "oil drop model for protein[115),116)]" and X-ray analysis of proteins,[117)] it has been revealed that hydrophobic amino acid

residues of protein (such as valine, isoleucine, phenylalanine, tryptophan, etc.) tend to avoid the aqueous phase and adhere to one another. On the other hand, some papers[108),118),119)] reported that hydrophobic amino acid residues which were masked in the native protein molecules were unfolded and exposed to the aqueous phase in the presence of urea. Therefore, this result is probably due to the increment of the hydrophobic interaction between unfolded BSA molecule (denatured by urea) and PMMA latex. Further, the steps in the adsorption isotherms are hardly observed. Hence, in the presence of urea, it appears that the adsorbed BSA molecule cannot be altered any more. The pH at maximum plateau value shifts to a more alkaline side as compared with that in the absence of urea (i.e., pH 4.8→6.2, cf. Figure 2 in chapter I with Figure 24). This result will be discussed in the following section.

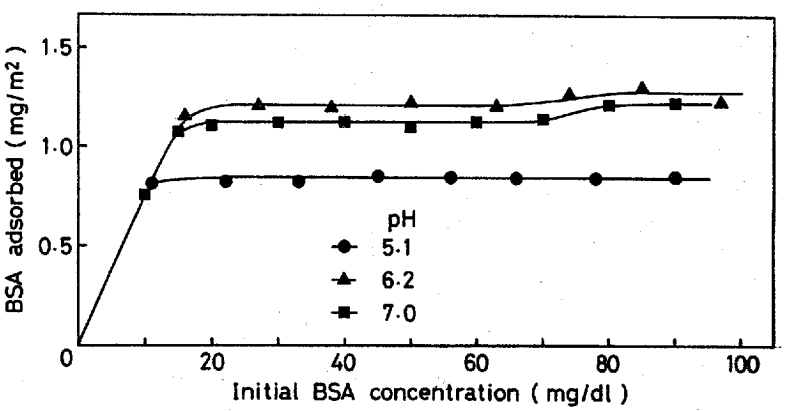

Fig. 24. Adsorption isotherms of BSA onto PMMA latex in 8M urea solution (25°C , ionic strength 0·01).

3.2. Effects of pH and ionic strength

Figure 25 shows the effects of pH and ionic strength on the adsorption of BSA onto PMMA latex in the presence of urea. In comparison with the results in the absence of urea, it appears that the most distinguishable point is the shift of the pH at maximum adsorption. To better illustrate this, the results in the absence and presence of urea are given in Figure 26 for an ionic strength of 0.01. It can be seen from Figure 26 that the pH at maximum adsorption in the presence of urea shifts to a more alkaline region, i.e., from pH ca.5 to pH ca.6. It has hitherto been reported that the maximum adsorption is obtained near the isoelectric point (iep) of proteins.[10),16),42),65)-68)]

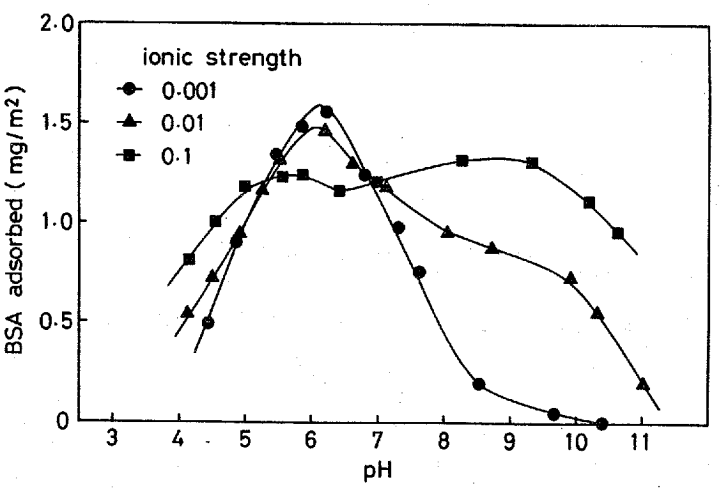

Fig. 25. pH dependence of BSA adsorption onto PMMA latex in 5 M urea solution (25°C , initial BSA concentration 50 mg/dl).

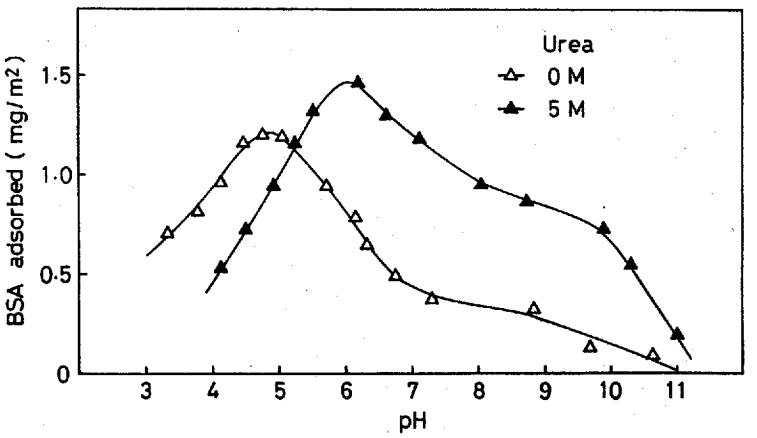

Fig. 26. Effect of urea on BSA adsorption onto PMMA latex (25°C, ionic strength 0.01, initial BSA concn. 50 mg/dl).

Foster and Aoki [105] investigated the isomerization equilibrium of BSA in the presence of urea, and found that the iep of BSA shifted to a more alkaline region as compared with that in the absence of urea. They suggested that this fact should be due to the shift of the N-F transition of BSA to an alkaline region by urea. In recent years, Salaman and Williamson [112] analyzed the urea-denatured BSA at 4℃ in 6M urea solution by isoelectric focusing without fractionating it into components, and found that urea-denatured BSA focused at pH 5.9. Aoki et al.[120] also analyzed the urea-denatured BSA by the same method with fractionating it into components (1, 1', 2, and 3 ; here component 1 is an undenatured monomer, 1', 2, and 3 are denatured components (modified monomer, dimer, and probably trimer, respectively)). They found that the iep of 1 was pH 4.9 and those of 1', 2 and 3 were pH 5.9.

Moreover, the electrophoretic mobilities of BSA-covered latex particles were measured to confirm the shift of the iep of BSA in the adsorbed state. The results are given in Figure 27. As can be seen from this figure, the iep of BSA adsorbed onto PMMA latex shifts to a more alkaline region with increasing urea concentration. At 5M urea, the iep is pH 6, which agrees with that obtained by isoelectric focusing.

From the above discussion, it is suggested that the shift of pH at maximum adsorption in the presence of urea to a more alkaline region is related to the shift of the iep of urea-denatured BSA in aqueous solution to a more alkaline region. However, in the acidic and alkaline pH regions, the amount adsorbed in the presence of urea increases with increasing ionic strength similarly to that in the absence of urea.

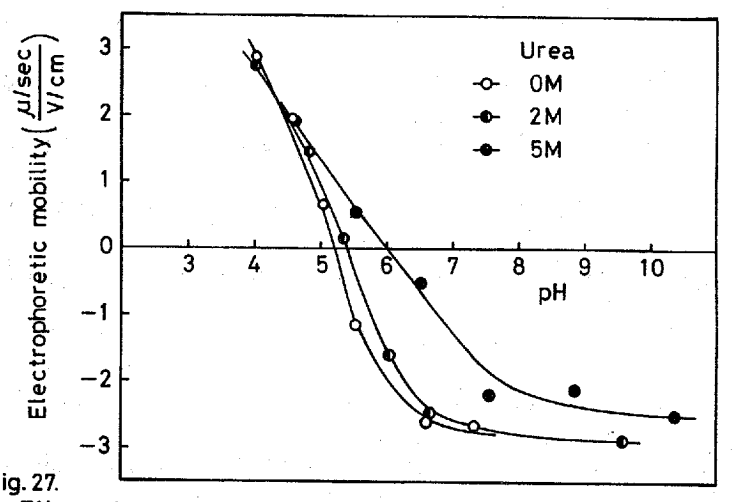

Fig. 27.
Effect of urea concn. on electrophoretic mobilities of BSA-adsorbed PMMA latex (25°C , ionic strength 0.01).

Figures 28 and 29 show the effects of pH and ionic strength on BSA adsorption onto P(St/MMA/MAA) latex in the absence and presence of urea, respectively. In the presence of urea, the maximum adsorption is obtained at the same pH (ca.6) as for PMMA latex.

In the alkaline pH region especially at higher ionic strengths (i. e., at ionic strength 0.01 and 0.1), the amount of BSA adsorbed in the presence of urea is considerably greater than that in the absence of urea similarly to PMMA latex. In concentrated urea solution particularly in the neutral and alkaline pH regions, BSA molecules are unfolded and tend to aggregate by an intermolecular SH/S-S exchange reaction.[107),112),114)] These facts suggest that denatured BSA components(1',2, and 3) are more hydrophobic than an undenatured component (1), hence, the hydrophobic interaction between denatured components and the latex is greater than that between component 1 and the latex. This probably leads to the increment of the amount adsorbed in the alkaline pH region, as observed in Figure 29. That the aggregates of BSA molecules adsorb onto the latex in an "end-on" or a "loop" mode may also contribute to this increase in the amount adsorbed. As observed in Figure 26, similar results are obtained in the case of PMMA latex. However, the amount adsorbed is considerably smaller than that onto P(St/MMA/MAA) latex, because the hydrogen bonding between BSA molecule and PMMA latex may be negligible.

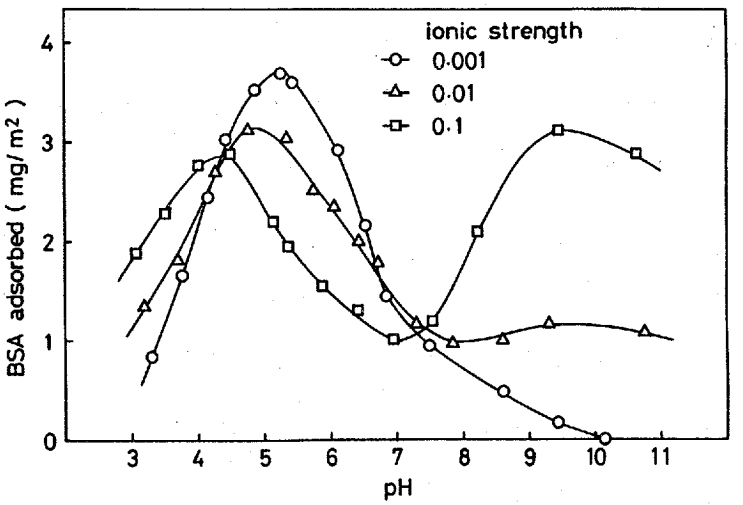

Fig. 28. pH dependence of BSA adsorption onto P(St/MMA/MAA) latex (25°C, initial BSA concn. 50 mg/dl).

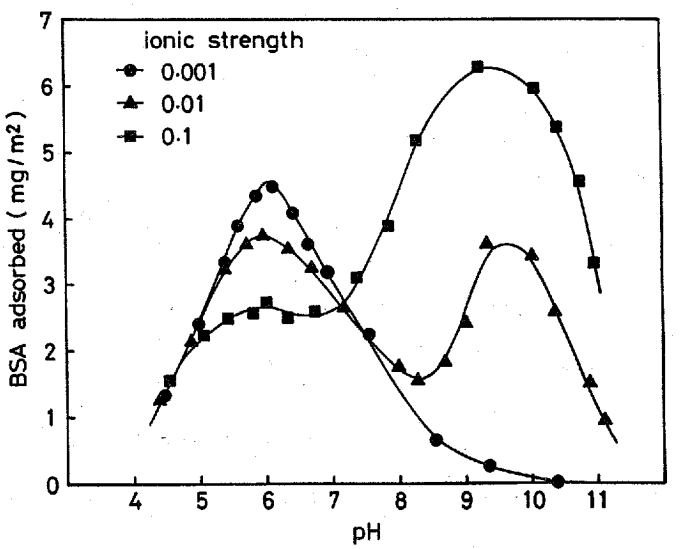

Fig. 29. pH dependence of BSA adsorption onto P(St/MMA/MAA) latex in 5 M urea soln. (25°C, initial BSA concn. 50 mg/dl)

SUMMARY

The adsorbability of bovine serum albumin (BSA) onto various polymer latices was investigated as a function of pH and ionic strength, etc. The latices used were hydrophobic homopolymers and hydrophilic copolymers. First, in part I, the preparation and surface characterization of polymer latices were dealt with. Subsequently, in part II, BSA adsorption onto those latices was discussed.

Part I

Chapter I : Hydrophobic homopolymer latices, i. e., polystyrene (PS) and polymethyl methacrylate (PMMA) latices, were prepared without emulsifier using potassium persulfate (KPS) as the initiator. Electron micrographs of these latices revealed the particles to be highly monodisperse. The conductometric titration curve of PS latex showed both strong and weak acid groups to exist on the latex surface, though that of PMMA latex showed only strong acid groups to exist on the surface. The surface charge density and ζ-potential of PS latex were greater than those of PMMA latex in proportion to the quantity of KPS used in the polymerization.

Chapter II : Hydrophilic copolymer latices, i. e., carboxylated latices — styrene / acrylic acid (AA) copolymer (P(St/AA)) and styrene / methacrylic acid (MAA) copolymer (P(St/MAA))—, styrene / 2-hydroxyethyl methacrylate (HEMA) copolymer (P(St/HEMA)) latices, and

styrene / acrylamide (AAm) copolymer (P(St/AAm)) latices were prepared without emulsifier using KPS as the initiator. PS latex was used as a reference sample. Carboxylated and P(St/HEMA) latices were prepared by a special polymerization technique, i. e., by the seed polymerization method with the successive addition of monomer, though P(St/AAm) latices were prepared by the same method as PS latex. All these latices were found to be highly monodisperse from those electron micrographs. The conductometric titration curves of these latices except P(St/AAm) latex showed that both strong and weak acid groups existed on the surface of latex particles. The surface charge density (σ) for P(St/AA) latices was proportional to the quantity of AA used in the copolymerization (i. e., the quantity of surface carboxyl groups of the latices). The σ for P(St/MAA_5) latex was smaller than that for P(St/AA_5) latex, although the mol % of acid monomers used in the copolymerization was the same for both latices. The σ for carboxylated latices increased with increasing pH, but the pH dependence of σ for PS latex was not very pronounced. The pH dependence of σ for P(St/HEMA) latex was similar to that for PS latex. This result suggested that the surface of P(St/HEMA) latex was more hydrophilic than that of PS latex despite its having much the same surface charge as PS latex. The ζ-potentials of copolymer latices were smaller than that of PS latex over the whole range of measured pH. This result was explained by the difference in the structure of the electrical double layer between PS and copolymer latices. That is,

because the hydrated polymer (such as poly-HEMA) layers existing on the copolymer latex surfaces shifted the shear plane of the electrical double layer away from their particle surfaces, the ζ-potentials of copolymer latices probably decreased as compared with that of PS latex. From the results of the viscosity measurement etc. of P(St/AAm) latex dispersion, it was found that the thickness of polyacrylamide (PAAm) layer existing on the latex surface increased with increasing the quantity of AAm used in the copolymerization. Methylene Blue (basic dye) adsorption onto PS, P(St/AA), and P(St/HEMA) latices was measured as a function of pH. The overall tendency of the dye adsorption was more similar to the σ-pH curves than the ζ-pH curves. This may indicate that Methylene Blue adsorption onto latices mainly occurs electrostatically.

Part II

Chapter I : The adsorbability of BSA onto hydrophobic PS and PMMA latices was investigated in this chapter. Affected by the electrostatic interactions between BSA molecules and the latices, the initial slopes of the adsorption isotherms of BSA decreased with increasing pH. The isotherms for these latices showed steps at some concentrations of BSA. The cross-sectional area of an adsorbed BSA molecule and the thickness of the adsorbed BSA monolayer suggested that BSA molecules adsorbed onto PS latex in a "side-on" mode near the isoelectric point (iep) of this protein. With an increase of ionic

strength, the amount of BSA adsorbed onto these two latices increased except in the iep region of BSA. For both latices, the amount adsorbed showed a maximum near the iep (pH ca.5) of BSA, and the pH at maximum adsorption shifted to a more acidic region with increasing ionic strength. Over the whole range of measured pH, BSA adsorption onto PS (more hydrophobic) latex was greater than that onto PMMA latex.

Chapter Ⅱ; section Ⅱ- Ⅰ: This section was concerned with BSA adsorption onto carboxylated latices. In addition to the carboxylated latices mentioned in chapter Ⅱ of part Ⅰ, styrene/methyl methacrylate/methacrylic acid copolymer (P(St/MMA/MAA)) latex was also used. The amount of BSA adsorbed onto carboxylated latices except in the alkaline pH region was greater than that onto PS latex. Moreover, the amount adsorbed onto carboxylated latices was proportional to the quantity of surface carboxyl groups of the latices throughout almost the range of measured pH. These results are probably due to the hydrogen bonding between BSA molecule and carboxylated latices. At a high ionic strength, the amount of BSA adsorbed onto all carboxylated latices increased again from pH ca. 7. This tendency was most remarkable for P(St/MMA/MAA) latex. Therefore, not only the hydrogen bonding but also the hydrophobic interaction between the methyl group of the latex (containing MMA unit) and BSA molecule probably contributes to this re-increase in the amount adsorbed. With repect to other results of BSA adsorption, similar tendencies to those for hydrophobic latices were obtained.

Section Ⅱ- Ⅱ: In this section, BSA adsorption onto P(St/HEMA) latex was investigated. In the acidic pH region lower than the iep of BSA, the adsorbability of the protein onto this latex was similar to that onto PS latex. However, in the alkaline pH region, the amount adsorbed onto P(St/HEMA) latex was scarcely discernible regardless of ionic strength. This tendency was proportional to the quantity of HEMA used in the copolymerization. These results are probably because the hydrophobic interaction between this latex and BSA molecule is rather smaller than that between PS latex and BSA molecule. Furthermore, the effect of the hydrogel (poly-HEMA) layer existing on P(St/HEMA) latex, i. e., the diffuse layer effect probably affects this decrease in the amount of BSA adsorbed greatly.

Section Ⅱ- Ⅲ: Moreover, in this section, the effect of the hydrogel layer on BSA adsorption, i. e., the adsorbability of BSA onto P(St/AAm) latex having polyacrylamide (PAAm) layer on its surface was studied. At a high ionic strength, the amount of BSA adsorbed onto P(St/AAm) latex was rather smaller than that onto PS latex; this tendency was proportional to the quantity of AAm used in the copolymerization (in other words, to the thickness of PAAm layer). Further, in contrast to P(St/HEMA) latex, this decrease in the amount adsorbed was observed throughout the entire range of measured pH. Therefore, the diffuse layer effect of PAAm layer on BSA adsorption is probably greater than that of poly-HEMA layer.

Chapter Ⅲ: The effects of coexistent electrolyte anions on BSA

adsorption onto PS latex were investigated in this chapter. Three electrolyte anions (viz., Cl^- , CH_3COO^-, and SCN^-) were used as the sodium salt. The adsorbability of BSA onto the latex in both Cl^- and CH_3COO^- media showed a similar tendency. However, BSA adsorption in SCN^- medium especially at a high ionic strength was very different from that in other anions (Cl^- and CH_3COO^-) media. That is, in SCN^- medium , the pH at maximum adsorption shifted to a more acidic region and the maximum adsorption was greater than those in other anions media. These results were explained by the difference in the binding affinity of those small anions to BSA molecule.

Chapter IV: The adsorbability of urea-denatured BSA onto PMMA and P(St/MMA/MAA) latices was investigated in this chapter. In the presence of urea, the initial slopes of the adsorption isotherms of BSA were very sharp regardless of pH. The pH at maximum adsorption of urea-denatured BSA shifted to a more alkaline region by ca. 1 pH unit as compared with that of native one. This pH shift agreed with the shift of the iep of BSA to a alkaline pH region in urea solution. In the alkaline pH region particularly at a high ionic strength, the amount adsorbed of urea-denatured BSA was considerably greater than that of native one. The amount adsorbed onto P(St/MMA/MAA) latex was greater than that onto PMMA latex in the presence and absence of urea.

As described above, it was found that the adsorbability of BSA was greatly dependent on not only pH and ionic strength but also the surface characteristics of polymer latices, the kinds of electrolyte

anions, and the denaturation state of BSA molecule. In particular, the most important conclusion obtained in this study is that BSA adsorption onto the latices having hydrogel layers on their surfaces (i. e., onto P(St/HEMA) and P(St/AAm) latices) is hardly discernible at least near the physiological pH (about 7.4) region. Moreover, the surfaces of these latices are considered to resemble those of living cells. This similarity probably makes the interaction between the latices and living cells (or blood components) very small. Therefore, hydrophilic polymers modified by such monomers as HEMA and AAm seem to be most suitable for biocompatible materials, especially for an antithrombogenic one.

REFERENCES

1) J.L.Brash, D.J.Lyman, J.Biomed. Mater. Res., 3, 175 (1969).

2) D.J.Lyman, K.Knutson, B.McNeill, K.Shibatani, Trans. Am. Soc. Artif. Int. Organs, 21, 49 (1975).

3) A. Van Der Scheer, C.A.Smolders, J.Colloid Interface Sci., 63, 7 (1978).

4) D.J.Lyman, L.C.Metcalf, D.Albo, Jr., K.F.Richards, J.Lamb, Trans. Am. Soc. Artif. Int. Organs, 20, 474 (1974).

5) S.W.Kim, R.G.Lee, H.Oster, D.Coleman, J.D.Andrade, D.J.Lentz, D. Olsen, Trans. Am. Soc. Artif. Int. Organs, 20, 449 (1974).

6) S.D.Bruck, J.Biomed. Mater. Res., 7, 387 (1973).

7) J.L.Brash, S.Uniyal, Q.M.Samak, Trans. Am. Soc. Artif. Int. Organs, 20, 69 (1974).

8) W.Norde, J.Lyklema, J.Colloid Interface Sci., 66, 257 (1978).

9) B.D.Fair, A.M.Jamieson, J.Colloid Interface Sci., 77, 525 (1980).

10) T.Suzawa, T.Murakami, J.Colloid Interface Sci., 78, 266 (1980).

11) P.Bagchi, S.M.Birnbaum, J.Colloid Interface Sci., 83, 460 (1981).

12) H.Kitano, K.Nakamura, N.Ise, "Abstracts, 2nd Polymer Microspheres Symposium", Fukui (Japan), November 11-13, p.123, 1982.

13) E.W.Bermes, Jr., J.H.Isaacs, Am. J.Obst. & Gynec., 104, 865 (1969).

14) A.Rembaum, S.P.S.Yen, E.Cheong, S.Wallace, R.S.Molday, I.L.Gordon, W.J.Dreyer, Macromolecules, 9, 328 (1976).

15) A.Bini, D.Collen, Throm. Res., 12, 389 (1978).

16) W.Norde, Ph.D. thesis, Agricultural University Wageningen, The Netherlands, 1976.

17) A.Kotera, K.Furusawa, Y,Takeda, Kolloid Z. Z. Polym. 239, 677 (1970).

18) H.Ono, H.Saeki, Br. Polym. J., 7, 21 (1975).

19) Y.Ohtsuka, H.Kawaguchi, Y.Sugi, J.Appl. Polym. Sci., 26, 1637 (1981).

20) H.Tamai, A.Iida, T.Suzawa, Colloid Polym. Sci., 262, 77 (1984).

21) G.Scatchard, I.H.Scheinberg, S.H.Armstrong, J.Am.Chem. Soc., 72, 535 (1950).

22) C.W.Carr, Arch. Biochem. Biophys., 40, 286 (1952).

23) For example, C.F.Fryling, J.Colloid Sci., 18, 713 (1963); J.B. Brodnyan, E.L.Kelley, J.Colloid Sci., 20,7 (1965); C.G.Force, E. Matijević, J.P.Kratohvil, Kolloid Z.Z.Polym., 223, 31 (1968).

24) H.J.van den Hul, J.W.Vanderhoff, J.Colloid Interface Sci., 28, 336 (1968).

25) P.H.Wiersema, A.L.Loeb, J.Th.G.Overbeek, J.Colloid Interface Sci., 22,78 (1966).

26) R.H.Ottewill, J.N.Shaw, Kolloid Z.Z.Polym., 218, 34 (1967).

27) J.Hearn, R.H.Ottewill, J.N.Shaw, Br. Polym. J., 2,116 (1970).

28) I.M.Kolthoff, I.K.Miller, J.Am.Chem. Soc., 73,3055 (1951).

29) J.W.Vanderhoff, in "Vinyl Polymerization," G.E.Ham, Ed., Vol. 1, Part 2, Chap. 1, Dekker, New York, 1969.

30) A.Homola, R.O.James, J.Colloid Interface Sci., 59, 123 (1977).

31) M.E.Labib, A.L.Robertson, J.Colloid Interface Sci., 77, 151 (1980).

32) T.Matsumoto, M.Shimada, Kobunshi Kagaku, 22, 172 (1965).

33) E.Ohmori, in "Akurirusan-esuteru To Sono Porimā〔II〕(Acylic Esters and Their Polymers 〔II〕," Shokodo (Japan), 1975, p.70.

34) W.G.Eversole, W.W.Boardman, J.Chem. Phys., 9, 798 (1941).

35) C.M.Ma, F.J.Micale, M.S.El-Aasser, J.W.Vanderhoff, in "Emulsion Polymers and Emulsion Polymerization," D.R.Bassett and A.E. Hamielec, Eds., American Chemical Society, Washington, D.C., 1981, p.251.

36) H.Tamai, T.Murakami, T.Suzawa, J.Appl. Polym. Sci., 30, 3857 (1985).

37) G.J.Fleer, J.K.Koopal, J.Lyklema, Kolloid Z.Z.Polym., 250, 689 (1972).

38) T.Suzawa, H.Shirahama, S.Kawasaki, unpublished data.

39) J.L.Brash, D.J.Lyman, in "The Chemistry of Biosurfaces," M.L. Hair, Ed., Dekker, New York, 1971, Vol. 1, p. 177.

40) F.MacRitchie, J.Colloid Interface Sci., 38, 484 (1972).

41) W.Dillman, I.F.Miller, J.Colloid Interface Sci., 44, 221 (1973).

42) B.W.Morrissey, R.R.Stromberg, J.Colloid Interface Sci., 46, 152 (1974).

43) J.L.Brash, Q.M.Samak, J.Colloid Interface Sci., 65, 495 (1978).

44) J.L.Brash, S.Uniyal, Polym. Symp., 66, 377 (1979).

45) V.Hlady, H.Füredi-Milhofer, J.Colloid Interface Sci, 69, 460 (1979).

46) T.Okano, S.Nishiyama, I.Shinohara, T.Akaike, Y.Sakurai, Kobunshi Ronbunshu, 36, 209 (1979).

47) M.E.Soderquist, A.G.Walton, J.Colloid Interface Sci., 75, 386 (1980).

48) P.van Dulm, W.Norde, J.Lyklema, J.Colloid Interface Sci., 82, 77 (1981).

49) B.Jansen, G.Ellinghorst, J.Biomed. Mater. Res., 18, 655 (1984).

50) G.Scatchard, W.T.Yap, J.Am. Chem. Soc., 86, 3434 (1964).

51) F.Karush, J. Am. Chem. Soc., 72, 2705 (1950).

52) H.Terada, K.Hiramatsu, in "Kessei Arubumin (Serum Albumin), Seitai niokeru Sono Yakuwari (Its Role in Vitals)," K.Aoki, T.Takagi, H.Terada, Eds., Kodansha, Tokyo, 1984, p.81.

53) V.M.Rosenoer, M.Qrsatz, M.A.Rothschild, Eds., "Albumin Structure, Function and Uses," Pergamon Press (1977).

54) P.F.Spahr, J.T.Edsall, J.Biol. Chem., 239, 850 (1964).

55) R.G.Reed, F.W.Putnam, T.Peters, Jr., Biochem. J., 191, 867 (1980).

56) L.Andersson, Biochim. Biophys. Acta, 117, 115 (1966).

57) V.Luzzati, J.Witz, A.Nicolaieff, J.Mol. Biol., 3, 379 (1961).

58) K.Aoki, in "Kessei Arubumin (Serum Albumin), Seitai niokeru Sono

Yakuwari (Its Role in Vitals) ," K.Aoki, T.Takagi, H.Terada, Eds., Kodansha, Tokyo, 1984, p.13.

59) K.Aoki, J.F.Foster, J.Am. Chem. Soc., 79, 3385 (1957).

60) K.Aoki, J.F.Foster, J.Am.Chem.Soc., 79, 3393 (1957).

61) L.G.Longsworth, C.F.Jacobsen, J.Phys. Colloid Chem., 53, 126 (1949).

62) J.F.Foster, in "The Plasma Proteins," F.W.Putnam, Ed., Academic Press, New York, 1960, Vol.1, p.179.

63) R.F.Itzhaki, D.M.Gill, Anal. Biochem., 9, 401 (1964).

64) T-H. Chiu, E.Nyilas, D.M.Lederman, Trans. Am. Soc. Artif. Int. Organs, 22, 498 (1976).

65) R.W.Watkins, C.R.Robertson, J.Biomed. Mater. Res., 11, 915 (1977).

66) E.I.Hitchcock, J.Gen. Physiol., 8, 61 (1925).

67) A.D.Mularen, J.Phys. Chem., 58, 129 (1954).

68) H.B.Bull, Biochim. Biophys. Acta, 19, 464 (1956).

69) H.B.Bull, J.Am. Chem. Soc., 80, 1901 (1958).

70) C.Tanford, S.A.Swanson, W.S.Shore, J.Am.Chem.Soc., 77, 6414 (1955).

71) T.Suzawa, H.Shirahama, K.Terasawa, unpublished data.

72) H.Tanzawa, in "Iyo Kobunshi (Biomedical Polymer)," M.Seno, Ed., Kyoritsu Shuppan, Tokyo, 1979, p.95.

73) M.Toyama, T.Ito, H.Moriguchi, J.Appl. Polym. Sci., 14, 2039 (1970).

74) O.Wichterle, D.Lim, Nature, 185, 117 (1960).

75) J.D.Andrade, J.Assoc. Advan. Med. Inst., 7, 110 (1973).

76) B.D.Ratner, A.S.Hoffman, in "Hydrogels for Medical and Related Applications," J.D.Andrade, Ed., Am. Chem. Soc. Symp. Ser., 31, 1 (1976).

77) Y.Ikada, M.Suzuki, Polym. Preprints, Japan, 31(No.8), 1789 (1982).

78) P.Stamberger, J.Colloid Sci., 17, 146 (1962).

79) S.Muroi, Kogyo Kagaku Zasshi, 68, 1796 (1965).

80) S.Muroi, J.Nomura, Kogyo Kagaku Zasshi, 68, 1800 (1965).

81) A.C.Nussle, B.B.Kine, Am. Dyestuff Rep., 50, 1007 (1961).

82) S.Muroi, K.Hosoi, Kogyo Kagaku Zasshi, 69, 1545 (1966).

83) Du Pont, Br.Patent, 1 114 133 (1968).

84) S.W.Kim, R.G.Lee, in "Applied Chemistry at Protein Interfaces," R.E.Baier, Ed., Am. Chem. Soc., New York, 1975, pp. 218-229.

85) E.J.Williams, J.F.Foster, J.Am.Chem.Soc., 81, 865 (1959).

86) G.Markus, F.Karush, J.Am.Chem.Soc., 79, 3264 (1957).

87) W.J.Leonard, Jr., K.K.Vijai, J.F.Foster, J.Biol.Chem., 238, 1984 (1963).

88) T.Matsumoto, in "Gosei Jushi Emarujon (Synthetic Resin Emulsion)", H.Inagaki, T.Okuda, Eds., Kobunshi Kankokai, Tokyo, 1978, p.26.

89) T.Nakashima, K.Takakura, Y.Komoto, J.Biomed. Mater. Res., 11, 787 (1977).

90) T.Okano, S.Nishiyama, I.Shinohara, T.Akaike, Y.Sakurai, K.Kataoka, T.Tsuruta, J.Biomed. Mter. Res., 15, 393 (1981).

91) Y.Ikada, H.Iwata, F.Horii, T.Matsunaga, M.Taniguchi, M.Suzuki, W.Taki, S.Yamagata, Y.Yonekawa, H.Handa, J.Biomed. Mater. Res., 15, 697 (1981).

92) S.Nagaoka, H.Takiuchi, K.Yokota, Y.Mori, H.Tanzawa, T.Kikuchi, Kobunshi Ronbunshu, 39, 165 (1982).

93) For example, A.S.Kramer, J.Pharm. Sci., 63, 1647 (1974).

94) I.M.Klotz, J.M.Urquhart, J.Phys. Colloid Chem., 53, 100 (1949).

95) G.Scatchard, E.S.Black, J.Phys. Colloid Chem., 53, 88 (1949).

96) G.Scatchard, J.S.Coleman, A.L.Shen, J.Am.Chem. Soc., 79, 12 (1957).

97) K.Miyajima, in "Mizu No Kozo To Bussei (Structure and Physical Property of Water)," M.Nakagaki, Ed., Nankodo, Tokyo, 1974, p.90.

98) C.V.Eadsforth, D.M.Power, E.W.Thomas, J.V.Davies, Int. J.Radiat. Biol. Relat. Stud. Phys., Chem. Med., 30, 449 (1976).

99) I.M.Klotz, Ann. New York Acad. Sci., 226, 18 (1973).

100) T.Akaike, Y.Sakurai, K.Kosuge, Y.Senba, K.Kuwana, S.Miyata, K.Kataoka, T.Tsuruta, Kobunshi Ronbunshu, 36, 217 (1979).

101) W.Kauzmann, R.B.Simpson, J.Am. Chem. Soc., 75, 5154 (1953).

102) H.K.Frensdorf, M.T.Watson, W.Kauzmann, J.Am.Chem.Soc., 75, 5167 (1953).

103) W.Kauzmann, R.G.Douglas, Jr., Arch. Biochem. Biophys., 65, 106 (1956).

104) M.D.Sterman, J.F.Foster, J.Am. Chem. Soc., 78, 3652 (1956).

105) J.F.Foster, K.Aoki, J.Am. Chem. Soc., 80, 1117 (1958).

106) P.Callaghan, N.H.Martin, Biochem. J., 83, 144 (1962).

107) H.A.McKenzie, M.B.Smith, R.G.Wake, Biochim. Biophys. Acta, 69, 222 (1963).

108) C.Tanford, J.Am. Chem. Soc., 86, 2050 (1964).

109) T.G.Ferris, S.Katz, Nature (London), 211, 586 (1966).

110) S.Katz, J.Denis, Biochem. Biophys. Res. Commun., 28, 711 (1967).

111) S.Katz, J.Denis, Biochim. Biophys. Acta, 188, 247 (1969).

112) M.R.Salaman, A.R.Williamson, Biochem. J., 122, 93 (1971).

113) M.Nakagaki, Y.Sano, Yakugaku Zasshi (Japan), 93 (7), 902 (1973).

114) K.Aoki, M.Murata, K.Hiramatsu, Anal. Biochem., 59, 146 (1974).

115) W.Kauzmann, in "The Mechanism of Enzyme Action," W.D.McElory and B. Glas, Eds., John Hopkins Press, Baltimore, 1954, p.51.

116) T.Takagi, Yukagaku (Japan), 28 (4), 242 (1979).

117) S.Rackovsky, H.A.Scherage, Proc. Natl. Acad. Sci. U.S.A., 74, 5234 (1977).

118) W.Kauzmann, Advan. Protein Chem., 14, 1 (1959).

119) Y.Nozaki, C.Tanford, J.Biol. Chem., 238, 4074 (1963).

120) K.Aoki, private communication.

LIST OF PUBLICATIONS

1. Toshiro SUZAWA, Hiroyuki SHIRAHAMA, Tetsuya FUJIMOTO, "Adsorption of Bovine Serum Albumin onto Homo -and Copolymer Latices," J.Colloid Interface Sci., 86, 144 − 150 (1982); which relates to Chapter Ⅰ, Ⅱ(Ⅱ − Ⅰ), and Ⅳ in Part Ⅱ.

2. Toshiro SUZAWA, Hiroyuki SHIRAHAMA, Tetsuya FUJIMOTO, "Effect of Urea on the Adsorption of Bovine Serum Albumin onto Polymer Latices," J.Colloid Interface Sci., 93, 498 − 503 (1983); which relates to Chapter Ⅰ, Ⅱ(Ⅱ − Ⅰ), and Ⅳ in Part Ⅱ.

3. Hiroyuki SHIRAHAMA, Toshiro SUZAWA, "Surface Characterization of Soap-Free Carboxylated Polymer Latices," Polym. J., 16, 795 − 803 (1984); which relates to Chapter Ⅰ and Ⅱ in Part Ⅰ.

4. Hiroyuki SHIRAHAMA, Toshiro SUZAWA, "Surface Characterization of Styrene/2-Hydroxyethyl Methacrylate Copolymer Latex," J.Appl. Polym. Sci., 29, 3651− 3661 (1984); which relates to Chapter Ⅰ and Ⅱ in Part Ⅰ.

5. Hiroyuki SHIRAHAMA, Toshiro SUZAWA, "Adsorption of Bovine Serum Albumin onto Styrene/Acrylic Acid Copolymer Latex," Colloid Polym. Sci., 263, 141−146(1985); which relates to Chapter Ⅰ and

Ⅱ(Ⅱ－Ⅰ) in Part Ⅱ.

6. Hiroyuki SHIRAHAMA, Toshiro SUZAWA, "Adsorption of Bovine Serum Albumin onto Styrene/2-Hydroxyethyl Methacrylate Copolymer Latex," J.Colloid Interface Sci., 104, 416－421 (1985); which relates to Chapter Ⅰ and Ⅱ(Ⅱ－ Ⅱ) in Part Ⅱ.

7. Hiroyuki SHIRAHAMA, Hisashi TAMAI, Ikunori SAKAI, Toshiro SUZAWA, "Adsorption of Bovine Serum Albumin onto Styrene-Acrylamide Copolymer Latex," Nippon Kagaku Kaishi, 1985 (No.6), 1285 － 1292; which relates to Chapter Ⅱ in Part Ⅰ and Chapter Ⅱ(Ⅱ－Ⅲ) in Part Ⅱ.

8. Hiroyuki SHIRAHAMA, Kazuhiro TAKEDA, Toshiro SUZAWA, "Adsorption of Bovine Serum Albumin onto Polystyrene Latex: Effects of Coexistent Electrolyte Anions," J.Colloid Interface Sci., in press; which relates to Chapter Ⅲ in Part Ⅱ.